Identifying the novel GTPase function of FLCN and characterizing its role in aging

Abbas Ghazi

Department of Biochemistry

McGill University, Montreal

Submitted in December 2010

A thesis submitted to McGill University in partial fulfillment of the requirements of the degree of Master of Science

Abstract

Birt-Hogg-Dube syndrome (BHD) is an inherited neoplasia syndrome that predisposes affected individuals to skin hamartomas, lung cysts, pneumothorax and renal carcinoma. Mutations within the BHD locus (also known as FLCN) have been found associated with the disease. Almost all mutations in BHD patients cause a truncated FLCN protein product suggesting a loss-of-function mechanism leading to tumor formation. FLCN is highly conserved across species from yeast to humans suggesting an important biological function. Earlier this year, the exact molecular function of FLCN was still unclear. However, with the aid of the first crystal structure of folliculin carboxy-terminal domain we provide the first insight into the function of folliculin as a novel GTPase. Interestingly this GTPase activity is lost in a naturally occurring disease-causing mutant (C1844G). We then characterize the role of FLCN-1 in the nematode *Caenorhabditis elegans* in an attempt to determine the signalling pathway(s) to which FLCN-1 belongs. We report a novel role of FLCN-1 in *C. elegans* aging as a component of the insulin/IGF-1 signalling pathway. FLCN-1 regulates lifespan via a mechanism that is AAK-2/AMPK, DAF-16/FOXO and autophagy dependent. We demonstrate that FLCN-1 negatively regulates AAK-2 phosphorylation independent of the constitutively active PAR-4 kinase. Moreover, *flcn-1* null mutants have elevated levels of β oxidation of fatty acids, mitochondrial respiration and ROS generation all of which are dependent on AAK-2. We hypothesis that ROS generation stimulates autophagy activation as a downstream mechanism required for lifespan extension of *flcn-1* null mutants. Taken together, these studies are aimed to identify the functional role of FLCN and to clarify its metabolic role in relation to AMPK in order to better understand its tumor suppressor function.

Resume

Le syndrome de Birt-Hogg-Dubé (BHD) est un syndrome néoplasique héréditaire, qui rend les personnes atteintes plus susceptibles de développer les maladies telles que les harmatomes de la peau, kystes pulmonaires, pneumothorax et carcinomes rénaux. Des mutations dans le locus BHD au niveau du gène de la folliculine (FLCN) sont souvent associées à cette maladie. La majorité des patients présentent des mutations entrainant la troncation de la protéine FLCN, suggèrant un mécanisme de perte de fonction qui entraine la formation de tumeurs. Très conservée à travers les espèces de la levure à l'homme, la FLCN semble avoir une fonction biologique importante, cependant son mécanisme d'action est encore obscure. Néanmoins l'obtention récente de la structure cristallographique du domaine carboxyle terminal de la folliculine suggère qu'elle pourrait fonctionner telle une GTPase. Chose intéressante, cette activité GTPase est perdue naturellement chez les malades portant la mutation C1844G. Afin de déterminer dans quelle voie de signalisation la folliculine appartient, nous avons analysé son rôle chez le nématode Caenorhabditis elegans. Nous rapportons ici le nouveau rôle de la FLCN-1 dans le vieillissement de C. elegans, comme étant un acteur de la voie de signalisation insuline/IGF-1. La FLCN-1 régule la durée de vie à travers un mécanisme dépendant de l'AMPK/aak-2, FOXO/DAF-16 et de l'autophagie. Nous démontrons qu'elle régule négativement la phosphorylation de AAK-2 indépendamment de la kinase constitutivement active PAR-4. Chez les mutants nul flcn-1, les acides gras B oxydes, la respiration mitochondriale ainsi que la production de ROS présentent des niveaux élevés, qui dépendent de AAK-2. Nous proposons que la production de ROS stimule l'activation de l'autophagie, nécessaire pour l'extension de la durée de vie des mutants flcn-1 nul. Ainsi, nos études ont permis d'identifier le rôle fonctionnel de la FLCN et de clarifier son rôle métabolique en lien avec l'AMPK, permettant de mieux comprendre sa fonction de suppresseur de tumeur.

Acknowledgements

First and foremost I would like to thank my supervisor and mentor Dr. Arnim Pause who believed in me when I stopped. He provided invaluable support throughout my degree on a professional and personal level. I want to thank him for the great projects that were assigned to me. He is open and supportive to new ideas. If I only learned one thing from Arnim, it would be being humble and maintaining scientific integrity. I am great full to all the Pause lab members for the unique experience and great discussions on scientific and non-scientific topics. I wish them all the best on their future experiments and dreams. I will dearly miss Dmitri Kharitidi (chicken boy), Sanaz Manteghi, Ming Yan and the superstar Nathalie Ng Kuet Leong whom were so easy to work with. I am sure that the BHD group (Anders Bondo, Nathalie Ng Kuet Leong, Ming Yan, Yann Nouet, Sebastien Latapie, Zahra Jalali, and Elite Possik) will make great discoveries in the very near future. Sylvie, Vanessa and Vicky (the crazy gang) will always be the sunshine and I wish them all the best in whatever they plan on doing.

I will never be able to put into words how I feel towards the Roy lab and Dr. Richard Roy. They are just an amazing gang of researchers and friends namely: Chris St-Francois, Shaolin Li, Yu Lu, Julie Mantovani, Emilie Demoinet, Meng Xie and Gilbert Velasquez. You guys just made me love the worms and doing science. I will never forget "Knowledge is free and for everyone on this side" Richard Roy.

To my great friend and brother Chris St-Francois, for the priceless conversations on life and science. Nicky I am so blessed to have you in my life. You both are the source of my positive and constructive behavior and I will value our friendship forever.

To my family: Mother, father and siblings, thank you for the support from across the seas. You all will always be my definition of love and support. I miss you and love you.

Preface-Contributions of authors

All the work presented in this thesis was done by me for the following exceptions: In chapter 1, all the cloning, protein expression, purification and crystallization of the recombinant folliculin-CT was performed by Dr. Ravi K. Nookala (University of Cambridge, UK). In chapter 2, the generation of the following double mutant genotypes: *flcn-1;daf-2, flcn-1;aak-1, flcn-1;aak-2, flcn-1;daf-16,* and *flcn-1;par-4* by matings single mutants was performed by Nathalie Ng Kuet Leong (undergraduate student) in our laboratory. Chris St-Francois and Nathalie Ng Kuet Leong also assisted in conducting many of the survival curves, triglyceride quantification, ROS measurement assays and ROS resistance assays in this chapter. Chris St-Francois, Shaolin Li and Yu Lu (Roy Lab members) provided indispensable technical and research advice to conduct the *C.elegans* experiments. *C.elegans* strains used in chapter 2 were either provided by the laboratory of Dr. Richard Roy (McGill University) or purchased from the Caenorhabditis Genetics Center (CGC, University of Minnesota).

Table of Contents

List of Tables and Figures

Chapter 1:

Chapter 2:

General Introduction

Renal cancer

Kidney cancer affected 4900 Canadians in 2009 and has been identified as the cause of death of 1650 patients. Therefore, one in sixty four Canadians have the risk of developing renal cancer and almost half of diagnosed patients die from it. This is due to the fact that the disease is detected during late stages when most of the available treatments are ineffective. Moreover, patients with advanced disease have a two-year survival of just 18% [1]. Understanding the genetic basis of renal cancer through identifying genetic predispositions leading to the development of the tumors will allow early screening, thus helping for the detection of tumors at early stages, when they have a better response to available treatments. In addition, identifying the basic mechanisms leading to tumor development will proved sufficient knowledge in order to design effective therapies to cure this disease.

While most renal cancers are sporadic cases, 1-4% are due to inherited predispositions and this proportion is likely to increase in the future [2]. Sporadic renal cancer is often unifocal (one tumor), unilateral (one kidney affected) and has a later onset in life whereas, hereditary renal cancer tends to be bilateral (both kidney affected), multifocal (more than one tumor) and has an early onset in life [3]. Kidney cancer includes various types of renal cell carcinomas (RCC), which are classified in several morphological subtypes based on different histology and causative gene: clear cell RCC (80%), papillary type I and type II RCC (10%), oncocytoma RCC (< 5%) and chromophobe RCC (5%) [3-5]. In fact, a number of genetic diseases predispose to the development of specific subtypes of renal tumors and for some of them, associated genes have been identified. Mutations in the von Hipped-Lindau (*VHL*) tumor suppressor gene, the *MET* proto-oncogene, the fumarate hydratase (*FH*) gene, the tuberous sclerosis (*TSC1* and *TSC2*) genes, and the Birt-Hogg- Dube (BHD) tumor suppressor gene were previously identified to predispose to renal cancer of various subtypes [6, 7].

vhl tumor suppressor gene encodes a protein possessing ubiqutin ligase E3 activity responsible for the ubiquitin-mediated degradation of the hypoxia-inducible factors (HIF1-α and HIF2-α). Mutations in *vhl* leading to the development of the von Hipped-

Lindau disease give rise to renal tumors that are almost exclusively clear cell RCC [3, 8]. Another gene, the *c-MET* proto-oncogene encodes a receptor tyrosine kinase. Patients with missense mutations in the juxtamembrane domain of *c-MET* have a constitutively active receptor leading to the development of hereditary papillary renal carcinoma (HPRC) [9]. Furthermore, tumors in patients affected with HPRC are usually of the papillary type 1 histology [9]. In addition, the fumarate hydratase (*FH*) gene encodes a protein responsible for the conversion of fumarate to s-malate in the Krebs cycle [10]. Missense or frameshift germline mutations in *FH* were shown to be associated with hereditary leiomyomatosis renal cell carcinoma (HLRCC), a cancer syndrome characterized by tumors of papillary type 2 histology [2, 10, 11]. Moreover, Tuberous Sclerosis Complex syndrome (TSC) is a hereditary renal cancer syndrome characterized by benign tumors of the skin, brain and viscera caused by germline mutations in *TSC1* and *TSC2* genes [2, 12, 13]. It is interesting to note that *TSC1* and *TSC2* encode tuberin and its interacting partner hamartin respectively. Both proteins have been reported to downregulate the mammalian target of rapamycin complex 1 (mTORC1) which is deregulated in multiple human diseases [14]. Recently, the predisposing gene for chromophobe renal carcinoma and renal oncocytoma subtypes was identified. Indeed, germline mutations in a novel gene, *BHD*, were discovered in patients with the Birt-Hogg-Dube (BHD) syndrome [15, 16].

Birt-Hogg-Dube disease

Birt-Hogg-Dube syndrome is an inherited neoplasia syndrome that was originally described in 1977 by three Canadian physicians who studied families with history of small papular lesions (called fibrofolliculomas) from the hair follicle on the scalp, forehead, face and neck, inherited in an autosomal dominant manner [2, 15]. In addition to the fibrofolliculomas or skin hamartomas, BHD patients have an increased risk of pulmonary cysts, spontaneous peumothorax and renal neoplasms of multiple histological types [17, 18]. BHD patients have a 50-fold increased risk of developing spontaneous peumothorax and 7-fold increased risk of developing kidney tumors as compared to unaffected siblings [5, 18]. Actually, 15-30% of BHD patients with fibrofolliculomas will develop kidney tumors. It is important to mention that multiple different histological types of kidney tumors were observed within BHD families and even within kidneys of

individual BHD patients [3]. BHD associated renal tumors display diverse histology including chromophobe RCC (34%), clear cell RCC (9%), oncocytoma RCC (5%) and papillary type I RCC (3%) [19]. Moreover, the most common histological type in 50% of BHD renal tumors is a hybrid carrying features of both chromophobe and oncocytoma RCC [5, 19].Taken together; these findings suggest a general role of *BHD* in the development of many different histological types of kidney cancer. Interestingly, *BHD* gene mutations were also found in endometrial carcinomas, gastric cancer, and colon polyps and carcinomas [20-24].

The *BHD* gene locus was mapped to chromosome 17p11.2 by linkage analysis and later identified by positional cloning [16, 25, 26]. It encodes a cytoplasmic protein called folliculin (FLCN). Interestingly, the chromosomal band 17p11.2 was reported to be a genomic unstable region in multiple diseases such as Smith-Magenis syndrome, medulloblastomas and neuroectodermal tumors [27-29]. Moreover, loss of heterozygocity (LOH) on chromosome 17p was also reported in multiple different types of cancers including liver, colorectal, breast, ovarian and lung [30-34].

More than 60 families affected with the BHD syndrome have been analyzed for germline mutations in the *BHD* locus. A total of 22 novel mutations located along the entire length of the coding region of the *BHD* gene were reported [16, 35]. These mutations include insertion/deletion mutations (frameshift leading to premature truncation), nonsense mutations (leading to premature truncation) and putative splice-site mutations. Thus, the majority of the mutations in *BHD* lead to a truncated protein suggesting a loss-of-function mechanism leading to tumor development. More than half of all germline mutations (53%) were reported within the cytosine occurring in a poly (C) tract within exon 11 of the *BHD* gene which is considered a mutational hotspot [16, 35]. Somatic “second hit” mutations and LOH were identified in several sporadic as well as BHD-associated kidney tumors suggesting that both copies of the *BHD* gene can be inactivated for renal tumorigenesis to occur. This result conforms to the Knudson two-hit tumor suppressor model [36-38]. Conversely, other reports suggested that complete loss of FLCN function is not required for cutaneous tumors to develop in BHD patients.

Instead, haplo-insufficiency of FLCN is sufficient to initiate the uncontrolled growth that precedes tumorigenesis in susceptible tissue [39, 40].

The human *BHD* comprises 14 exons (3 non-coding and 11 coding) and *BHD* full length mRNA sequence is 3674 nucleotides (GenBank accession number AF517523). It was reported that *BHD* mRNA is widely expressed in adult human tissues including kidney, skin, lung, muscle, heart, liver, and epithelial strands of fibrofolliculomas. On the other hand, *BHD* mRNA expression is downregulated in kidney tumors regardless of the histological type suggesting its tumor suppressor role [16, 41]. The *BHD* cDNA encodes the novel cytoplasmic protein folliculin (FLCN) with an open reading frame of 579 amino acids and predicted molecular weight of 64 kDa. Two isoforms of FLCN have been identified with the second isoform predicted to be shorter with a distinct C-terminus of only 342 amino acids. FLCN has no significant sequence homology to any other known protein and it is highly conserved across species suggesting an important biological role [16]. To this end, human folliculin is more than 90% identical to the monkey, rat, cow, dog and mouse homologs and it is 22%-36% identical to the *Drosophila melanogaster* and 27 -28% identical to the *Caenorhabditis elegans*.

Cellular functions of FLCN

Mutation analysis in human BHD patients and presence of multiple animal models of inherited forms of renal cancer where germline mutations of BHD homologs were identified strongly support a tumor suppressor role of BHD [16, 35, 42, 43]. However, the molecular mechanism by which loss of *BHD* causes tumorigenesis in mammalian cells is still unclear.

As described previously, tuberous sclerosis complex (TSC) syndrome is caused by germline mutations of either the *TSC1* or *TSC2* tumor suppressor genes that lead to dysregulation of the mTOR signalling pathway [44, 45]. Moreover, BHD syndrome has multiple clinical manifestations including skin harmatomas, pneumothorax, lung cysts and kidney tumors. Interestingly, these manifestations can also occur in tuberous sclerosis complex (TSC) syndrome suggesting that FLCN and TSC proteins could act within a common signalling pathway leading to tumor development. A study in yeast (*Schizosaccharomyces pombe*) addressed this hypothesis and surprisingly revealed

opposing roles for FLCN and TSC homologs through the regulation of Tor2 (homolog of mTOR in yeast) [46]. In the study, FLCN was found to activate mTOR signalling independent of TSC1/2 [46]. Whether this regulation of mTOR signalling by FLCN is conserved in mammalian cells and involved in renal tumorigenesis appears to be highly controversial as further described below. Another study in *Drosophila*, demonstrated that the *BHD* homolog (*DBHD*) regulates male germline stem cells maintenance in the fly by interacting with both the JAK-STAT and decapentaplegic (Dpp) signalling transduction pathways [47]. The study also suggests that FLCN could control tumorigenesis by regulating the JAK/STAT pathway. It is important to mention that the JAK/STAT signalling pathway influences cell survival and growth mechanisms while abnormal JAK/STAT signalling is associated with multiple cancers [48-50].

In 2006, a report identified a 130 kDa folliculin-interacting protein 1 (termed FNIP1) which in turn interacts with AMPK (AMP-activated protein kinase) [51]. FNIP1 binds to the C-terminus of FLCN [51]. AMPK act as a negative regulator of the mammalian target of rapamycin (mTOR) and is a key metabolic regulator in energy sensing in cells. FNIP1 phosphorylation by AMPK modulates FNIP1 protein expression levels. Moreover, FLCN phosphorylation is mediated by FNIP1 expression but reduced by inhibition of AMPK or mTOR signalling [51]. More recently, two independent reports identified folliculin-interacting protein 2 (termed FNIP2) [52, 53]. Interestingly FNIP2 is highly homologus to FNIP1 with a sequence identity of 49% suggesting a functional conservation. Indeed, similar to FNIP1, FNIP2 is also able to interact with FLCN at its C-terminus and with AMPK as well [52]. This year, further biochemical analysis of the nature of this interaction identified Ser62 amino acid residue as the rat FLCN phosphorylation site that is indirectly upregulated by AMPK [54]. Interestingly, upon binding with folliculin-interacting proteins (FNIP1 and FNIP2), Ser62 phosphorylation is increased. Furthermore, a phospho-mimic mutation at Ser62 enhanced the formation of the FLCN-AMPK complex independent of FNIP1 and FNIP2 [54]. Another report by the same group identified Ser302 as another novel rat FLCN phosphorylation site and concluded that both sites (Ser62 and Ser 302) may be phosphorylated by an unknown kinase downstream of tuberin-mTORC1 [55]. Taken together, interaction of FLCN with FNIP1, FNIP2 and AMPK suggests a role for FLCN FNIP1, and FNIP2 in nutrient/ energy

sensing through the AMPK and mTOR signalling pathways. However, the nature of this regulation is still unclear as a matter of fact it is highly controversial and the molecular role of FLCN in these pathways is not yet understood.

The controversy in the FLCN research field stems from determining the exact role of FLCN in regulating mTORC1. It is important to note that mTOR acts as a nutrient sensor and a master regulator of protein translation in cell growth and proliferation. A study that used a conditional KSP-Cre FLCN knockout mouse showed an activation of mTOR via the PI3K-AKT pathway in the renal tumors and polycystic kidneys [56]. Upon treatment of the knockout mice with rapamycin (mTOR inhibitor), they showed smaller kidneys and longer median lifespan [56]. In the same study, the authors report that knockout of FLCN led to the activation of Raf-extracellular signal-regulated protein kinase (Erk)1/2 in the kidneys which is also known to be involved in increased expression of cell cycle proteins and cell proliferation in multiple cancers [56]. This study strongly suggests that FLCN is acting upstream and negatively regulating these two pathways. Similiarly, another report also described an activation of the AKT-mTOR signalling in polycystic kidneys upon the reduction of FLCN expression levels [57]. Conversely, multiple studies show the exact opposite, were downregulation of FLCN using siRNA in multiple human cancer cell lines also shows a reduction in positive markers of the mTORC1 signalling pathway. This was done using phospho- specific antibodies against phospho-ribosomal protein S6 (pS6) and phospho-70 ribosomal protein S6 kinase 1 (p70-S6K1) both of which are considered positive markers of the mTOR pathway [53, 58]. In our laboratory, we observe that solid tumors and normal kidneys show decreased pS6 upon diminished FLCN expression [59]. Our *in vivo* experiments, pS6 was found to be elevated or absent in FLCN-negative renal cysts. Moreover, when growing RCC cells *in vitro*, regardless of culture conditions and FLCN expression status, we observed no differences in pS6 levels. Therefore, loss of FLCN expression leads to context-dependent effects on S6 activation (pS6 levels) and the contradictory mTOR activation/repression reports are probably due to the second hit mutations in FLCN [59].

It is very important to note that the BHD syndrome shares many clinical manifestations (harmatomas, pneumothorax, lung cysts and kidney tumors) with other harmatoma

syndromes namely the Peutz-Jeghers syndrome (*LKB1* tumor suppressor gene), the Cowden syndrome (*PTEN* tumor suppressor gene) and the tuberous sclerosis complex syndrome (*TSC1* and *TSC2* tumor suppressor genes) [60-64]. This phenotypical link between the BHD syndrome and other harmatoma syndromes strongly suggests that FLCN might be involved in functions universal to the development of these malignancies. Moreover, although FLCN is considered to act as a tumor suppressor, the mechanisms by which it causes tumor formation is still unclear. To this date, no functional role of FLCN has been reported in the mammalian systems. Taken together, more research should be performed to shed some light on characterizing a functional role of FLCN which will undoubtedly give great insight on the mechanism by which the tumor formation occurs. This is also clear any controversies that have been reported in the BHD syndrome research field. Finally understanding the genetic and functional basis of the BHD syndrome will hopefully lead to the development of efficient therapies for this disease and kidney cancer as well.

References

1. Linehan, W.M., et al., *The genetic basis of cancer of kidney cancer: implications for gene-specific clinical management.* BJU Int, 2005. **95 Suppl 2**: p. 2-7.
2. Choyke, P.L., et al., *Hereditary renal cancers.* Radiology, 2003. **226**(1): p. 33-46.
3. Pavlovich, C.P. and L.S. Schmidt, *Searching for the hereditary causes of renal-cell carcinoma.* Nat Rev Cancer, 2004. **4**(5): p. 381-93.
4. Kovacs, G., et al., *The Heidelberg classification of renal cell tumours.* J Pathol, 1997. **183**(2): p. 131-3.
5. Schmidt, L.S., *Birt-Hogg-Dube syndrome, a genodermatosis that increases risk for renal carcinoma.* Curr Mol Med, 2004. **4**(8): p. 877-85.
6. Linehan, W.M., M.M. Walther, and B. Zbar, *The genetic basis of cancer of the kidney.* J Urol, 2003. **170**(6 Pt 1): p. 2163-72.
7. Bjornsson, J., et al., *Tuberous sclerosis-associated renal cell carcinoma. Clinical, pathological, and genetic features.* Am J Pathol, 1996. **149**(4): p. 1201-8.
8. Latif, F., et al., *Identification of the von Hippel-Lindau disease tumor suppressor gene.* Science, 1993. **260**(5112): p. 1317-20.
9. Schmidt, L., et al., *Germline and somatic mutations in the tyrosine kinase domain of the MET proto-oncogene in papillary renal carcinomas.* Nat Genet, 1997. **16**(1): p. 68-73.
10. Tomlinson, I.P., et al., *Germline mutations in FH predispose to dominantly inherited uterine fibroids, skin leiomyomata and papillary renal cell cancer.* Nat Genet, 2002. **30**(4): p. 406-10.
11. Toro, J.R., et al., *Mutations in the fumarate hydratase gene cause hereditary leiomyomatosis and renal cell cancer in families in North America.* Am J Hum Genet, 2003. **73**(1): p. 95-106.
12. Cheadle, J.P., et al., *Molecular genetic advances in tuberous sclerosis.* Hum Genet, 2000. **107**(2): p. 97-114.
13. Kandt, R.S., et al., *Linkage of an important gene locus for tuberous sclerosis to a chromosome 16 marker for polycystic kidney disease.* Nat Genet, 1992. **2**(1): p. 37-41.
14. Inoki, K., M.N. Corradetti, and K.L. Guan, *Dysregulation of the TSC-mTOR pathway in human disease.* Nat Genet, 2005. **37**(1): p. 19-24.
15. Birt, A.R., G.R. Hogg, and W.J. Dube, *Hereditary multiple fibrofolliculomas with trichodiscomas and acrochordons.* Arch Dermatol, 1977. **113**(12): p. 1674-7.
16. Nickerson, M.L., et al., *Mutations in a novel gene lead to kidney tumors, lung wall defects, and benign tumors of the hair follicle in patients with the Birt-Hogg-Dube syndrome.* Cancer Cell, 2002. **2**(2): p. 157-64.
17. Toro, J.R., et al., *Birt-Hogg-Dube syndrome: a novel marker of kidney neoplasia.* Arch Dermatol, 1999. **135**(10): p. 1195-202.
18. Zbar, B., et al., *Risk of renal and colonic neoplasms and spontaneous pneumothorax in the Birt-Hogg-Dube syndrome.* Cancer Epidemiol Biomarkers Prev, 2002. **11**(4): p. 393-400.
19. Pavlovich, C.P., et al., *Renal tumors in the Birt-Hogg-Dube syndrome.* Am J Surg Pathol, 2002. **26**(12): p. 1542-52.
20. Fujii, H., et al., *Birt-Hogg-Dube gene mutations in human endometrial carcinomas with microsatellite instability.* J Pathol, 2006. **209**(3): p. 328-35.

21. Hornstein, O.P., *Generalized dermal perifollicular fibromas with polyps of the colon.* Hum Genet, 1976. **33**(2): p. 193-7.
22. Hornstein, O.P. and M. Knickenberg, *Perifollicular fibromatosis cutis with polyps of the colon--a cutaneo-intestinal syndrome sui generis.* Arch Dermatol Res, 1975. **253**(2): p. 161-75.
23. Jiang, W., et al., *Birt-Hogg-Dube (BHD) gene mutations in human gastric cancer with high frequency microsatellite instability.* Cancer Lett, 2007. **248**(1): p. 103-11.
24. Le Guyadec, T., et al., *[Multiple trichodiscomas associated with colonic polyposis].* Ann Dermatol Venereol, 1998. **125**(10): p. 717-9.
25. Khoo, S.K., et al., *Birt-Hogg-Dube syndrome: mapping of a novel hereditary neoplasia gene to chromosome 17p12-q11.2.* Oncogene, 2001. **20**(37): p. 5239-42.
26. Schmidt, L.S., et al., *Birt-Hogg-Dube syndrome, a genodermatosis associated with spontaneous pneumothorax and kidney neoplasia, maps to chromosome 17p11.2.* Am J Hum Genet, 2001. **69**(4): p. 876-82.
27. Smith, A.C., et al., *Interstitial deletion of (17)(p11.2p11.2) in nine patients.* Am J Med Genet, 1986. **24**(3): p. 393-414.
28. Seranski, P., et al., *Transcription mapping in a medulloblastoma breakpoint interval and Smith-Magenis syndrome candidate region: identification of 53 transcriptional units and new candidate genes.* Genomics, 1999. **56**(1): p. 1-11.
29. Scheurlen, W.G., et al., *High-resolution deletion mapping of chromosome arm 17p in childhood primitive neuroectodermal tumors reveals a common chromosomal disruption within the Smith-Magenis region, an unstable region in chromosome band 17p11.2.* Genes Chromosomes Cancer, 1997. **18**(1): p. 50-8.
30. Piao, Z., et al., *Allelotype analysis of hepatocellular carcinoma.* Int J Cancer, 1998. **75**(1): p. 29-33.
31. Laurent-Puig, P., H. Blons, and P.H. Cugnenc, *Sequence of molecular genetic events in colorectal tumorigenesis.* Eur J Cancer Prev, 1999. **8 Suppl 1**: p. S39-47.
32. Hoff, C., et al., *Allelic imbalance and fine mapping of the 17p13.3 subregion in sporadic breast carcinomas.* Cancer Genet Cytogenet, 2001. **129**(2): p. 145-9.
33. Phillips, N., et al., *Allelic loss on chromosome 17 in human ovarian cancer.* Int J Cancer, 1993. **54**(1): p. 85-91.
34. Konishi, H., et al., *Detailed deletion mapping suggests the involvement of a tumor suppressor gene at 17p13.3, distal to p53, in the pathogenesis of lung cancers.* Oncogene, 1998. **17**(16): p. 2095-100.
35. Schmidt, L.S., et al., *Germline BHD-mutation spectrum and phenotype analysis of a large cohort of families with Birt-Hogg-Dube syndrome.* Am J Hum Genet, 2005. **76**(6): p. 1023-33.
36. Vocke, C.D., et al., *High frequency of somatic frameshift BHD gene mutations in Birt-Hogg-Dube-associated renal tumors.* J Natl Cancer Inst, 2005. **97**(12): p. 931-5.
37. Khoo, S.K., et al., *Inactivation of BHD in sporadic renal tumors.* Cancer Res, 2003. **63**(15): p. 4583-7.

38. Knudson, A.G., Jr., *Mutation and cancer: statistical study of retinoblastoma.* Proc Natl Acad Sci U S A, 1971. **68**(4): p. 820-3.
39. van Steensel, M.A., et al., *Novel mutations in the BHD gene and absence of loss of heterozygosity in fibrofolliculomas of Birt-Hogg-Dube patients.* J Invest Dermatol, 2007. **127**(3): p. 588-93.
40. Toro, J.R., et al., *Lung cysts, spontaneous pneumothorax, and genetic associations in 89 families with Birt-Hogg-Dube syndrome.* Am J Respir Crit Care Med, 2007. **175**(10): p. 1044-53.
41. Warren, M.B., et al., *Expression of Birt-Hogg-Dube gene mRNA in normal and neoplastic human tissues.* Mod Pathol, 2004. **17**(8): p. 998-1011.
42. Lingaas, F., et al., *A mutation in the canine BHD gene is associated with hereditary multifocal renal cystadenocarcinoma and nodular dermatofibrosis in the German Shepherd dog.* Hum Mol Genet, 2003. **12**(23): p. 3043-53.
43. Okimoto, K., et al., *A germ-line insertion in the Birt-Hogg-Dube (BHD) gene gives rise to the Nihon rat model of inherited renal cancer.* Proc Natl Acad Sci U S A, 2004. **101**(7): p. 2023-7.
44. Mak, B.C. and R.S. Yeung, *The tuberous sclerosis complex genes in tumor development.* Cancer Invest, 2004. **22**(4): p. 588-603.
45. Astrinidis, A. and E.P. Henske, *Tuberous sclerosis complex: linking growth and energy signaling pathways with human disease.* Oncogene, 2005. **24**(50): p. 7475-81.
46. van Slegtenhorst, M., et al., *The Birt-Hogg-Dube and tuberous sclerosis complex homologs have opposing roles in amino acid homeostasis in Schizosaccharomyces pombe.* J Biol Chem, 2007. **282**(34): p. 24583-90.
47. Singh, S.R., et al., *The Drosophila homolog of the human tumor suppressor gene BHD interacts with the JAK-STAT and Dpp signaling pathways in regulating male germline stem cell maintenance.* Oncogene, 2006. **25**(44): p. 5933-41.
48. Ihle, J.N., *Cytokine receptor signalling.* Nature, 1995. **377**(6550): p. 591-4.
49. Garcia, R., et al., *Constitutive activation of Stat3 in fibroblasts transformed by diverse oncoproteins and in breast carcinoma cells.* Cell Growth Differ, 1997. **8**(12): p. 1267-76.
50. Liu, K.D., et al., *Janus kinases in interleukin-2-mediated signaling: JAK1 and JAK3 are differentially regulated by tyrosine phosphorylation.* Curr Biol, 1997. **7**(11): p. 817-26.
51. Baba, M., et al., *Folliculin encoded by the BHD gene interacts with a binding protein, FNIP1, and AMPK, and is involved in AMPK and mTOR signaling.* Proc Natl Acad Sci U S A, 2006. **103**(42): p. 15552-7.
52. Hasumi, H., et al., *Identification and characterization of a novel folliculin-interacting protein FNIP2.* Gene, 2008. **415**(1-2): p. 60-7.
53. Takagi, Y., et al., *Interaction of folliculin (Birt-Hogg-Dube gene product) with a novel Fnip1-like (FnipL/Fnip2) protein.* Oncogene, 2008. **27**(40): p. 5339-47.
54. Wang, L., et al., *Serine 62 is a phosphorylation site in folliculin, the Birt-Hogg-Dube gene product.* FEBS Lett. **584**(1): p. 39-43.
55. Piao, X., et al., *Regulation of folliculin (the BHD gene product) phosphorylation by Tsc2-mTOR pathway.* Biochem Biophys Res Commun, 2009. **389**(1): p. 16-21.

56. Baba, M., et al., *Kidney-targeted Birt-Hogg-Dube gene inactivation in a mouse model: Erk1/2 and Akt-mTOR activation, cell hyperproliferation, and polycystic kidneys.* J Natl Cancer Inst, 2008. **100**(2): p. 140-54.
57. Chen, J., et al., *Deficiency of FLCN in mouse kidney led to development of polycystic kidneys and renal neoplasia.* PLoS One, 2008. **3**(10): p. e3581.
58. Hartman, T.R., et al., *The role of the Birt-Hogg-Dube protein in mTOR activation and renal tumorigenesis.* Oncogene, 2009. **28**(13): p. 1594-604.
59. Hudon, V., et al., *Renal tumour suppressor function of the Birt-Hogg-Dube syndrome gene product folliculin.* J Med Genet. **47**(3): p. 182-9.
60. Jenne, D.E., et al., *Peutz-Jeghers syndrome is caused by mutations in a novel serine threonine kinase.* Nat Genet, 1998. **18**(1): p. 38-43.
61. Hemminki, A., et al., *A serine/threonine kinase gene defective in Peutz-Jeghers syndrome.* Nature, 1998. **391**(6663): p. 184-7.
62. Toro, J.R., et al., *Exclusion of PTEN, CTNNB1, and PTCH as candidate genes for Birt-Hogg-Dube syndrome.* J Med Genet, 2002. **39**(2): p. E10.
63. Marsh, D.J., et al., *PTEN mutation spectrum and genotype-phenotype correlations in Bannayan-Riley-Ruvalcaba syndrome suggest a single entity with Cowden syndrome.* Hum Mol Genet, 1999. **8**(8): p. 1461-72.
64. Liaw, D., et al., *Germline mutations of the PTEN gene in Cowden disease, an inherited breast and thyroid cancer syndrome.* Nat Genet, 1997. **16**(1): p. 64-7.

Rational and Objectives of the study

To date the exact molecular and functional role of the tumor suppressor folliculin (FLCN) is still unclear. Multiple contradictory reports have shown opposing roles of FLCN in regulating AMPK and mTOR signalling. The results presented in this study identify FLCN as a novel GTPase in the AMPK/mTOR pathway. We then use the nematode *C.elegans* as a novel FLCN study system. *C.elegans* offers an ideal simple genetic model organism to further characterize the metabolic role of FLCN. Identifying and characterizing a FLCN phenotype in the nematode will allow us as well as the FLCN research field to better understand its molecular function in the cell.

The two specific objectives of this study are:

A) Use the first crystal structure of folliculin carboxy-terminal domain to further elucidate its functional role.
   i) Identify the novel role of FLCN as a GTPase.
   ii) Determine whether this GTPase function is lost in naturally occurring mutants.

B) Use *C.elegans* as a novel model organism to study the metabolic role of FLCN-1.

i) Identify the novel role of FLCN-1 in *C.elegans* aging.

ii) Determine the genetic pathway(s) by which FLCN-1 extends lifespan in the nematode.

iii) Characterize the role of FLCN-1 in the insulin/IGF-1 signalling pathway to extend lifespan via elevated autophagy.

iv) Elucidate the functional and phenotypical link between FLCN-1 and AAK-2(AMPK).

Chapter 1: Crystal structure of renal tumor suppressor protein, folliculin: a novel GTPase in AMPK/mTOR pathway

Ravi K. Nookala[1, *], Abbas Ghazi[2], Dimitri Y. Chirgadze[1], Anders C. Dydensborg[2], Tom L. Blundell[1, †] and Arnim Pause[2, †]

1. Department of Biochemistry, University of Cambridge, Sanger Building, 80 Tennis Court Road, Cambridge CB2 1GA, United Kingdom.

2. Goodman Cancer Center, Department of Biochemistry, McGill University, McIntyre Building, 3655 Sir William Osler Promenade, Montreal, Quebec, H3G1Y6, Canada.

†Joint senior authors: Tom L. Blundell (tom@cryst.bioc.cam.ac.uk) and Arnim Pause (arnim.pause@mcgill.ca).

* Corresponding author: Ravi K. Nookala (rn229@cam.ac.uk).

Manuscript in preparation

Authors Contributions

A.P, R.K.N and T.L.B conceived the idea. R.K.N cloned, expressed, purified and crystallized the recombinant folliculin-CT. A.G performed all the mutagenesis, immuno-precipitation and nucleotide binding and hydrolysis experiments. D.Y.C helped in structure building and refinement. All authors contributed towards the preparation of the manuscript.

Abstract

Single and biallelic mutations in the tumor suppressor gene folliculin predispose affected individuals to proliferative lesions such as hair follicle tumors, lung and renal cysts resulting in pneumothorax and several histological types of renal cancer[1, 2]. Folliculin has been reported to be a component of the target of rapamycin - mTOR - pathway, interacting through its carboxy-terminal domain with AMP-activated kinase, and thus playing a role in regulation of cell growth and energy metabolism[3]. Importantly, most naturally occurring cancer causing mutations lead to carboxy-terminal truncations of folliculin pointing to a functional importance of this domain in tumor suppression[4]. We present here the first crystal structures of folliculin carboxy-terminal domain in its apo- and nucleotide-bound forms. The structures reveal that folliculin has an unconventional GTPase fold and that the protein dimerizes upon nucleotide binding. Although the protein lacks the Walker motifs and the G3 guanine base recognition motif characteristic of conventional GTPases, we demonstrate that folliculin is able to bind GTP. The nucleotide-bound structure reveals that the folliculin dimerisation is uniquely mediated by the NKIE helical motif (similar to the N/TKxD or G4 motif), wherein lysine 485 residues from each protomer are in close contact with the N7 of the guanine ring. Significantly, we show that folliculin is capable of efficiently hydrolyzing GTP to GDP and that the mutation of the lysine 485 residue to an alanine in the NKIE motif renders folliculin unable to hydrolyze GTP. Furthermore, we also show that a naturally occurring disease-causing mutant is unable to hydrolyze GTP. These crystal structures provide a first insight into the function of folliculin as a novel GTPase in the AMPK/mTOR pathway.

Introduction

Genetically inherited syndromes offer an important insight into molecular mechanisms underlying biological processes of medical importance, such as carcinogenesis. One such hereditary cancer syndrome is the Birt-Hogg-Dubé syndrome (BHD), an autosomal dominant disease characterized by multifocal, bilateral renal cancers, benign skin tumors, colon polyps, and lung cysts, which lead to pneumothorax [1, 2]. Folliculin, the tumor suppressor gene responsible for the BHD disease, and its interacting partners, FNIP1 and FNIP2, were shown to form a complex with AMP-activated protein kinase (AMPK) [3, 5]. AMPK regulates the energy homeostasis in the cell and becomes activated upon energy deprivation, resulting in negative regulation of mammalian Target of Rapamycin Complex 1 (mTORC1)[6, 7]. AMPK inhibits mTORC1 directly through phosphorylation of Raptor[8] as well as indirectly through its effects on the Tuberous Sclerosis complex 1/-2 (TSC1/-2 complex) [7]. Whether folliculin, via AMPK, is directly involved in the mTORC1 pathway or whether it functions independently of mTORC1 remains unclear as conflicting evidence to the role of folliculin in this pathway has been reported[9-12]. The knowledge of the molecular structure of folliculin will help in better understanding its function and role in this multi-component signaling pathway.

Results and Discussion

We began by carrying out a bioinformatical analysis of secondary structure content of the amino acid sequence using JPred[13] and Disopred[14] software. The ClustalW[15] alignment of the sequences of various folliculin homologues shows that the carboxy terminus of the protein is well conserved in higher vertebrates (Fig. S1). Based on these findings, folliculin is seen to comprise at least two structural domains: an amino-terminal region (89-290 aa) organized as a globular structure (comprising of α helices and β strands), followed by a relatively well-conserved, globular region - the carboxy terminus (340-579 aa). These are linked by a central region, which is predicted to have little secondary structure and some intrinsically disordered sequence (Fig.1a). Most germline mutations produce a truncated folliculin protein that lacks the carboxy terminus[4]. Assuming that the amino terminal region folds independently to give a stable protein and that there are no stabilizing interactions between the structural domains, a potential role of the carboxy-terminal region, called folliculin-CT henceforth, in tumorigenesis may be inferred.

We, therefore, determined the 3-dimensional structure of folliculin-CT at 1.9 Å resolution using phases calculated by multi-wavelength anomalous dispersion (MAD) data collected for the selenium anomalous scatterer (see Methods). The apo-form of folliculin-CT crystallized in $C222_1$ space group with 2 molecules in the asymmetric unit related by 2-fold non-crystallographic symmetry. The overall structure of folliculin-CT comprises an αβ fold with 6 α helices that stack on one side of the β sheet followed by an α helical region (Fig. 1b). The β sheet comprises of 5 strands, which form a characteristic order, E-D-A-C-B (each strand is represented by a letter of the alphabet). A database search using DALI server[16] and NCBI's VAST[17] search program returned several NTPases as having similar spatial arrangement of secondary structures to the folliculin-CT. The carboxy-terminal domain of VirB11 protein (pdb id: 1nlz), a transport ATPase from *Helicobacter pylori*[18], with 7% structural identity to folliculin-CT was the top hit in the searches performed using the two aforementioned servers. Superposition of the two structures shows that the overall architecture of the proteins is similar with a root mean square deviation of 2.6 Å on the C-alpha atoms but over the alignment length of only 88 amino acids spanning residues 347 to 469 representing five β strands and one helix (Fig 2a). These NTPases from diverse genera such as the VirB11 transport ATPase from *Helicobacter pylori*, the *Archaeoglobus fulgidus* secretion superfamily ATPase, afGspE, the replicative helicase-primase protein from bacteriophage T7 and the human RAD51 recombinase all contain the characteristic Walker A and B motifs that are required for their function. However, these motifs are absent not only in the folliculin-CT domain but also in the full length folliculin protein.

In order to determine whether folliculin binds nucleotides, we performed UV mediated nucleotide cross-linking. This assay is used to characterize direct binding of NTPs to NTPases by incubating α-^{32}P-labelled NTP with recombinant NTPase protein under UV light[19]. We observed that purified recombinant folliculin-CT specifically binds GTP and ATP, the latter with significantly lower affinity (Fig. 2b). In all known GTP binding proteins and conventional GTPases, two sets of residues, the G3 (DxxG) and the G4 (N/TKxD) motifs that form the guanine nucleotide binding 'fingerprint' have been considered essential for recognition/stabilization of the guanine ring[20]. The ability of folliculin to bind GTP is surprising given the lack of the G3 motif in the carboxy terminal

region and the full length protein sequences. Evolutionarily the GTPase superclass can be divided into two large classes: the TRAFAC GTPases (consisting of translation factors) and the SIMIBI GTPases (named after signal recognition particle, MinD and BioD proteins). These two classes of GTPases differ from each other both at the structure and at the sequence levels[20]. In order to investigate whether there are any structural similarities with TRAFAC GTPases, we compared the structure of human ras GTPase[21] (pdb id: 1Q21) with folliculin-CT (Fig 2c). The 3-dimensional superposition of the two structures showed that the arrangement of the β strands in human ras is similar to that of the β strands in folliculin (i.e. E-D-A-C-B) but with one significant difference – the orientation of the strands B and E. In folliculin-CT, strand B is parallel and strand E is anti-parallel to the rest of the strands, whereas in human ras and other conventional GTPases strand B is anti-parallel and strand E is parallel to the rest of the strands (Fig. S2). Similarly, we compared folliculin-CT structure with a SIMIBI GTPase, the signal sequence recognition protein (Ffh) [22] from *Thermus aquaticus* (pdb id: 2NG1, Fig. 2d). The Ffh protein has a β sheet comprised of seven parallel strands and the comparison with folliculin-CT structure showed that the arrangement of the strands is not similar to each other but the directionality of the strand B is the same (Fig. S2). These analyses suggest that 1) folliculin-CT shares similarities with both classes of GTPases, 2) there is an apparent 'strand swap' in folliculin-CT and 3) that folliculin does not fall in either of the two classes of GTPases.

Next, we set out to verify whether folliculin is merely a GTP binding protein or a GTP hydrolyzing protein as our analysis suggested. To this end, the immuno-precipitated FLAG tagged folliculin from HEK 293T cells was subjected to GTPase and ATPase assays. While no ATP hydrolysis was observed (Fig. 3a), there was a clear dose-response relationship between the folliculin input and GTP hydrolysis, demonstrating that immuno-purified folliculin possesses GTPase activity (Fig. 3b, 4b and 4d). As previously mentioned, the majority of disease causing mutations in the BHD patient population result in carboxy terminal truncations[4]; we therefore tested the GTPase activity of a common cancer causing folliculin mutant that results in a truncated protein at Tyr 463 residue as well as the recombinant folliculin-CT domain. The patient mutation protein was found devoid of GTPase activity (Fig. 3c), while the recombinant folliculin-CT

domain expressed and purified from *E. coli* had very little activity compared to the full length protein (Fig. 3b). These data demonstrate that folliculin harbors a carboxy terminal GTPase activity that 1) is dependent on the full length protein and 2) is lost in a common, naturally occurring disease causing mutation. Together, this points out the potential importance of the GTPase activity for the tumor suppressor function of folliculin.

In order to identify the putative GTP binding region in folliculin-CT, we co-crystallized nucleotide bound folliculin-CT (see Methods). The complex crystallized in C2 space group with 2 molecules in the asymmetric unit. The structure of folliculin-CT and nucleotide complex was determined to 2.7 Å resolution by the molecular replacement (MR) method using the folliculin-CT protomer from the apo-crystal-form as the MR search probe. In this crystal structure, folliculin-CT forms a dimer and the nucleotide is bound between the short helices from both protomers forming a compact pocket to stabilize the nucleotide (Fig. 4a). This mode of nucleotide-dependent dimerisation is commonly seen in a subset of GTP binding proteins called the *G proteins activated by nucleotide-dependent dimerisation* (GADs). For example, the Ffh and FtsY proteins (both are GADs that belong to the SIMIBI class GTPases) undergo a pseudo-trans dimerisation upon GTP binding wherein identical active site residues present on the G4 motif from both proteins interact with the nucleotide[23]. In folliculin-CT, the Lys 485 residues from the NKIE motifs of both protomers make a hydrogen bond (3.5 Å) with the N7 of guanine ring similar to the conserved Lys residue from the N/TKxD motif of all the conventional GTPases. However, the distinctive feature of the nucleotide-binding mode of folliculin-CT is that the putative G4 motif forms a small helix unlike the conventional GTPases where the motif exists as a loop[20]. Next, we sought to establish whether the Lys 485 residue is critical for the GTPase activity of folliculin and hence mutated the lysine to an alanine. Strikingly, the Lys 485 Ala point mutation in folliculin completely abolished the GTPase activity even at very high protein concentrations (Fig. 4c). We also observed that even though GTP was used in crystallization, only GDP could be fitted in the electron density (Fig. 4e). As the folliculin-CT has weak GTPase activity (Fig. 3b), we conclude that the GTP used in crystallization was hydrolyzed by the protein prior to crystal formation, and hence only GDP is visible in the structure.

Here, we present the first crystal structure of folliculin-CT domain, a tumor suppressor protein that interacts with AMPK, an important energy sensor in cells that negatively regulates mTOR, the master switch for cell growth and proliferation. Folliculin may play a role in cellular energy and nutrient sensing through interactions with the AMPK-mTOR signaling pathway. Mutations in several other tumor suppressor genes, including LKB1, PTEN, VHL and TSC1/2, have been shown to lead to dysregulation of AKT/mTOR signaling and to the development of other cancer syndromes. We show for the first time structural and biochemical evidence that folliculin-CT harbors a GTP binding domain. We also show that folliculin-CT has an unconventional GTPase fold and that upon GTP binding undergoes dimerisation similar to some G proteins that are categorized as GADs. Folliculin hydrolyzes GTP to GDP, and this activity is lost when a key amino acid (Lys 485) in the nucleotide-binding pocket is mutated to an alanine. Furthermore, the GTPase activity is also lost in a very frequently occurring patient mutation that produces a truncated protein. We hypothesize that the loss of GTPase activity could contribute to the symptoms of the disease. Taken together these data, we propose that folliculin may be a unique GTPase that has evolved in higher vertebrates to perform a more specialized function.

Materials and Methods

Protein Purification

The folliculin-CT was cloned into the Gateway system (Invitrogen, UK) and the recombinant protein was expressed as a thioredoxin fusion protein in BL21 (DE3) Star® (Invitrogen, UK) *E. coli* competent cells. The recombinant protein was initially purified over a 1 mL nickel-immobilized metal affinity chromatography column (Ni-IMAC). A proteolytic cleavage using Tobacco Etch Virus Protease (TEV-protease) was carried out for 1h at room temperature to separate the affinity tag from folliculin-CT. The reaction was subsequently passed over the Ni-IMAC column for removal of the tag and the remaining uncleaved fusion protein. The target protein was further purified using a Superdex® 75 (GE Healthcare) size exclusion chromatography column to obtain homogeneous recombinant protein for crystallization trials. The protein was concentrated to 5 mg/mL using Amicon ultra filter concentrators (Millipore, UK) with a 10,000

daltons molecular weight cut-off membrane. The concentrated protein was frozen in liquid nitrogen and stored at -80^{o}C until further use.

Mutagenesis

Crystallization of the folliculin-CT required mutation of three cysteine residues Cys454, Cys 503, and Cys 506 to alanines. These cysteine residues could have been forming covalent intermolecular disulphide mediated cross-links that were causing folliculin-CT to form multimers thereby inhibiting crystallization. Mutagenesis of the cysteine residues to alanines in folliculin-CT as well as mutagenesis of full length folliculin was carried out using the Quick Change® mutagenesis kit (Stratagene) according to the manufacturer's protocol. For mutagenesis of folliculin-CT, the PCR reaction mixture contained 1 µL of template DNA (5 ng and 25 ng), 1 µL of forward primer (10 µM), 1 µL of reverse primer (10 µM), 1 µL of dNTPs (100 mM), 1 µL of P*fu* Turbo Polymerase (2 U), 5 µL of 10x reaction buffer and 40 µL of Milli Q water. The PCR cycles comprised of 1 cycle of 95^{o}C for 30 sec and 16 cycles of 95^{o}C for 30 sec, 55^{o}C for 1 min, and 68^{o}C for 8 min 20 sec. For the mutagenesis of full length folliculin, the PCR reaction mixture contained 1 µL of template DNA (100ng), 1.5 µL of forward primer (10µM), 1.5 µL of reverse primer (10µM), 1 µL of dNTPs (100 mM), 1 µL of P*fu* Turbo Polymerase (2 U), 5 µL of 10x P*fu* reaction buffer and 39 µL of Milli Q water. The PCR cycles comprised of 1 cycle of 94^{o}C for 2 min and 16 cycles of 94^{o}C for 30 sec, 55^{o}C for 1 min, and 68^{o}C for 14 min. Following the PCR, the reactions were treated for 1 hr with 1 µL *DpnI* restriction enzyme at 37^{o}C to remove methylated DNA. Subsequently, 1µL of the treated reaction was transformed into XL1-Blue Super-competent *E. coli* (DH5α for the full length folliculin reaction) and plated onto LB Agar plates with 100 µg/mL of Ampicillin. The Plates were incubated at 37^{o}C over night to facilitate the growth of bacterial colonies. A few colonies from each plate were sub-cultured into 5 mL LB broth medium with Ampicillin. The DNA from the cultures was extracted using Qiagen Miniprep kit and the DNA sequence was verified for the desired mutations. The following primers were used for mutagenesis: Cys 454 Ala forward primer CTC CAC CCT GTG GGG GCT GAG GAT GAC CAG TCT and Cys 454 Ala reverse primer AGA CTG GTC ATC CTC AGC CCC CAC AGG GTG GAG; Cys 503, 506 Ala forward primer GAT GTG GTG GAC CAG GCC CTC GTC GCC CTC AAG GAG GAG TGG and Cys 503, 506 Ala reverse primer CCA CTC

CTC CTT GAG GGC GAC GAG GGC CTG GTC CAC CAC ATC. The following primers were used for mutagenesis of the Lys 485 Ala forward primer CAC CAT CCT GAA TGC GAT TGA AGC GGC and Lys 485 Ala reverse primer CAG AGC CGC TTC AAT CGC ATT CAG GAT G.

Crystallization

Initially, the crystallization trials were set up with 5 mg/mL folliculin-CT using 96 well crystallization plates (Griener, UK) and JCSG Crystal Screen (Molecular Dimensions, UK) and incubated at 12^{o}C. Initial crystals appeared over night in condition H9 which corresponds to 0.2 M $LiSO_4$, 0.1 M Bis-Tris pH 5.5, and 25% PEG 3350 (henceforth referred to as the 'mother liquor'). The crystals were reproduced by optimizing the mother liquor using vapor diffusion method and Linbro plates. Crystals were harvested in cryo-protectant solution containing 30% Polypropylene Glycol (PPG, Sigma, UK) along with the original mother liquor using crystallization loops (Hampton Research Inc, USA and stored in liquid nitrogen). To obtain crystals with GTP bound, the protein solution at the 5 mg/ml was mixed with 5 mM GTP (Sigma, UK), and 10 mM $MgCl_2$ and a 1:1 ratio of protein mixture with the above mentioned mother liquor. The drops were equilibrated for 2h before they were seeded with the native crystal seed stock. The seed stock was prepared by harvesting a single crystal and mixing it with 250 µL of mother liquor and mixing vigorously using a vortex and subsequently was stored at -20^{o}C.

Structure determination

Initial structure of folliculin-CT was determined by collecting multi-wavelength anomalous diffraction data (MAD) from selenomethionine crystals by exploiting the anomalous signal of the incorporated selenium at Diamond Light source beam line I02. Three data sets corresponding to the peak, inflection and remote energies for selenium were acquired on a single folliculin-CT crystal. The data for selenium peak was collected at 12,657.42 eV (λ = 0.9796Å), the inf lection data was collected at 12,656.42 eV (λ = 0.9797 Å) and finally the remote data was collected at 12700.42 eV(λ = 0.9763 Å). The diffraction data were processed in Imosflm[S1] and merged in SCALA[S2] of CCP4i[S3]. The positions of the selenium atoms in the asymmetric unit were determined in PHENIX[S4], and used as for the phasing calculations in AUTOSOL wizard of PHENIX. The solvent-modified map calculated by AUTOSOL was interpreted by AUTOBUILD wizard which

produced an almost complete model of the structure. Refinement of the structure was carried out in REFMAC5[S5], together with minor manual protein structure rebuilding in COOT[S6]. It was observed that the electron density was missing in the following regions: residues 341-344 in both chain A and B (gstgsRK); residues 443-458 (in chain A) and 447-459(in chain B); residues 469-477 in chain B only; residues 523-528 (chain A) and 523-527 (chain B); residues 557-568 (chain A and chain B). Hence, it was not possible to build these regions. Subsequently, higher resolution data to 1.9 Å resolution using native protein crystals were collected at Diamond Light Source beam line I03. The final structure of apo-form folliculin-CT at 1.9 Å was obtained by using PHASER_MR[S7] module of CCP4i suite by combining the original model built at 2.7 Å and the electron density maps from the native data. To improve the residual R and R_{free} the initial refined structure was used to generate a two segment TLS (translation/libration/screw) model using the TLSMD server (TLS motion determination) [S8, S9]. The resultant TLS parameters were used in further refinement to obtain the final R/R_{free} values of 0.21/0.27 respectively with Ramachandran statistics showing that 363 residues are present in the preferred regions (98.64%), 4 residues in allowed regions (1.09%) and 1 outlier (0.27%). The diffraction data for the determination of the structure of folliculin-CT nucleotide-bound complex were collected at Swiss Light Source beamline PX III. The structure was determined by the molecular replacement method using PHASER_MR and folliculin protomer from the apo-form as the search model. The structure solution from PHASER_MR was refined using BUSTER[S10] and additional electron density in a region near the NKIE peptide (aa 484-487) was observed. Into this additional density, a GDP molecule was fitted and the structure was refined further using BUSTER. The Ramachandran statistics for the nucleotide bound folliculin-CT structure shows that 365 residues (97.59%) were in the preferred regions, 4 (1.07%) were in allowed regions and 5 (1.34%) were outliers. The final R/R_{free} values were 0.22/0.29 respectively.

Immuno-precipitation

FLAG tagged FLCN wild type, C1844G mutant and K485A constructs were transfected into HEK 293T cells using FuGENE 6 (Roche Applied Science) according to manufacturer's protocol. Cells were lysed in 50 mM Tris-HCl (pH 7.4), 120 mM NaCl, 5% glycerol, 0.5% TritonX-100, complete protease inhibitor cocktail (Roche Applied

Science) lysis buffer. The soluble portions were immuno-precipitated at 4°C for 3 hr with anti-FLAG M2 beads (Sigma Aldrich). Immuno-precipitates were washed three times with 50 mM Tris-HCl (pH 7.4), 120 mM NaCl, 0.5% TritonX-100, complete protease inhibitor cocktail (Roche Applied Science) followed by elution with 3x FLAG-peptide (Sigma Aldrich) at a final concentration of 150 ng/µl for 30 min on ice while gently shaking. Eluted protein was diluted with sample buffer followed by boiling and subjected to SDS-PAGE. Protein expression levels were viewed by staining the SDS-PAGE gels with colloidal blue staining kit (Invitrogen) according to manufacturer's protocol.

GTP Cross-linking

The α-^{32}P labeled nucleotides were cross linked using UV light. In the assay, 0.3 µL of 10 µCi/µl of radioactivity was used for each cross linking reaction. In all reactions, 5 µg of FLCN protein and BSA (negative control) were used. The complexes were then boiled in SDS sample buffer and resolved by SDS-PAGE.

GTPase activity assay

Protein (0.05ug - 4ug) was incubated with 1 µM γ - ^{32}P GTP (10 Ci/mmol) at 37^{o}C for 1h or 2h. Following incubation, equal volume of 25 mM EDTA was added to each sample. Inorganic phosphate and γ - ^{32}P GTP were separated by thin layer chromatography technique as described previously by Lorsch and Herschlag[S11] (1998), with the exception of using 0.8 M acetic acid and 0.8 M $LiCl_2$ as a running buffer. The chromatograms were quantified using a Fujix BAS 2000 phosphor-imager with a Fuji imaging screen. The fraction of Pi at t=0 was typically 1-3% and subtracted as background.

Acknowledgements

The authors would like to thank Julia Forman and Cat Donaldson for carrying out initial bioinformatic analysis and initial cloning of folliculin domains respectively. The authors would like to thank the Myrovlytis Trust for their funding to R.K.N. and A.G., D.Y.C and T.L.B are funded by the Wellcome Trust.

References

1. Adley, B. P, Smith, N. D, Nayar, R, Yang, X. J. Birt-Hogg-Dubé syndrome: clinicopathologic findings and genetic alterations. Arch Pathol Lab Med. **130**, 1865-1870 (2006)

2. Murakami, T, Sano, F, Huang, Y, Komiya, A, Baba, M, Osada, Y, Nagashima, Y, Kondo, K, Nakaigawa, N, Miura, T, Kubota, Y, Yao, M, and Kishida T. Identification and characterization of Birt-Hogg-Dubé associated renal carcinoma. J. Pathol. **211 (5)**, 524-31 (2007)

3. Baba, M, Hong, S, Sharma, N, Warren, M. B, Nickerson, M. L, Iwamatsu, A, Esposito, D, Gillette, K. W, Hopkins III, R. F, Hartley, J. L, Furihata, M, Oishi, S, Zhen, W, Burke Jr, T. R, Linehan, W. M, Schmidt, L. S and Zbar, B. Folliculin encoded by the BHD gene interacts with a binding protein, FNIP1, and AMPK, and is involved in AMPK and mTOR signalling. Proc. Natl. Acad. Sci. **103 (42)**, 15552-15557 (2006)

4. Schmidt, L. S, Nickerson, M .L, Warren, M. B, Glenn, G. M, Toro, J. R, Merino, M. J, Turner, M. L, Choyke, P. L, Sharma, N, Peterson, J, Morrison, P, Maher, E. R, Walther, M. M, Zbar, B, Linehan, W. M. Germline BHD-mutation spectrum and phenotype analysis of a large cohort of families with Birt-Hogg-Dubé syndrome. Am. J. Hum. Genet. **76 (6)**, 1023-33 (2005)

5. Takagi, Y, Kobayashi, T, Shiono, M, Wang, L, Piao, X, Sun, G, Zhang D, Abe, M, Hagiwara, Y, Takahashi, K and Hino, O. Interaction of folliculin (Birt-Hogg-Dubé gene product) with a novel Fnip1-like (FnipL/Fnip2) protein. Oncogene. **27,** 5339–5347 (2008)

6. Cheung, P.C.F, Salt, I.P, Davies, S.P, Hardie, D. G, and Carling, D. Characterization of AMP-activated protein kinase g-subunit isoforms and their role in AMP binding. Biochem. J. **346**, 659-669 (2000)

7. Chan, A.Y.M., and Dyck, J. R. B, Activation of AMP-activated protein kinase (AMPK) inhibits protein synthesis: a potential strategy to prevent the development of cardiac hypertrophy. Can. J. Physiol. Pharmacol. **83**, 24–28 (2005)

8. Gwinn, D. M, Shackelford, D. B, Egan, D.F, Mihaylova, M. M, Mery , A, Vasquez, D.S, Turk, B. E, and Shaw, R. J. AMPK phosphorylation of raptor mediates a metabolic checkpoint. Mol. Cell. **30 (2)**, 214-226 (2008)

9. Hasumia, Y, Babaa, M, Ajimab, R, Hasumia, H, Valeraa, V. A, Kleina, M. A, Hainesc, D.C, Merinod, M. J, Honga, S, Yamaguchib, T. P, Schmidt, L. S, and Linehan, W. M. Homozygous loss of BHD causes early embryonic lethality and kidney tumor development with activation of mTORC1 and mTORC2. Proc. Nat. Acad. Sci. **106 (44)**, 18722-18727 (2009)

10. van Slegtenhorst, M, Khabibullin, D, Hartman, T. R, Nicolas, E, Kruger, W. D and Henske, E. P. The Birt-Hogg-Dube and tuberous sclerosis complex homologs have opposing roles in amino acid homeostasis in Schizosaccharomyces pombe. J. Biol. Chem. **282 (34)**, 24583-90 (2007)

11. Chen, J, Futami, K, Petillo, D, Peng, J, Wang, P, Knol, J, Li, Y, Khoo, S. K, Huang, D, Qian, C. N, Zhao, P, Dykema, K, Zhang, R, Cao, B, Yang, X. J, Furge, K, Williams, B. O, and Teh, B. T. Deficiency of FLCN in mouse kidney led to development of polycystic kidneys and renal neoplasia. PLoS One **3(10)**, e3581 (2008)

12. Hudon, V, Sabourin, S, Dydensborg, A. B, Kottis, V, Ghazi, A, Paquet, M, Crosby, K, Pomerleau, V, Uetani, N, and Pause, A. Renal tumour suppressor function of the Birt-Hogg-Dubé syndrome gene product folliculin. J. Med. Genet. **47(3)**, 182-9 (2009)

13. Cole, C, Barber, J. D and Barton, G. J. The Jpred 3 secondary structure prediction server. Nucl. Acids Res. **36 (2),** W197-W201 (2008)

14. Ward, J. J, McGuffin, L. J, Bryson, K, Buxton, B. F. and Jones, D. T. The DISOPRED server for the prediction of protein disorder. Bioinformatics **20 (13)**, 2138-2139 (2004)

15. Thompson, J. D, Gibson, T. J, and Higgins, D. G. Multiple sequence alignment using ClustalW and ClustalX. Curr. Protoc. Bioinformatics **Chapter 2, Unit 2.3**, 2.3.1-2.3.22 (2003)

16. Holm L and Rosenström, P. Dali server: conservation mapping in 3D. Nucl. Acids Res. **38**, W545-549 (2010)

17. http://www.ncbi.nlm.nih.gov/Structure/VAST/vast.shtml

18. Savvides, S. N, Yeo, H. J, Beck, M. R, Blaesing, F, Lurz, R, Lanka, E, Buhrdorf, R, Fischer, W, Haas, R, Waksman, G. VirB11 ATPases are dynamic hexameric assemblies: new insights into bacterial type IV secretion. EMBO J. **22 (9)**, 1969-80 (2003)

19. Sarkar, G, Edery, I, and Sonenberg, N. Photoaffinity labeling of the cap-binding protein complex with ATP/dATP. Differential labeling of free eukaryotic initiation factor 4A and the eukaryotic initiation factor 4A component of the cap-binding protein complex with [alpha-32P] ATP/dATP. J Biol Chem. **260 (25)**, 13831-7 (1985)

20. Leipe, D. D, Wolf, Y. I, Koonin, E. V. and Aravind, L. Classification and Evolution of P-loop GTPases and Related ATPases. J. Mol. Biol. **317**, 41-72 (2002)

21. Tong, L. A, de Vos, A. M, Milburn, M. V and Kim, S. H. Crystal structures at 2.2 A resolution of the catalytic domains of normal ras protein and an oncogenic mutant complexed with GDP. J Mol. Biol. **217 (3)**, 503-16 (1991)

22. Freymann, D. M, Keenan, R. J, Stroud, R. M and Walter, P. Functional changes in the structure of the SRP GTPase on binding GDP and Mg2+GDP. Nat. Struct. Biol. **6 (8)**, 793-801 (1999)

23. Gasper, R, Meyer, S, Gotthardt, K, Sirajuddin, M and Wittinghofer, A. It takes two to tango: regulation of G proteins by dimerisation. Nat. Rev. Mol. Cell Biol. **10**, 423-429 (2009)

Supplementary References

S1. http://www.mrc-lmb.cam.ac.uk/harry/imosflm/ver104/

S2. http://www.ccp4.ac.uk/html/scala.html

S3. http://www.ccp4.ac.uk/ccp4i_main.php

S4. Adams, P. D, Afonine, P. V, Bunkóczi, G, Chen, V. B, Davis, I. W, Echols, N, Headd, J. J, Hung, L.-W, Kapral, G. J, Grosse-Kunstleve, R. W, McCoy, A. J, Moriarty, N. W, Oeffner, R, Read, R. J, Richardson, D. C, Richardson, J. S, Terwilliger,T. C and Zwart P. H. PHENIX: a comprehensive Python-based system for macromolecular structure solution. Acta Cryst. **D66**, 213-221 (2010)

S5. Murshudov, G. N, Vagin, A. A and Dodson, E. J. Refinement of Macromolecular Structures by the Maximum-Likelihood method. Acta Cryst. **D53**, 240-255 (1997)

S6. Emsley, P and Cowtan, P. Coot: model-building tools for molecular graphics. Acta Cryst. D**60**, 2133-2143 (2004)

S7. McCoy, A. J, Grosse-Kunstleve, G. W, Adams, P. D, Winn, M. D, Storoni, L.C and Read, R.J. Phaser crystallographic software. J. Appl. Cryst. **40**, 658-674 (2007)

S8. Painter, J and Merritt, E. A. Optimal description of a protein structure in terms

of multiple groups undergoing TLS motion. *Acta Cryst.* **D62**, 439-450 (2006)

S9. Painter, J and Merritt, E. A. *TLSMD* web server for the generation of multi-group TLS models. *J. Appl. Cryst.* **39**, 109-111. (2006)

S10. http://www.globalphasing.com/buster

S11. Lorsch, J. R and Herschlag, D. The DEAD box protein eIF4A: A minimal kinetic and thermodynamic framework reveals coupled binding of RNA and nucleotide. Biochemistry **37**, 2180–2193 (1998)

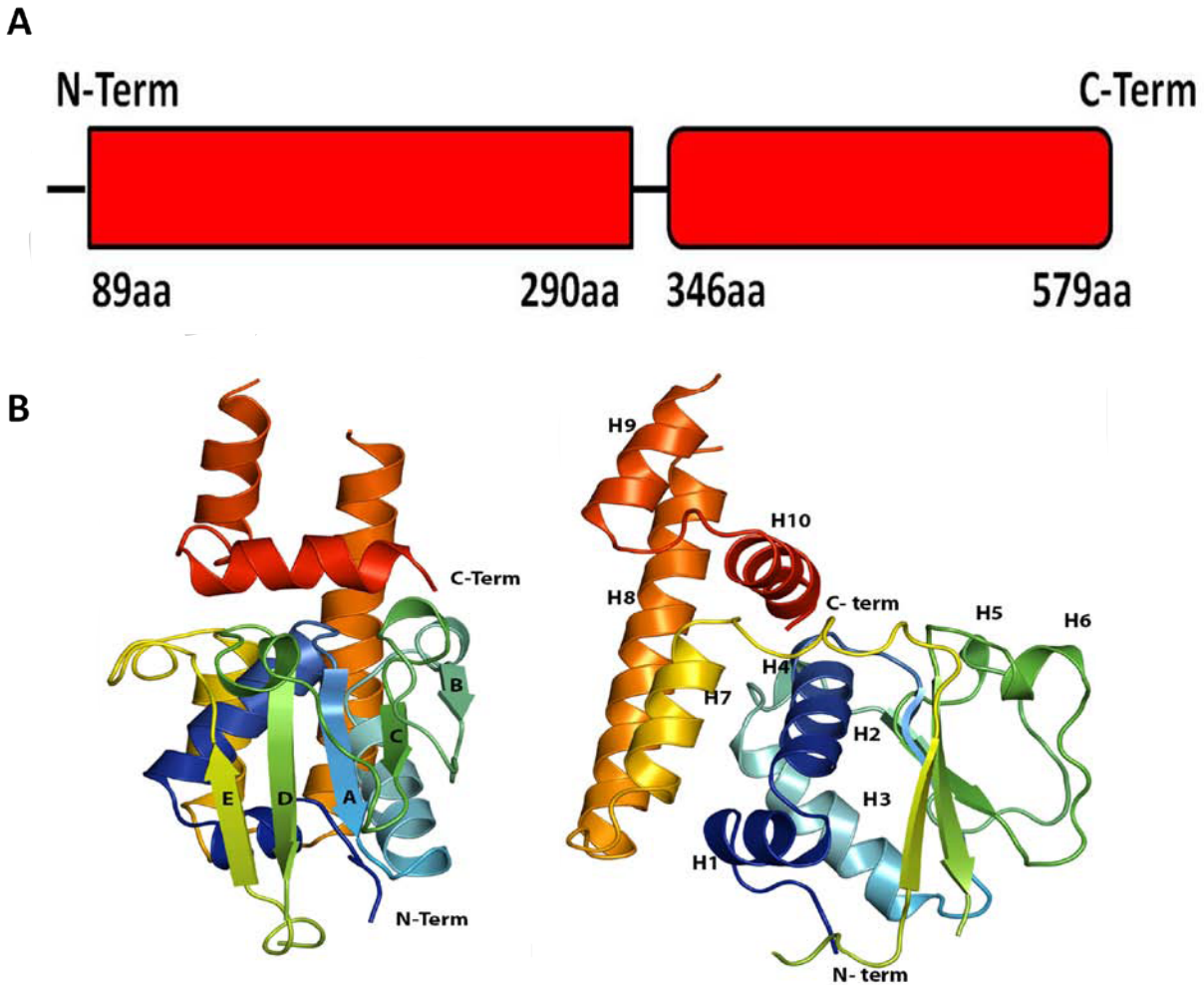

Figure 1: Domain architecture and folliculin-CT crystal structure.

A) Schematic representation of the predicted globular domain boundaries in the amino acid sequence of full length folliculin based on Jpred. The predicted globular domains represented as solid red rectangles and the regions with low secondary structure are represented by small lines.

B) Cartoon representation of the crystal structure of the folliculin-CT determined at 1.9 Å resolution. The protein chain is represented as cartoon, rainbow colored from blue at the N-terminal end to red at the C-terminal end. The front view shows the arrangement of the beta strands (labeled A-E) with the characteristic GTPase strand order E-D-A-C-B. The side view of the structure shows the ten helices (labeled H1-10) stacked onto the side of the protein.

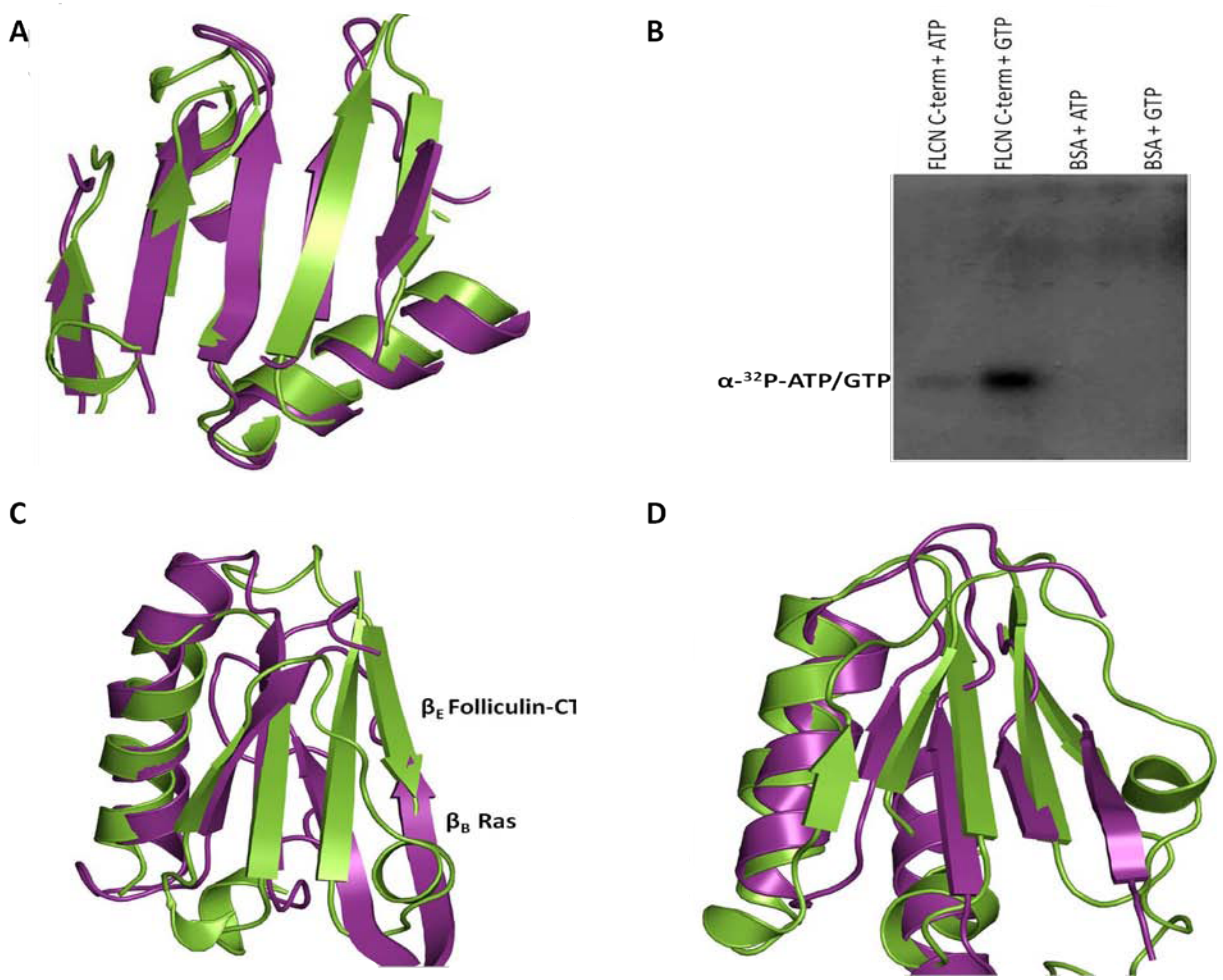

Figure 2: Folliculin binds nucleotides and shares structural similarities with NTPases.

A) Superposition with VirB11 protein (pdb id. 1NLZ) with folliculin-CT domain. The protein chains are represented as cartoon tubes with VirB11 represented in purple and folliculin-CT in green.

B) Autoradiograph of the α^{32}P-labelled ATP and GTP cross-linking using folliculin-CT and Bovine serum albumin as a negative control.

C) and D) Superposition of folliculin-CT domain with two prototypical GTPases from TRAFAC and SIMIBI class: human ras GTPase (pdb id. 1Q21) and signal recognition protein, Ffh (pdb id. 2NG1). The protein chains are represented as cartoon tubes with folliculin-CT in green and the two GTPases in purple respectively.

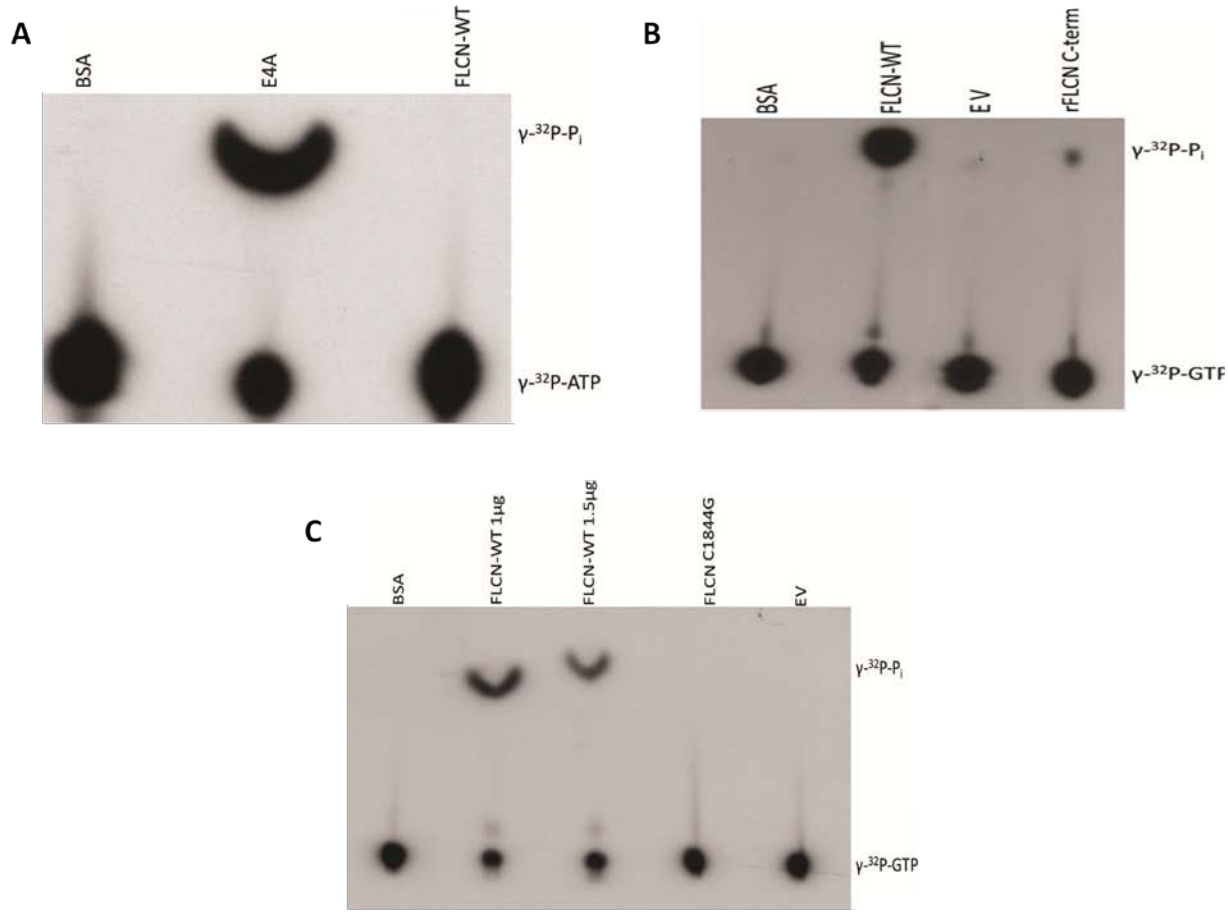

Figure 3: ATP and GTP hydrolysis assays with foliculin.

A) Autoradiograph showing thin layer chromatography of ATP hydrolysis assay. While eIF-4A a known ATPase catalyzes ATP, wild type folliculin is incapable of hydrolyzing γ - ^{32}P ATP to ADP and Pi.

B) Autoradiography of the GTPase assay showing that endogenous wild type full length folliculin and recombinant folliculin-CT exhibit GTPase activity.

C) Autoradiograph showing a patient mutation, C1844G, which results in a truncated folliculin is incapable of hydrolyzing GTP. Bovine serum Albumin (BSA) and empty vector (EV) are used are negative controls in all the assays.

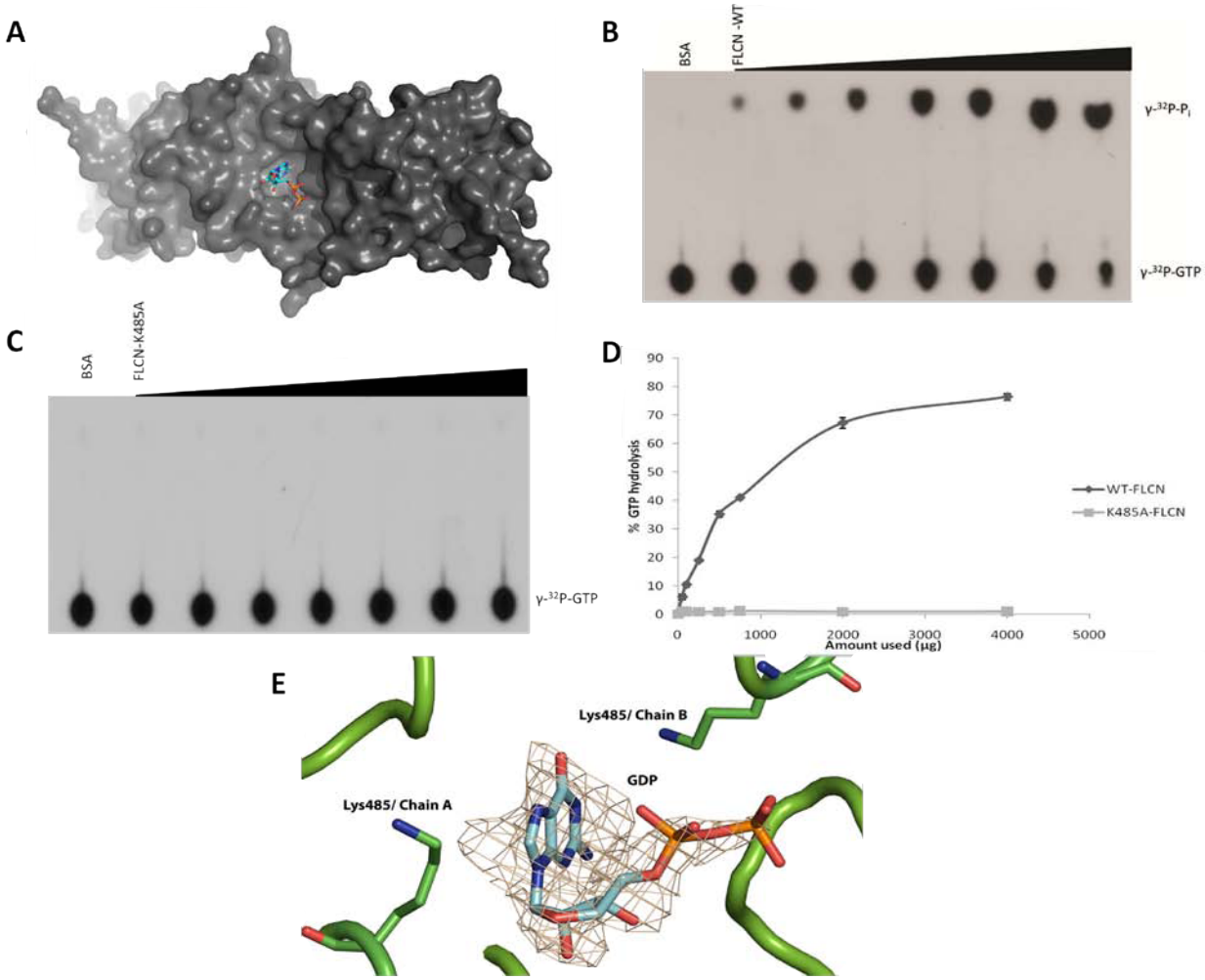

Figure 4: Co-crystal structure of folliculin-CT with GDP showing key Lysine 485 residue that is important for the GTPase activity.

A)Surface representation of the nucleotide binding pocket of folliculin-CT dimer. The protein is represented as a grey surface map and the GDP is represented as a stick model.

B)and C) Autoradiograph of the thin layer chromatography showing the protein concentration (50 ng to 4 µg) dependent GTPase activity of folliculin wild type and that the GTPase activity is completely lost as a result of lysine 485 mutation to an alanine even at very high protein concentrations (up to 4 µg of protein).

D) Quantification of the concentration dependent GTP hydrolysis by folliculin wild type and the K485A mutant. Folliclun wild type is represented by black solid diamonds and black curve and the folliculin K485A mutant is represented by solid grey squares and grey curve.

E) Electron density map ($F_o - F_c$) at 2.7 Å showing GDP molecule fitted after refinement (wheat colored mesh); also showing is the lysine 485 residues (represented as sticks) from each protomer of folliculin-CT.

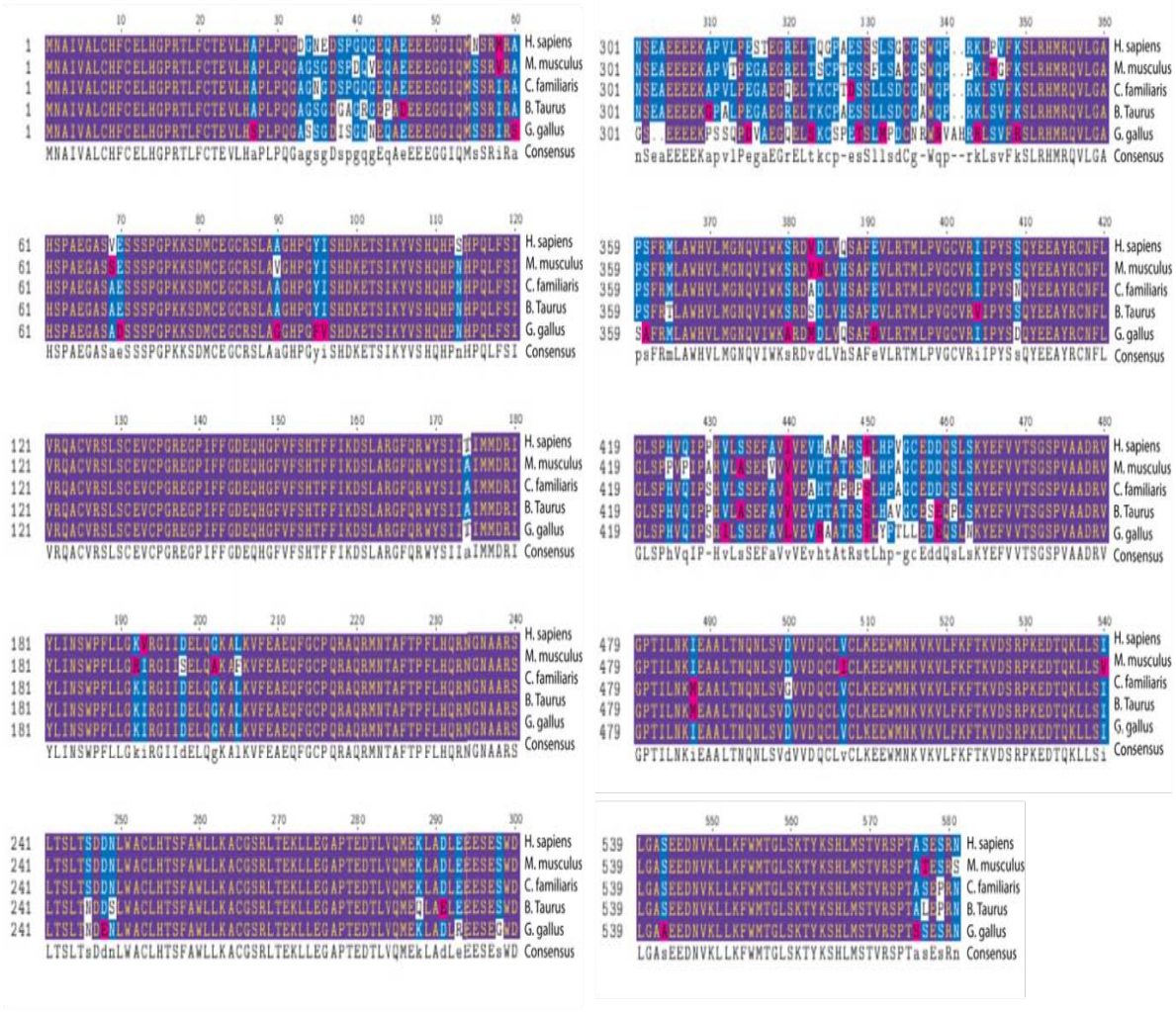

Figure S 1: Textbox representation showing the ClustalW sequence alignment of vertebrate folliculins.

The protein sequences from vertebrate folliculins including *Homo sapiens, Mus musculus*, *Canis familiaris, Bos taurus,* and *Gallus gallus* were aligned using ClustalW.

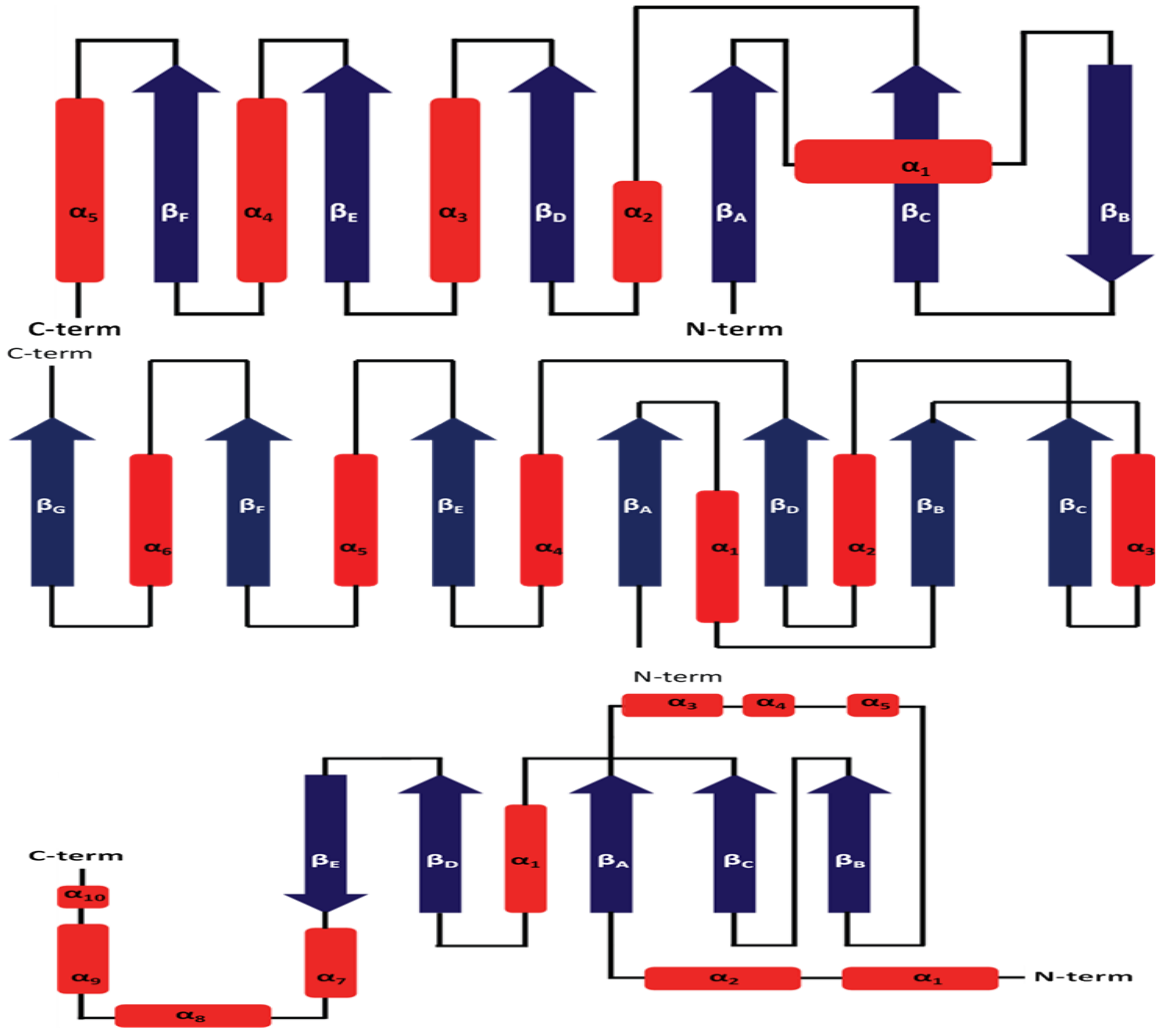

Figure S 2: Topological diagram of human ras, signal recognition protein Ffh from *T.acquaticus* and human folliculin-CT.

The α- helices in the diagram are represented by cylinders and β-strands are represented by thick arrows. The direction of the arrows indicates the direction of the β-strands.

Table 1: X-Ray data collection and refinement statistics for folliculin-CT and folliculin-CT with the bound nucleotide.

	Folliculin-CT	Folliculin-CT with GDP
Data collection		
Space group	$C222_1$	C2
Cell dimensions		
a, *b*, *c* (Å)	86.05, 99.95, 107.58	98.9, 85.41, 65.850
α, β, γ (°)	90, 90, 90	90, 125.15, 90
Resolution (Å)	1.92	2.7
R_{sym} or R_{merge}	0.22356	0.2239
$I/\sigma I$	2.6	3.9
Completeness (%)	97.43	96.93
Redundancy	4.8	2.6
Refinement		
Resolution (Å)	1.92	2.7
No. reflections	32,843	12,386
$R_{work/}$ R_{free}	0.22/0.28	0.22/0.29
No. atoms	4185	3194
Protein	3090	3089
Ligand/ion	None	1
Water	258	116
B-factors		
Protein		
Ligand/ion		
Water		
R.m.s deviations		
Bond lengths (Å)	0.022	0.009
Bond angles (°)	1.812	1.17

Chapter 2: Characterizing the Role of FLCN in *Caenorhabditis elegans* aging

Abbas Ghazi and Arnim Pause

What is aging?

A common feature of living and non living organisms is that they tend to lose their structural and functional integrity over time. In the case of non-living organisms this loss is irreversible. For example, a ship in the absence of proper maintenance will fall apart after few years of sailing in the ocean. On the other hand, shortly after birth, living organisms are capable of maintaining their structure, repair various damages to their components and sometimes further enhance their fitness in order to adapt to their environment. However, the damage repair machinery is either imperfect or requires more energy than that which is available leading to the accumulation of various deleterious damages over time causing the loss of structural and functional integrity and eventually death. This process is appropriately termed as aging.

Aging has been reported even in the simplest single-cell organisms. Under nutrient deficient conditions, prokaryotic single-cell organisms like bacteria, which were once believed to be incapable of aging, will enter a hibernation- like phase. When this stage is maintained for too long, the organism will lose their ability to recover to an optimal proliferative stage and ultimately die [1]. Moreover, in eukaryotic single-cell organisms like yeast, the mother cell has limited capacity to bud and will eventually die. The lifespan of a yeast mother cell is measured by the number of times it is able to bud [2]. With the purpose of identifying the specific genetic pathways regulating the aging process in humans, researchers have studied different organisms, including yeast, nematodes, fruit flies, mice, monkeys, and dogs in the laboratory. The importance of such studies is reflected in the fact that the incidence of many diseases increases significantly with age. Examples of such diseases are cancer, cardiovascular disease, arthritis, osteoporosis, Alzheimer's disease, type 2 diabetes, and hypertension; all of which create a major cause for concern in the medical field. These diseases can be viewed as a result of the failure to maintain a particular function during the normal aging process. Furthermore, aging is the loss of a certain function due to impaired maintenance. Intuitively, slowing or stopping the aging process should subsequently delay or stop the onset of age-related diseases.

C. elegans as a model organism for aging research

Caenorhabditis elegans is a small (1mm long), free-living, soil-dwelling nematode that can be easily cultured in a controlled laboratory environment. The first gene mutation that was identified with the ability to extend the lifespan of the worm was *age-1* in 1988 [3]. Since then, the nematode has been used as a model organism for aging studies. A quarter of a century later, loss-of-function mutations or altered function of protein produces of close to 200 genes have been reported to regulate the worm's lifespan [4]. The advantages of using the worm as a model organism in the field of developmental research are evident. Firstly, it has small size, rapid life cycle, and large number of progeny allow it to be cultured in a time effective and economical way in large-scale genetic analysis. Secondly, transgenic worm models are easily generated, allowing for the *in vivo* labeling of specific proteins using multiple fluorescent protein tags [5]. Thirdly, knowledge of the *C. elegans* complete genome greatly aids gene analysis. Fourthly, it is easy to knockdown any given gene in the *C. elegans* genome by either feeding, soaking or injecting double-stranded RNA for efficient genome wide screens and the use of reverse genetic approaches [6]. Also, the transparency of the worm cuticle allows for *in vivo* imaging of cells using differential interference contrast microscopy. Lastly, it has a short lifespan (2-3 weeks) which makes it an ideal model organism for aging research.

Genetics of aging in *C. elegans*

Insulin/ *IGF-1* signalling (IIS) pathway

Under optimal growth conditions, insulin is produced to promote the synthesis of various macromolecules such as proteins, carbohydrates and lipids. The IGF-1 (DAF-2 in *C. elegans*) receptor consists of two β transmembrane subunits with tyrosine kinase activity and two extracellular α subunits that bind insulin. The binding of insulin initiates auto and trans-phosphorylation between the β subunits, leading to an increase in the kinase activity of the receptor towards other downstream protein substrates [7]. This results in the immediate activation of PI-3 kinase (PI3K). PI3K is composed of an adaptor protein, AAP-1, and a catalytic subunit, AGE-1, and it catalysis the phosphorylation of PIP_2 to PIP_3 [8]. The reverse reaction is catalyzed by DAF-18 phosphate. PIP_3 binds the plextrin domain of PDK-1, thus activating it to phosphorylate the downstream serine/ threonine kinases AKT-1, AKT-2 and SGK-1[9]. These kinases

phosphorylate several key effectors that play a role in growth, apoptosis, cell cycle and metabolism [10]. One of downstream targets is a FOXO forkhead transcription factor (DAF-16) which upon phosphorylation is transported from the nucleus to the cytosol, preventing it from subsequently altering gene transcription [11].

Under stressful or sub-optimal growth conditions, the insulin signalling must be reduced to shut down biosynthetic pathways in order to conserve energy recourses. Both the L1 and dauer diapauses in C. *elegans* are characterized by reduced insulin like signalling, resulting in multiple defects such as abnormal metabolism and tissue hyperplasia [12, 13]. In addition to cell metabolism and growth, insulin signaling is involved in the survival of cells and organisms. Thus, *C. elegans* mutations that decrease the activity of *daf-2* and *age-1* and those affecting the downstream PI3K/AKT/PDK kinase cascade result in a more than two-fold increase in the lifespan of the animal [3, 14]. The change in the lifespan is mediated by alterations in gene expression through three downstream targets of the insulin signalling pathway: the DAF-16 transcription factor; the heat-shock transcription factor HSF-1; and SKN-1 (Nrf-like response factor) [14, 15]. These transcription factors regulate the expression of multiple downstream stress-response genes such as glutathione S-transferase, methallothioneinsm, Catalases, chaperones, apolipoproteins, lipases, channels and multiple genes encoding antimicrobial peptides [16-20]. The regulation of lifespan by insulin signalling occurs in a cell non-autonomous fashion. Thus, the presence of a limited number of cell types with reduced insulin signalling is sufficient to increase the worms lifespan [21]. For example, reduced insulin signalling in the nervous system and the intestine appears to play the most critical regulation of lifespan [22, 23]. Therefore, increasing the activity of DAF-16 in just one tissue can increase its activity elsewhere and this is through a feedback regulation of the insulin gene expression [24]. In addition to DAF-16, both SKN-1 and HSF-1 transcription factors are able to affect lifespan by influencing cells other than those in which they act [16, 25].

Among all the genetic pathways involved in lifespan extension (discussed below), the insulin signalling pathway seems to be evolutionarily highly conserved since homologs of the upstream and downstream components of the signalling cascade have been shown

to affect lifespan in yeast, fruit flies, mice, dogs and humans [16, 26]. In *Drosophila*, over-expressing FOXO (homolog of DAF-16) in the adipose tissues or inhibiting the insulin/ IGF-1 signalling results in an extension of lifespan. Similar to the *C.elegans* DAF-16, the *Drosophila* FOXO acts in a cell non-autonomous fashion, highlighting the conservation of this longevity regulation. Mutations reducing the activity of the insulin receptor, IGF-1 receptor, upstream and downstream components of the insulin/IGF-1 signalling pathway result in lifespan extension among inbred cohorts of mice [26-29]. Moreover, smaller dogs with mutations in the IGF-1 receptor live longer than larger dogs. In humans, mutations that impair the function of the insulin and IGF-1 receptors have been linked to longevity in Japanese and Ashkenazi Jewish cohorts respectively. It is important to mention that variants of AKT, FOXO3A and FOXO1 are more frequent in centenarians than ninety year olds in three, seven and two human cohorts respectively [30-36].

Dietary restriction

Different environmental and physiological stressors mediate lifespan extension among various species. Dietary restriction (DR), which is defined as the limitation of food intake without malnutrition, is the most effective environmental stressor that results in the extended lifespan of organisms ranging from yeast to rodents. Furthermore, even complete food starvation can lead to longevity in *C. elegans* [37-39]. Throughout the last decade, more evidence has been shown to support the notion that different techniques of DR induce different signalling pathways necessary to affect lifespan [40]. The longevity response to DR is mediated by multiple nutrient sensing pathways involving the kinase target of rapamycin (TOR), insulin/IGF-1 signalling, sirtuins, and AMP kinase [41-47]. The way that DR is imposed (liquid media, *eat-2* mutants, every-other-day feeding, weak *eat-2* mutants, and food limitation starting middle age) determines which of the above nutrient sensor pathways is activated or repressed leading to lifespan extension.

1.1 Chronic limitation of food intake

The first DR method discussed in this section is the *eat-2* mutant worms that carry mutations causing reduction in pharyngeal pumping leading to decreased eating rate. This mimicks DR by living in a state of chronic limitation of food intake leading to lifespan extension [48, 49]. The inhibition of TOR has been shown to be required for the DR-

induced longevity of *eat-2* mutants as TOR reduction does not further extend the *eat-2* mutant lifespan [50]. TOR is a highly conserved serine/threonine protein kinase which acts as a master regulator of protein translation. Under optimal growth conditions, TOR up-regulates translation by activating the ribosomal subunit S6 Kinase (S6K) and inhibiting 4E-BP (a translation inhibitor). PHA-4/ FOXA, a forkhead transcription factor plays a critical role in the extension of longevity induced by chronic limitation of food intake [50]. PHA-4/FOXA is required for lifespan extension by inhibition of TOR induced by DR. Thus, when the expression of the PHA-4 target genes is down-regulated, *eat-2* mutant worms live shorter under chronic limitation of food intake and inactivation of *let-363* (homolog of *TOR* in *C.elegans*). Moreover, activation of PHA-4 promotes longevity by increasing the expression of a set of reactive oxygen species (ROS) resistance genes (*sod-1, sod-2, sod-4* and *sod-5*) [50]. PHA-4 activation is also required for autophagy response induced by the inhibition of TOR in *eat-2* mutants leading to prolonged lifespan [51]. Interestingly, activation of SKN-1 (Nrf-like) transcription factor leads to longevity in response to chronic limitation of food intake. However, its relationship with *let-363* has not been tested. In another DR method, in which food is restricted in liquid medium, activation PHA-4 transcription factor is required for lifespan extension [50]. Furthermore, expression of SKN-1 in two sensory neurons is also required for lifespan extension induced by this DR regime [25]. Interestingly, SKN-1 was shown to function by increasing oxygen consumption due to elevated respiration rates in *C.elegans* [25].

2.1 Mild chronic food limitation

Weak *eat-2* mutations can induce longevity due to a mild chronic food limitation DR method. The increase in lifespan of these mutants requires a functional *sir-2.1* gene and is independent of *let-363* [52]. It is important to note that all other known modes of DR in the worm are capable of extending the lifespan of *sir-2.1* mutants, suggesting that SIR-2.1 activity is specifically required for the mild chronic DR method [40, 43]. *sir-2.1* is the *C.elegans* ortholog of the yeast *sir2,* which was initially identified as a key regulator of lifespan replication [53]. Sirtuins are a family of NAD-dependent protein deacetylases whose overexpression has been reported to extend lifespan in yeast, worms, and flies [16]. In *C.elegans,* over-expression of *sir-2.1* extends lifespan by directly activating

DAF-16 transcription factor through deactylation [54]. Moreover, oxidative stress induces the binding of SIR-2.1 to DAF-16, which extends the lifespan in a *sir-2.1*- and *daf-16*- dependent manner [55]. However, the insulin/IGF-1 signalling mutants don't require the expression of *sir-2.1* for longevity, which strongly suggests that the regulation of DAF-16 by SIR-2.1 is independent of the insulin/IGF-1 pathway. The deactylation of FOXO proteins by SIRT1 in response to oxidative stress and the subsequent increase in stress resistance was reported in mammalian systems, suggesting a functional conservation of sirtuins across species [16].

3.1 Food limitation starting in the middle age

AMP-activated protein kinase (AMPK) is a master metabolic switch that is activated in response to energy deprivation (high AMP/ATP ratio). Upon its activation, AMPK down-regulates biosynthetic pathways and activates alternative catabolic pathways to restore the energy balance in all eukaryotic organisms. A third dietary restriction method involves feeding the worms diluted concentrations of OP50 bacteria starting from middle age [47]. This food limitation starting in the middle age extends lifespan in the worms by activating the AMPK catalytic subunit (AAK-2), which in turn activates DAF-16 through direct phosphorylation [47]. Activation of DAF-16 induces stress resistance by stimulating a set of superoxide dismutase genes (*sod-1*, *sod-3* and *sod-5*) [47, 50]. The regulation of DAF-16 by AAK-2 in this DR method is independent of the insulin/IGF-1 signalling pathway [56]. In fact, this AMPK pathway is also unnecessary for the extension of lifespan achieved by the chronic food limitation method of DR (*eat-2* mutants). In support of this finding is that the PHA-4/FOXA and SKN-1 transcription factors which are required for chronic food limitation longevity are not required for the lifespan extension induced by food limitation starting middle age [40]. Therefore, it seems that the longevity of *C.elegans*, is not only a result of the quantity of food that they are given but it is also a result of the temporal control of the food limitation.

4.1 Every-other-day feeding

The last method of DR involves feeding the worms every-other-day. Lifespan extension induced by this DR mode is due to inhibition of the insulin/ IGF-1 singalling which is dependent on the downstream transcription factor DAF-16 [45]. Indeed, every-other-day feeding does not further extend the long lifespan of the *daf-2* mutants and other

components of the insulin/ IGF-1 pathway. Interestingly, the longevity phenotype induced by this DR method requires the activity of the small GTPase RHEB-1 and partially requires the activity of TOR, which is a known RHEB-1 target [45]. Thus, different dietary restriction (DR) modes induce independent nutrient/sensory signalling pathways leading to the extension of the *C.elegans* lifespan. Furthermore, while many of these DR methods have been shown to induce longevity in flies and mice the unanswered question remains whether or not calorie restriction is able to slow down the aging process in higher organisms such as humans.

Protein translation

The process of protein translation is tightly regulated by various factors that can sense nutrient levels and energy levels. The master regulator of protein translation is the mammalian target of rapamycin (TOR) kinase which is highly conserved across species. Under nutrient limitation, TOR is down-regulated leading to inhibition of protein synthesis [57]. This occurs by reducing the phosphorylation of S6K which leads to the dephosphorylation and subsequent inactivation of the small ribosomal subunit protein S6 (rpS6) and the translation elongation factor (eEF2) kinase [58]. Moreover, down-regulation of TOR reduces the phosphorylation of translation initiation factor 4 binding proteins (eIF4-BP) thereby allowing it to bind to eIF4E. Consequently, the recruitment of the 40S ribosomal subunit to the cap structure at the 5'-end of the mRNA is impaired, resulting in protein translation inhibition [59-61].

In *C.elegans*, inhibition of global protein translation has been shown to extend lifespan. A knockdown of *let-363* (ortholog of *TOR*) by RNAi feeding extends the adult lifespan 1.5 fold in comparison to its wild type counterpart [43, 62-64]. Heterozygous mutants of *daf-15* (ortholog of RAPTOR) also leads to increased longevity [65]. Furthermore, knocking down three translation initiation factors (homologs of eIF4E, eIF4G and eIF2β), ribosomal proteins or *rsks-1* (ortholog of S6K) extends the adults nematode lifespan [43, 62, 66]. Interestingly, the observed lifespan extension due to the down-regulation of translation initiation factors is *daf-16* dependent, whereas lifespan extension due to down-regulation of ribosomal proteins, *rsks-1* and *let-363* is *daf-16* independent [43]. Moreover, the lifespan extension stimulated by inhibiting various components of the

protein translation machinery is due to a switch from a state of optimal growth to a state of cell maintenance and increased stress resistance (thermal stress or oxidative stress) [43]. The inhibition of the global protein translation mechanism leading to longevity has been shown to be conserved across species from yeast to mice. Therefore, inhibiting the TOR pathway also leads to lifespan extension in yeast, flies and mice [42, 44, 67]. One of the most studied components of the TOR pathway is the downstream ribosomal kinase S6K. Multiple studies have shown that inhibition of S6K extends lifespan in yeast, flies and mice due to reduction in protein synthesis [42, 44, 68].

Mitochondrial dysfunction and ROS production

Mitochondria have always been known as the "power house" of the cell. They control essential processes involved in organismal aging such as cellular energy levels (ATP production), apoptosis, and reactive oxygen species (ROS) production/detoxification.[69]. In *C.elegans*, a knockdown or complete inhibition of gene expression of the various components of the electron transport chain (ETC) can either shorten or extend lifespan. The focus in this section will be on the mitochondrial dysfunction mutants that have increased lifespan phenotype.

Genetic studies in *C.elegans* presented the first evidence that different components of the ETC modulate organismal aging. The first loss-of-function mutation involved in the ETC that was found to extend lifespan up to 40% was in the gene *clk-1* [70]. *clk-1* encodes a mitochondrial hydroxylase (CLK-1) that is required for the biosynthesis of ubiquinone, which is essential for the shuttling of electrons from Complexes I and II to Complex III during respiration [71, 72]. However, the respiration levels in the *clk-1* mutants are not drastically lowered due to the supplementary Q_8 obtained from the bacterial diet that they feed on [71, 73-75]. The mechanism by which *clk-1* extends lifespan has been shown to be independent of the insulin/IGF-1 pathway. However, it might act in the chronic limitation of food intake (DR) pathway as the *clk-1* mutant doesn't further extend the long-life of the *eat-2* worms [49, 70]. Moreover, reduced activity of the mouse MCLK1 (ortholog of CLK-1) has been shown to extend the lifespan of mice, suggesting a strong functional and phenotypic conservation across species [76]. Another ETC mutant that was found to extend the lifespan of worms (by approximately

75%) was *isp-1(qm150)*[77]. *isp-1* encodes an iron-sulfur protein (ISP-1) of the mitochondrial complex III [77]. The effect of the *isp-1* mutant on lifespan is partially due to *daf-2* since the lifespan of the double mutant does not result in a synergistic effect. This might be due to the fact that both mutants affect a common downstream pathway or modify ROS metabolism [77]. However, the mechanism by which the *isp-1* mutant extends lifespan is still unclear. Knocking down *nuo-2* (subunit of Complex I), *cco-1* (subunit of Complex IV) and *atp-3* (subunit of complex V) by feeding RNAi in *C.elegans* led to lifespan extension due to reduced mitochondrial respiration [78]. On the other hand, mutations in various components of the ETC have the opposite phenotype. Deletion mutants in *nuo-1* (encodes NADH Ubiquinone Oxidoreducatase) are embryonic lethal, point mutations in *mev-1* (encodes succinate dehydrogenase subunit C) and *gas-1* (encodes an irons protein subunit of Complex I) shorten lifespan. This discrepancy could be explained by the level to which the mitochondrial function is being impaired. If the mitochondrial function is impaired to a certain extent, the animals will compensate for this functional defect by activating multiple stress response pathways (oxidative stress or thermal stress responses), resulting in longevity. However, if the damage to the mitochondrial function reaches a certain threshold then this leads to shorter lifespan or lethality during or post-embryogenesis [79]. To this date, the stress response mechanisms affected by knocking down mitochondrial genes are not well characterized. Interestingly, autophagy was recently proposed to contribute to the lifespan extension upon down regulating the expression of multiple components of the ETC [80].

Many studies in *C.elegans* have focused on the effects of ROS and oxidative stress on organismal aging. Anti-oxidant enzymes (such as superoxide dismutases and catalase) act to reduce the harmful effects of elevated levels of ROS on DNA and proteins. Elevated levels of these enzymes have been reported in many of the long-lived mutants which indicate increased stress resistance. For instance, catalase genes are up-regulated in *daf-2* mutants, *age-1* mutants, *eat-2* mutants, *clk-1* mutants, and upon inhibition of glycolysis in WT (N2) animals leading to lifespan extension [19, 81, 82]. Furthermore, elevated levels of *sod-3* have been reported in *daf*-2 mutants, *isp-1* mutants, *eat-2* mutants and DR method starting middle age leading to lifespan extension [22, 47, 50, 77]. Interestingly, while *daf-2* mutants have increased resistance to oxidative stress and decreased oxidative

damage, they were found to have higher levels of ROS compared to wild type counterparts [83, 84]. Similarly, inhibiting glycolysis by treating worms with 2-deoxyglucose results in an increase in ROS levels as well as an increase in oxidative stress resistance leading to lifespan extension [19]. On the other hand, the short-lived mitochondrial mutants (*mev-1* and *gas-1*) have elevated levels of ROS, high sensitivity to treatment with paraquat (pro-oxidant) and increased oxidative damage [73, 85]. Another approach used to test the effect of ROS on aging was to suppress anti-oxidant enzymes and score for organismal lifespan thereafter. Increasing oxidative stress by knocking out *sod-1* or *ctl-2* (catalase) leads to a shorter nematode lifespan (up 30% less in *sod-1* mutants and 16% less in *ctl-2* mutants) [86, 87]. Moreover, under certain conditions, the use of SOD mimics (compounds with SOD activity such as Euk-134 and Euk-8) increases resistance to oxidative stress resulting in a lifespan increase [88]. Treatment with Pt-nano (platinum nanoparticles which have a SOD/catalase activity), leads to a 20% increase in *C.elegans* lifespan. These animals are less sensitive to treatment with paraquat suggesting that higher resistance to oxidative stress is the cause of lifespan extension [89].

Autophagy and aging

During development and under stressful conditions (such as starvation), eukaryotic cells undergo a process called autophagy. It is a (self-eating) catabolic process during which cells degrade long-lived proteins and damaged cytoplasmic organelles in order to generate metabolic substrates required for ATP production, protein and fatty acid synthesis therefore maintaining survival [90]. Decline in autophagy as well as accumulation of damaged organelles and macromolecules are known characteristics of aging cells [91]. In the last decade, more experimental evidence supports an essential role of autophagy in lifespan extension. Moreover, autophagy is believed to act as a downstream effector of some of the above discussed lifespan regulatory pathways.

In *C. elegans*, autophagy was first studied in the context of dauer diapause formation in *daf-2* mutants that show elevated levels of autophagy [92]. Therefore, autophagy is required for the remodelling process allowing the nematode to adapt to various environmental stresses (such as starvation and thermal stress) leading to dauer diapause.

More recent studies elucidated a role for autophagy in the longevity of the *daf-2* mutants (insulin/IGF-1 signalling pathway). Down-regulation of multiple autophagy genes by RNAi feeding during the adult stage significantly shorten the lifespan of *daf-2* mutants [51]. Consequently, the elevated levels of autophagy in the adult *daf-2* mutants are required for their longevity phenotype [92, 93]. As mentioned previously, *daf-2* mutants require the activity of DAF-16 (FOXO) transcription factor for lifespan extension since *daf-2;daf-16* double mutants are short-lived. Furthermore, *daf-2;daf-16* double mutants still have increased levels of autophagy similar to *daf-2* single mutants suggesting that elevated autophagy on its own is not sufficient to extend the lifespan of the insulin/IGF-1 signalling pathway mutants [51]. Taken together, DAF-16 could be either downstream of the autophagy process or acting independent of it. In the chronic food limitation DR method (*eat-2* mutants), inhibition of TOR is required for lifespan extension. TOR regulates multiple essential processes such as protein translation and autophagy [63]. DR mutants with reduced TOR signalling have increased levels of autophagy and require autophagy genes to extend lifespan as inhibition of autophagy specifically during adulthood shortens their long lifespan [51]. Moreover, PHA-4/FOXA transcription factor, which was also found to be required for the lifespan extension of the *eat-2* mutants, is required for their increased levels of autophagy suggesting that it might be regulating the transcription of multiple autophagy genes [51]. On the other hand, inhibiting various components in the protein translation machinery extends the nematode's lifespan (discussed previously in protein translation section). Autophagy has been reported not to be involved or required for the longevity induced by this pathway. For example, *rsks-1* mutants have normal levels of autophagy and do not require *bec-1* (ortholog of yeast *ATG6* and mammalian *beclin1*) to have an extended lifespan [51, 66]. Similarly, knockdown of *bec-1* by feeding RNAi during the adult stage doesn't significantly shorten the extended lifespan of *eIF4G* and *eIF4E* mutants [51, 66]. Finally, evidence of the longevity role of autophagy in long-lived mutants of the ETC (electron transport chain) is very controversial. Initially, knockdown of autophagy gene expression by feeding RNAi throughout development or in the adult stage in long-lived mitochondrial mutants did not show any significant effect on lifespan [51]. In contrast, down-regulating different components of the ETC (whose inhibition is known to extend life) by feeding RNAi in

mutants defective in autophagy could not fully extend the lifespan of the mutants suggesting that autophagy is required for mitochondrial dysfunction to extend lifespan [80]. Taken together, experimental evidence clearly support a longevity role for autophagy in mutants of the reduced insulin/ IGF-1 signalling pathway and dietary restriction (DR) pathway.

As described in the "Mitochondrial dysfunction and ROS production" section, the generation of ROS by the respiration process causes oxidative damage to the mitochondria and inhibits the ETC leading to the production of even more ROS which would subsequently cause aging and death [94]. Therefore, reducing ROS production might retard the aging process. Recently, it was suggested that mitochondrial ROS generation acts as a signal for autophagy activation [95]. Moreover, a selective elimination of damaged mitochondria by autophagy might be a key effector pathway downstream of mitochondrial dysfunction required for increased resistance to oxidative stress (by eliminating ROS) and the subsequent extension of lifespan. This role for autophagy in preventing ROS generation and maintaining redox homeostasis to promote cell survival has not been reported in the nematode *C.elegans*. Therefore, lower concentrations of ROS produced by damaged mitochondria might activate stress response mechanisms including autophagy for mitochondrial removal. However, if the ROS levels are too high due to more severe mitochondrial damage then the response might be the release of factors that activate cell death machineries such as apoptosis. Future experiments are clearly needed to fully clarify the longevity role of autophagy in *C.elegans*.

Role of *aak-2* in *C. elegans* aging

AMPK is a metabolite-sensing kinase that is found in all eukaryotes [96]. It is a kinase complex consisting of three subunits, one catalytic (α) and two regulatory subunits (β and γ). Two to three isoforms of each subunit exist and every combination seems to be possible. The β-subunit contains N-terminal glycogen binding domain and a C-terminal α γ-binding domain which makes it required to hold the entire complex together. The α-subunit contains N-terminal kinase domain and a C-terminal β binding domain. The γ-subunit contains N-terminal β binding domain and two C-terminal Bateman domains with

a high affinity for AMP [97]. Upon bindin g to AMP, the γ-subunit undergoes a conformational change which in turn allosterically activates the catalytic α-subunit [98]. AMPK functions as a master switch that is activated in response to energy deprivation (high AMP:ATP ratio) to stimulate alternative catabolic pathways thus maintaining energy homeostasis. It achieves its functions by directly phosphorylating multiple targets involved in various energy-related processes including cell growth, cell cycle regulation, glucose and lipid metabolism [97]. Therefore, AMPK has the opposite effect on many of the pathways that are also targeted by insulin /IGF-1 signalling. Under optimal growth conditions, insulin signalling is induced to stimulate growth, while the nutrient response kinase AMPK remains inactive. However, under stressful conditions, insulin signalling is turned off and AMPK is activated to further down regulate biosynthetic pathways and activate energy generating pathways. It has recently been observed that AMPK (like insulin/IGF-1 signalling) regulates organismal survival in both adult and dauer *C.elegans*. One of the initial observations in adult longevity was that over-expression of AAK-2 in the nematode extends lifespan significantly longer compared to wild type controls [56]. Moreover, AAK-2 activity was required for the full lifespan extension of *daf-2* mutants (animals with reduced insulin/IGF-1 signalling). As mentioned previously, DAF-16 (FOXO transcription factor) is required for lifespan extension of the insulin/IGF-1 signalling pathway mutants [99]. Furthermore, *daf-16;aak-2* double mutant worms have a significantly shorter lifespan than either single mutant suggesting that *aak-2* is able to influence lifespan of *daf-2* mutants in a DAF-16 independent manner [56]. Taken together, both *daf-16* and *aak-2* act in parallel to influence the lifespan extension of *daf-2* mutants [56].

AAK-2 activity was also reported to mediate the ability of one DR method (food limitation starting at middle age) to extend lifespan [47]. To this point, DAF-16 activity was never reported to be required for the lifespan extension induced by any DR method. Interestingly, *daf-16* like *aak-2* was required for the longevity phenotype of the food limitation starting at middle age DR method. Moreover, expression of a constitutively active AAK-2 extended lifespan in a DAF-16 dependent manner suggesting that *aak-2* acts via DAF-16 to extend lifespan in response to this DR method [47]. The cross-talk between *aak-2* and *daf-16* was direct, as AAK-2 was reported to directly phosphorylate

DAF-16 *in vitro* at six novel phosphorylation sites [47]. Therefore, activation of AAK-2 by food limitation result in the phosphorylation and activation of DAF-16 allowing its nuclear localization to increase the expression of genes involved in stress resistance (ROS resistance genes) leading to organismal longevity. This link between AAK-2 and DAF-16 was found to be highly conserved across species. *In vitro* kinase assays reveal that AMPK could phosphorylate all four human FoxO family members with a preference for FoxO3 and regulate its transcriptional activity [100]. Furthermore, compounds such as 2-deoxyglucose, phenformin, and metformin have the ability to mimic low glucose levels (a consequence of dietary restriction) leading to AMPK activation and in turn stimulation of adult longevity. Upon exposure to 2-deoxyglucose, which is a chemical inhibitor of glycolysis, the nematode *C.elegans* lives significantly longer then the wild-type untreated animals [19]. This lifespan extension due to impaired glucose metabolism is AAK-2 dependent [19]. Inhibition of glycolysis leads to AAK-2 activation by phosphorylation which in turn increases mitochondrial respiration and β-oxidation of fatty acids (less triglyceride levels) causing a significant elevation in ROS levels. The animals respond to this increase in ROS generation by activating downstream oxidative stress resistance pathways (increased catalase activity) leading to a lower net stress levels and thereby increased longevity. Meanwhile, the lifespan extension caused by mild chronic dietary DR method (discussed in details in the DR section) due to over-expression of the deacetylase (*sir-2.1*) is also *aak-2* dependent [99]. Conversely, *aak-2* was not required for lifespan extension of the *eat-2* mutants (chronic limitation of food intake DR method) [99]. Therefore, it seems that the requirement for AAK-2 activity in various DR methods to extend lifespan is dependent on the way these regimens trigger DR. These DR modes differ in the time at which the food limitation is applied (during development or at the adult stage), type of medium (solid versus liquid) and type of food limitation (either bacteria or chemical that are known to inhibit/activate specific pathways). Furthermore, the involvement of AAK-2 in the mitochondrial dysfunction pathway is still controversial. It was reported that loss of AAK-2 partially suppresses the long lifespan of *isp-1* and *clk-1* mutants [99]. Moreover, *isp-1* mutants also show a decrease in mitochondrial activity and an increase in AMP: ATP ratio suggesting that *aak-2* plays a role in its long-lived phenotype. However, *isp-1; aak-2* and *clk-1; aak-2* double mutant

animals live significantly longer than the *aak-2* single mutants that are short-lived [99]. This suggests that the involvement of *aak-2* in the lifespan extension of these mitochondrial mutants is at the most partial.

The role of AAK-2 in the nematode's survival is not only restricted to the adult developmental stage as it plays a very crucial role in the survival of the dauer diapause (developmental arrest stage). When the *C.elegans* larvae enter dauer, they remain active and motile, arrest feeding become stress resistant and extremely long-lived [101]. The physiological mechanism by which the dauer larvae is able to survive for a very long period of time (up to four months) in the absence of calorie intake was unknown. Narbonne *et al.* show that *C.elegans* larvae lacking AAK-2 signalling enter dauer normally then rapidly consume their stored fat/energy (lower levels of triglycerides) through the activation of adipose triglyceride lipase (ATGL-1) leading to premature organismal death [102]. *In vitro* kinase assays show that AMPK directly phosphorylate and inactivate a downstream lipase called ATGL-1 [102]. Therefore, AAK-2 signalling acts in adipose-like tissues (intestine and hypodermis) to downregulate triglyceride hydrolysis, through inhibiting ATGL-1, thus allowing the fat stores to last for the entire duration of the dauer arrest [102]. The novelty of the study stems from identifying the role of AAK-2 in fat metabolism that controls dauer survival and determining the molecular mechanism by which AAK-2 does so.

Tumor suppressors and aging

According to the "antagonistic pleiotropy" theory of aging natural selection has favored genes conferring short-term benefits for the organism at the expense of deterioration in later life. Multiple reports indicated that tumor suppression can occur at the cost of organsimal longevity [103]. For example mice that express altered isoforms of the tumor suppressor p53 with increased activity are more resistant to tumor development however age rapidly [104, 105]. One explanation could be that the cellular senescence and DNA damage responses triggered by the stimulation of p53 activity act as a defense mechanism against cancer formation meanwhile, causes deleterious changes in tissues leading to aging [106]. However, other studies argue that transgenic mice that are genetically engineered to over-express p53 under the control of the endogenous promoter age

normally. This suggests that the longevity phenotype observed is unique to the expression of these specific altered isoforms that drastically increase the activity of p53 [107, 108]. In *Drosophila*, over-expression of a dominant-negative form of p53 in the neurons extends organismal lifespan by up to 50% [109] which strongly suggests a phonotypical conservation across species. Moreover, a recent study in *C.elegans* shows that *cep-1* knockout mutants (ortholog of *p53*) live significantly longer than the wild-type control animals[110]. In addition, this lifespan extension of *cep-1* mutants is directly mediated by autophagy [110]. Another tumor suppressor that is involved in regulating organismal survival is VHL (responsible for Von Hippel-Lindau disease). VHL is a cullin E3 ubiquitin ligase that negatively regulates the hypoxic response by promoting ubiquitination and degradation of the hypoxic response transcription factor HIF-1 [111]. The effect of VHL on aging was initially described in a recent study in *C.elegans* showing that loss of VHL-1 activity in *vhl-1* null mutants significantly increased lifespan [112]. Furthermore, the deletion of HIF-1 reverted the longevity phenotype of *vhl-1* mutants, indicating that HIF-1 acts downstream of VHL-1 to modulate organismal aging [112]. This identifies a novel pathway where VHL-1 and HIF-1 control longevity by a mechanism distinct from insulin/IGF-1 singalling, dietary restriction (DR) and autophagy [112]. To this date, the effect of knocking out or over-expressing different isoforms of VHL on the survival phenotype of higher organisms is still not addressed. Taken together, over the years more evidence is presented which inversely link tumor suppression and longevity and seems to be highly conserved across species from *C.elegans* to mice. To this end, the need to characterize the physiological and molecular mechanisms by which novel tumor suppressors regulate organismal longevity is getting bigger.

Results and Discussion

In an attempt to resolve the reported controversial roles of FLCN in the mTOR signalling pathway (please refer to General Introduction), we decided to characterize its role in the nematode *C.elegans* which provides an ideal and simple model genetic organism for studying signalling pathways involved in highly conserved processes such as protein translation, aging, autophagy etc. *F22D3.2* is the ortholog of FLCN in the nematode and it shares a 28% overall sequence identity. For simplicity in the rest of this

text, *flcn-1* will be used instead of *F22D3.2*. Consequently, the protein encoded by *flcn-1* will be referred to as FLCN-1. To date, multiple reports have shown that the c-terminal region of mammalian FLCN is of significant functional importance for two major reasons. First, all the FLCN identified binding partners FNIP1, FNIP2 and AMPK bind to this region of the protein. Second, the majority of the naturally occurring mutations in BHD patients localize in this region leading to a truncated protein product suggesting a loss-of-function mechanism in the tumorigenesis process [117-120]. Interestingly, sequence analysis of the c-terminal region of the mammalian FLCN shows a 64% homology to FLCN-1 (Figure 1A) suggesting that FLCN might have a conserved molecular and functional role in the nematode. Our aim is to identify the molecular signalling pathway to which *flcn-1* belongs. To this end, we purchased *C.elegans flcn-1* mutant strain (strain name RB1035; allele name *ok975*) from the Caenorhabditis Genetics Center (CGC, University of Minnesota). The *flcn-1* mutant is 817bp deletion (including exons 5 and 6) that was generated by UV mutagenesis. This deletion causes a frameshift which introduces a stop codon after amino acid 149 leading to the expression of a truncated protein lacking the remaining 486 amino acid residues including the suggested functionally important c-terminal region of FLCN-1 (Figure 1B and 1C). Moreover, prior to characterizing the *flcn-1* mutant, we out-crossed it 8 times with WT worms to clear any additional mutational background.

Over the last three decades, *C.elegans* has been successfully used as a model organism for studying the molecular mechanisms of aging. The main advantage that this model offers with regards to studying longevity is a short lifespan of approximately 3 weeks. More than two hundred genes have so far been identified to modulate organismal aging in the nematode. Interestingly, the *flcn-1(ok975)* mutant worms showed extended adult longevity as compared to the wild-type (N2) [WT] adult worms. Under normal optimal growth conditions, when maintained at 20^{o}C the *flcn-1(ok975)* mutants have a maximal lifespan of 34 days as compared to adult WT worms with a maximal lifespan of 22 days (Figure 2A and Table 1). In order to confirm the *flcn-1* mutant longevity phenotype, we utilized a very powerful genetic tool in the nematode, RNA mediated interference (RNAi) by feeding WT nematodes bacteria that express double-stranded RNA (dsRNA) which corresponds to *flcn-1* leading to a gene knockdown and we scored for survival

thereafter. Indeed, knocking down *flcn-1* in WT animals leads to lifespan extension to 28 days confirming a novel *flcn-1* role in *C.elegans* aging (Figure 2A). Furthermore, in an attempt to determine whether the *flcn-1 (ok975)* mutant is carrying a null allele, we knocked down *flcn-1* by RNAi feeding during the development process of the *flcn-1(ok975)* mutant animals and scored for longevity. Our data shows no further extension of the lifespan phenotype of *flcn-1* mutant animals upon knocking down *flcn-1* suggesting that *ok975* is indeed a null allele (Figure 2B). To rule out any synergistic effect of potential background mutations in the *flcn-1* knockout on the longevity phenotype, we found that expression of a functional *flcn-1:: GFP* fusion construct under the endogenous *flcn-1* promoter rescued the extended lifespan of the *flcn-1* deletion mutant (Figure 2C). Taken together these findings suggest that under optimal growth conditions, knockout of *flcn-1* significantly extends the adult lifespan of the nematode compared to WT control animals.

Some evolutionary theories predict that longevity mutations are associated with reduced reproduction or other tradeoffs thus allowing animals to ensure a proper utilization of their resources [16]. To determine whether the long-lived *flcn-1* knockout worms have reduced total progeny production, we quantified the number of eggs laid over the period of 5 days post adult stage in the WT animals and *flcn-1* mutants. Our data clearly indicate no differences in the number of progeny between the WT and the long-lived *flcn-1* knockout animals (Figure 2D). Our findings support many long-lived mutants in various species, such as the *C.elegans* weak insulin/IGF-1 pathway mutants that extend lifespan but have little to no effect on reproduction and the *Drosophila indy* mutant, which produces even more progeny than WT [121, 122]. Interestingly, the insulin/IGF-1 pathway regulates both aging and reproduction, but it regulates the two processes independently of each another. Thus, knocking down *daf-2* (IGF-1 receptor) by RNAi feeding from the time of hatching extends life span and delays reproduction, but feeding WT animals *daf-2* dsRNA as young adults extends life span to the same extent with little or no effect on reproduction [123]. Therefore, longevity does not need to occur at the cost of reproduction. Another phenotype that is closely linked to longevity is slow developmental growth rate of the nematode. To this end, we looked at the growth rate of the *flcn-1* mutant during the different larval stages in comparison with the WT controls.

Our results show that both the WT and the *flcn-1* knockouts enter the first and second larval stages (L1 and L2) at the same time, however past the second larval stage, WT animals develop faster to become mixed population of L4 and young adults (48h post hatching) compared to the *flcn-1* mutants that delay their growth and stay in the L3 and L4 stage for longer period of time (Figure 2E and 2F). Taken together, under optimal growth conditions the *flcn-1* mutant worms show a delay in development by approximately 18 hours compared to WT control animals with no change in total progeny production.

After the discovery of *age-1* as the first gene with the ability to extend the lifespan of *C.elegans* in 1988, many longevity genome wide screens have been performed to further identify genes that regulate organismal aging [3]. To date close to 276 genes have been reported to have an effect on adult longevity and the majority of those genes are assigned to one or more of the four following genetic pathways: insulin/IGF-1 signalling pathway, dietary restriction pathway, protein translation pathway and mitochondrial respiration pathway [4]. The insulin/IGF-1 signalling pathway has been shown to be the most highly conserved longevity pathway across species from yeast to humans [16, 122]. Reducing the activity of this pathway by mutating *daf-2* (insulin/IGF-1 receptor) slows the aging process through doubling the adult lifespan of the nematode [14]. The lifespan extension of various mutated components of the insulin/IGF-1 signalling pathway requires the activity of the three downstream transcription factors: FOXO transcription factor DAF-16; heat-shock transcription factor HSF-1; and SKN-1 (Nrf-like response factor) [14, 15]. These transcription factors regulate the expression of multiple downstream stress-response genes such as glutathione S-transferase, methallothioneins, catalases, chaperones, apolipoproteins, lipases, channels and multiple genes encoding antimicrobial peptides [16-20]. The elevation of various stress response mechanisms reduces the net stress levels in adult *C.elegans* leading to lifespan extension. We next asked whether *flcn-1* plays a role in the insulin/IGF-1 signalling pathway leading to the lifespan extension. To this end, we measured the lifespan of *flcn-1(ok975)* mutants and *daf-2(e1370)* mutants, as well as *daf2(e1370); flcn-1(ok975)* double mutants. *daf2(e1370); flcn-1(ok975)* double mutants have a lifespan that is indistinguishable from those of the *flcn-1(ok975)* single mutants (Figure 3A). Therefore, a *flcn-1* dependent mechanism is

required to produce the exceptionally long lifespan of *daf-2* mutants. We further looked at DAF-16, the FOXO transcription factor, downstream of the insulin/IGF-1 pathway that is required for lifespan extension. If *flcn-1* extends adult lifespan independent of DAF-16 activity, then absence of *flcn-1* should further extend the short lifespan of *daf-16(mu86)* null mutants. Instead, *daf-16(mu86); flcn-1(ok975)* double mutants have a short lifespan similar to that of the *daf-16(mu86)* single mutants (Figure 3B). Therefore, *flcn-1* influences lifespan in a *daf-16* dependent manner. Taken together, these findings indentify *flcn-1* as a novel component of the insulin/IGF-1 signalling pathway acting downstream of *daf-2*. Moreover, both *flcn-1* and *daf-16* are required for the lifespan extension of *daf-2* mutants and *daf-16* acts downstream of *flcn-1*. However the exact functional role of *flcn-1* in this pathway is yet to be determined.

AMP-kinase (AMPK) functions as a master metabolic switch that is activated in response to energy deprivation (high AMP: ATP ratio) to stimulate alternative catabolic pathways and maintain energy homeostasis. It achieves this function by directly phosphorylating multiple targets involved in various energy-related processes including cell growth, cell cycle regulation, glucose and lipid metabolism [97]. In the last four years, multiple reports identified two FLCN interacting proteins FNIP1 and FNIP2 that bind to the c-terminal region of the protein and also directly interact with AMPK (please refer to General Introduction) [117-119]. In a recent study, FLCN was found to form a complex with AMPK independent of FNIP1 and FNIP2 and co-immunoprecipitation experimental data from our laboratory confirm these findings (data not shown) suggesting direct cross-talk between AMPK and FLCN. However, the nature of this regulation and the effects on AMPKs function is yet to be characterized [120]. In *C.elegans*, two isoforms of the catalytic subunit of AMPK has been identified as AAK-1 an AAK-2, both share a high sequence homology with the mammalian AMPKα1 and AMPKα2 isoforms respectively. In the insulin/IGF-1 signalling pathway, the link between *aak-2* and adult lifespan has been reported. It was shown that the lifespan extension of *daf-2* mutants is *aak-2* dependent. Moreover, since *daf-16;aak-2* double mutant worms have a significantly shorter lifespan than either single mutant then *aak-2* acts independent of *daf-16* downstream of *daf-2* [56]. Therefore, *daf-16* and *aak-2* act in parallel to influence the lifespan extension of *daf-2* mutants [56]. We asked whether

either of the two catalytic isoforms (*aak-1* and *aak-2*) play a role in the lifespan extension of the *flcn-1* mutant animals. Our data clearly shows that *aak-1* is not required for regulation of lifespan in the nematode since we see no significant effect on longevity in the *aak-1* null mutants compared to WT control animals. Furthermore, *aak-1;flcn-1* double mutants have an undistinguishable lifespan from the *flcn-1(ok975)* mutants (Figure 4A) [56]. We also measured the lifespan of *aak-2(ok524)* single mutants and *flcn-1(ok975)* single mutants in addition to *aak-2(ok524); flcn-1(ok975)* double mutants. If *flcn-1* extends lifespan solely by activating *aak-2* or mediating its activity, then absence of *flcn-1* should not further extend the short lifespan of the *aak-2* mutants. Indeed our experimental results confirm our hypothesis, *aak-2(ok524); flcn-1(ok975)* double mutants show a lifespan that is not significantly different from that of the *aak-2(ok524)* single mutants (Figure 4B). Therefore, *flcn-1* mutant adult lifespan extension is *aak-2* dependent. Taken together, *flcn-1* plays a key role in regulating organismal lifespan downstream of *daf-2* via a mechanism which is *aak-2* and *daf-16* dependent. This also suggests a potential role for *flcn-1* in modulating the activity of *aak-2* and *daf-16*.

AMPK kinase activity is induced by phosphorylation due to increasing intracellular levels of AMP and accordingly by decreasing levels of ATP [97]. The activation of this metabolic "switch" results in the repression of biosynthetic pathways and up-regulation of alternative catabolic pathways to maintain the cellular energy levels. The *C.elegans* AAK-2 kinase activity is increased by three fold upon treatment with AMP suggesting that AAK-2 exhibits the hallmarks of an AMPK in the nematode [56]. LKB1 is the upstream kinase that acts in concert with AMP to increase AMPK phosphorylation. Moreover, AAK-2 phosphorylation is required for its activity [56]. Given that the lifespan extension of the *flcn-1* mutants is *aak-2* dependent, we questioned whether absence of *flcn-1* does alter the phosphorylation status of AAK-2. Western blot analysis of whole worm lysates from WT and *flcn-1 (ok975)* mutant adult worms using a specific anti-phospho-AAK-2 antibody (phospho-Thr^{243} of the AAK-2 protein corresponding to Thr^{172} of the human AMPKα subunit [114]) shows increased abundance of the phosphorylated form of AAK-2 in flcn-1 mutant worms (Figure 4C). We further quantified the abundance of the phosphorylated form of AAK-2 and found a two fold increase in the *flcn-1* knockout worms compared to the WT control animals (figure 4D).

Take together; this negative correlation between FLCN-1 and AAK-2 phosphorylation suggest one of two possibilities: 1) The FLCN-1 effect on AAK-2 is indirect potentially due to a role for FLCN-1 in negatively regulating an energy consuming pathway (which in the absence of FLCN-1 results in the elevation of AMP:ATP ratio and consequently increase the phosphorylation/activation of AAK-2). 2) The FLCN-1 effect on AAK-2 is through a direct regulation mechanism involving known or novel kinase(s) that phosphorylates/activates AAK-2.

LKB1 acts as a tumour suppressor responsible for the Peutz-Jeghers syndrome (PJS) [124]. PJS is an autosomal dominant disorder that predisposes affected individuals to tumour formation in several organs [125]. LKB1 encodes a highly conserved serine/threonine kinase that phosphorylates and activates AMPK [126, 127]. The kinase activity and subcellular localization of LKB1 are modified upon its association with two cofactors, a Ste20-related adapter protein called STRAD and MO25, which together form the highly active heterotrimeric complex [126, 128, 129]. In *C.elegans*, the LKB1 homolog PAR-4 directly phosphorylates AAK-2 thus highlighting a conserved role of the kinase across species [114]. Furthermore, PAR-4 requires STRD-1 to activate AAK-2 by direct phosphorylation [113]. Given that *flcn-1* mutant worms have elevated phosphorylation of AAK-2, we asked whether FLCN-1 has an effect on the expression levels of PAR-4 and STRAD-1. Western blot analysis of total worm lysates from WT and *flcn-1* knockout worms using protein specific antibodies show no difference in the expression levels of PAR-4 and STRAD-1 (Figure 4C). This suggests that the elevated phosphorylation levels of AAK-2 in the *flcn-1* knockouts are not mediated by regulating the expression levels of PAR-4 and STRAD-1. To determine whether *par-4* activity plays a role in the lifespan extension of the *flcn-1* mutant animals, we measured the lifespan of *par-4(it57)* mutants and *flcn-1(ok975)* mutants in addition to *par-4(it57); flcn-1(ok975)* double mutants. If *flcn-1* extends lifespan solely by activating *aak-2* through directly influencing the PAR-4 mediated phosphorylation of AAK-2, then absence of *flcn-1* should not further extend the short lifespan of the *par-4* mutants. Instead, *par-4(it57); flcn-1(ok975)* double mutant worms have significantly longer lifespan compared to the *par-4* single mutants (Figure 4E). Therefore, *flcn-1* null mutants extend lifespan using a mechanism that is independent of *par-4* or at the most partially dependent on it. We

further asked whether *flcn-1* knockout affects the phosphorylation/activation status of AAK-2 independent of the kinase activity of PAR-4. To this end, we used a *par-4(it57)* mutant worms that have been previously reported to lack the ability to phosphorylate and activate AAK-2 [113]. Western blot analysis of whole worm lysates from WT, *flcn-1(ok975)* single mutants, *par-4(it57)* single mutants, and *par-4(it57); flcn-1(ok975)* double mutant adult worms using anti-phospho-AAK-2 specific antibody shows similar levels of AAK-2 phosphorylation in the *flcn-1* single mutants as well as in the *par-4; flcn-1* double mutants (Figure 4F). Therefore, FLCN-1 negatively regulates AAK-2 phosphorylation via a novel mechanism that is independent of PAR-4 activity leading to adult longevity. Taken together, our findings indicate an *aak-2* dependent mechanism leading to lifespan extension of the *flcn-1* knockout animals. Moreover, FLCN-1 negatively regulates AAK-2 phosphorylation/activation through a mechanism independent of the constitutively active PAR-4 kinase. This gives rise to two feasible scenarios for a FLCN-1 mechanism that directly regulates AAK-2 phosphorylation: either FLCN-1 is a phosphatase acting on AAK-2 or alternatively FLCN-1 could be negatively regulating the expression levels or activity of another known or novel kinase which functions to phosphorylate and activate AAK-2. Recently, Ca^{2+}/calmodulin dependent protein kinase kinase-β (CaMKK-β) was found to also phosphorylate and activate AMPK in mammalian cells in a mechanism independent of AMP and LKB1 [130, 131]. Instead, this activation of AMPK requires a change in intracellular Ca^{2+}[132]. In *C.elegans, ckk-1* has been reported as an ortholog of CaMKK [133-135]. The phosphorylation/activation of AAK-2 by CKK-1 is yet to be characterized in the nematode. However, based on its mammalian role, CKK-1 might function in a novel mechanism that phosphorylates/activates AAK-2 independent of PAR-4 kinase. Taken together, future experiments will clarify the FLCN-1 regulation of AAK-2 phosphorylation potentially through a novel FLCN-1/CKK-1 mechanism independent of PAR-4 activity.

AMPK is also capable of inhibiting protein translation by acting as a negative regulator of the mammalian target of rapamycin (mTOR), the master regulator of this process. Thus, under nutrient limitation, TOR is downregulated leading to inhibition of protein synthesis [57]. This occurs by reducing the phosphorylation of the kinase S6K which subsequently causes the dephosphorylation and inactivation of the translation elongation

factor (eEF2) kinase and the small ribosomal subunit protein S6 (rpS6) [58]. Moreover, down-regulation of TOR reduces the phosphorylation of translation initiation factor 4 binding proteins (eIF4-BP) thereby allowing it to bind to eIF4E thus inhibiting protein translation [58]. The inhibition of global protein translation by knocking down various components of the TOR pathway leading to longevity is a conserved process across species from yeast to mice [42, 44, 67]. This lifespan extension is due to switch from a state of optimal growth to a state of cell maintenance and increased stress resistance (thermal stress or oxidative stress) [43]. In *C.elegans*, inhibition of global protein translation has been shown to extend lifespan as well. A knockdown of *let-363* (ortholog of *TOR*) by RNAi feeding extends the adult lifespan by 1.5 folds compared to wild type control animals [43, 62-64]. Meanwhile, the puzzling controversy in the FLCN research field stems from identifying the exact role that FLCN plays in regulating mTOR activity as multiple contradictory studies reported opposing roles of FLCN in that aspect [136-139]. We asked whether *flcn-1* plays a role in the protein translation pathway that regulates lifespan by influencing the activity of LET-363. To this end, we measured the lifespan of *flcn-1(ok975)* mutants, *flcn-1(ok975)* mutants with *let-363* knockdown using RNAi feeding and WT animals with *let-363* knockdown. If *flcn-1* is part of the protein synthesis pathway which regulates adult longevity then knocking down *let-363* in the *flcn-1* knockout worms should not further extend their lifespan. Instead, the knockdown of *let-363* in the *flcn-1* mutant worms show a significant lifespan increase compared to the untreated *flcn-1* mutants and to the WT *let-363* knockdown animals (Figure 5A). This additive effect suggests that *flcn-1* extends lifespan via a mechanism that is independent of *let-363* and the protein translation process. One of the most studied components of the TOR pathway is the downstream kinase S6K. Various reports have shown that inhibition of S6K extends lifespan in yeast, *C. elegans*, flies and mice due to reduction in protein synthesis [42, 44, 68]. To confirm our previous findings, we measured the lifespan of *flcn-1(ok975)* mutants, *flcn-1(ok975)* with *rsks-1* knockdown (ortholog of S6K) using RNAi feeding and WT animals with *rsks-1* knockdown. Our results show that knocking down *rsks-1* results in an additive effect on the lifespan of the *flcn-1* null mutants (Figure 5B). This suggests that *flcn-1* extends lifespan in a mechanism independent of *rsks-1*.

Taken together, our findings indicate that *flcn-1* extends lifespan via a mechanism independent of the reduced protein translation pathway.

Autophagy is a well-conserved lysosomal catabolic pathway used to degrade long-lived proteins and damaged cytoplasmic organelles allowing eukaryotic cells to generate a source of metabolic substrates to maintain cellular ATP production, protein synthesis, and fatty acid synthesis in times of stress, thereby sustaining cellular activity needed for survival [90]. Decline in catabolic pathways (such as autophagy) as well as accumulation of damaged organelles and macromolecules are known characteristics of aging cells [91]. In *C.elegans*, the knockdown of multiple genes involved in the autophagy process shortens organismal lifespan. Previous studies have shown that of the longevity pathways, reduced insulin/IGF-1 signalling and dietary restriction appear to rely on autophagy to increase lifespan [51]. Given that *flcn-1* is a novel component of the insulin/IGF-1 signalling pathway that regulates lifespan in the nematode, we asked whether autophagy levels are affected in the *flcn-1* mutant worms. To this end, we visualized autophagy by using a transgenic WT animals that expressed a GFP-tagged version of the *C. elegans* gene product LGG-1 [92] (kindly provided to us by the laboratory of Dr. Richard Roy, McGill University) and generated a *flcn-1(ok975)* mutant that also expressed a GFP-tagged LGG-1, which is an ortholog of yeast Apg8/Aut7p and mammalian MAP-LC3. During autophagy, MAP-LC3 localizes to pre-autophagosomal and autophagosomal membranes, and their punctate staining pattern (versus a diffuse pattern in the absence of autophagy) provides a useful marker for autophagy [92]. We find a three-fold increase in the number of GFP::LGG-1 puncta in the seam cells of the *flcn-1* knockouts compared to WT animals (Figure 6A). This suggests an increase in autophagy levels in the *flcn-1* knockout animals compared to WT control animals. We further confirm our findings using western blot analysis on total worm lysates from WT and *flcn-1(ok975)* mutant worms that express the GFP-tagged LGG-1 reporter using anti-GFP specific antibody. We show an increase in the levels of both PE-LGG-1 and cytosolic LGG-1 in *flcn-1* knockout worms compared to the WT worms which confirm the up-regulation of autophagy in the *flcn-1* mutant animals (Figure 6B). To determine whether elevated levels of autophagy are required for the lifespan extension of the *flcn-1* knockout worms, we measured the lifespan of WT, *flcn-1 (ok975)* mutants, *flcn-1(ok975)*

mutants with *bec-1* knockdown using RNAi feeding and WT animals with *bec-1* knockdown. We focus on *bec-1*, the *C.elegan*s ortholog of yeast *APG6/VPS30*, because both its yeast and mammalian orthologues (mammalian *beclin 1*) are important components of the autophagy process. Apg6/Vps30/Beclin 1 is part of a Class III phosphatidylinositol 3-kinase (PI3K) complex that is important in mediating the localization of other Apg proteins to the pre-autophagosomal structures [140, 141]. A knockdown of *bec-1* by RNAi feeding thus inhibits the autophagy process. Our data shows that upon the inhibition of autophagy by knocking down *bec-1*, *flcn-1(ok975)* mutant worms have a lifespan that is indistinguishable from the WT animals (Figure 6C). This suggests that the *flcn-1* mutant longevity phenotype is indeed dependent on autophagy. Taken together, *flcn-1* regulates organismal lifespan via a mechanism that is autophagy, *aak-2* and *daf-16* dependent. Interestingly, to date in *C.elegans* a role of *aak-2* and *daf-16* in directly regulating autophagy leading to lifespan extension is still not reported. In contrast, in mammalian systems, a direct role for both FOXO3a (DAF-16 ortholog) and AMPK in the regulation of autophagy has been reported. FOXO3a transcription factor is activated either via Sirt1 mediated deacetylation or AKT mediated dephosphorylation. Upon its activation, FOXO3a translocates into the nucleus and upregulates the expression of multiple autophagy-related genes including *beclin-1* [142, 143]. Moreover, the interaction between AMPK and ULK1 which suggests that AMPK might be acting directly on the core components of the autophagy machinery [144]. It is important to mention that in mammalian systems, both FOXO3a and AMPK are capable of regulating autophagy independent of mTOR [145]. An intriguing, but not yet tested, possibility is that *C.elegans flcn-1* might be directly regulating *aak-2*, *daf-16*, or both upstream of autophagy to modulate longevity independent of *let-363*. Future experiments are required to measure the lifespan of *daf-16(mu86)* null mutant, *daf-16(mu86);flcn-1(ok975)* double mutants, *aak-2(ok524)* mutant, *aak-2(ok524);flcn-1(ok975)* double mutants and *daf-16(mu86); aak-2(ok524);flcn-1(ok975)* triple mutants upon inhibition of autophagy using *bec-1* RNAi. This set of experiments will clarify the involvement of *daf-16* and *aak-2* in the autophagy process downstream of *flcn-1* in regulating organismal lifespan. We also plan on identifying the set of autophagy genes that are up-regulated on the transcript level in the *flcn-1* null mutants using qRT-PCR.

AMPK has been shown to specifically induce mitochondrial metabolism in mammalian cells [98]. AMPK is also linked to altered β-oxidation of fatty acids and this role is conserved across species from *C.elegans* to mammals [19, 98, 102]. A recent study reported that upon treatment with a chemical inhibitor of glycolysis (2-deoxyglucose), the adult nematode *C.elegans* live significantly longer then the wild-type untreated animals [19]. This lifespan extension due to impaired glucose metabolism is AAK-2 dependent [19]. Furthermore, inhibition of glycolysis leads to phosphorylation/activation of AAK-2 which in turn increases mitochondrial respiration and β-oxidation of fatty acids (lower triglycerides levels) causing a significant elevation in ROS levels [19]. Given that we observe an increased abundance of the phosphorylated form of AAK-2 in the *flcn-1* null mutants, we asked whether adult *flcn-1* knockout nematodes have altered levels of triglycerides and whether this difference is dependent on the activity of AAK-2. We quantified the triglyceride content of WT, *flcn-1(ok975)* mutants, *aak-2(ok524)* mutants and *aak-2(ok524);flcn-1(ok975)* double mutants. Our results show a decrease in triglyceride content in the *flcn-1(ok975)* mutants indicating an increase in β-oxidation of fatty acids compared to WT control animals (Figure 7A). Moreover, this increase in β-oxidation of fatty acids in the *flcn-1* null mutants is dependent on the activity of AAK-2 since the triglyceride content of the *aak-2(ok524);flcn-1(ok975)* double mutants is indistinguishable from those of the *aak-2(ok524)* single mutants (Figure 7A). To confirm our findings, we performed oil-red-O staining as a method to assess major fat stores in the strains mentioned above. Oil-red-O provides another indicator to the fat accumulation at the organismal level [116]. The images confirm a lower fat accumulation in the *flcn-1(ok975)* compared to WT animals and a significant restoration of fat vesicles in *aak-2(ok524);flcn-1(ok975)* double mutants that is similar to the *aak-2(ok524)* single mutants (Figure 7 B-E). Taken together, our findings indicate that FLCN-1 could function to downregulate lipolysis via an AAK-2 dependent mechanism which might regulate adult lifespan. This gives rise to an intriguing possibility, that is yet to be tested, where *flcn-1* negatively regulates AAK-2 which might subsequently alter the activity of a downstream lipase and therefore influence adult lifespan. Further experiments are needed in order to identify the downstream lipase involved in this process. To this end, we will make use of a *C.elegans* lipase RNAi library (kindly provided to us by the laboratory of Dr. Richard

Roy, McGill University) to knockdown every known *C.elegans* lipase in the *flcn-1(ok975)* null mutants and score for triglyceride content thereafter. The down-regulated lipase that is able to restore the *flcn-1(ok975)* mutant triglyceride levels close to the *aak-2* mutant levels will be subsequently tested in longevity experiments to determine whether it has an effect on the lifespan of the *flcn-1* null mutants.

To gain insight into whether the hydrolyzed triglycerides are converted through the respiratory pathway, we measured the rate to which *flcn-1* knockout adult worms consume oxygen. Our data indicate that oxygen consumption in the *flcn-1* mutants is significantly higher than the control animals (Figure 7F). Therefore in the adult stage, in the absence of *flcn-1*, animals consume their lipid reserves at a faster rate compared to the WT controls and consequently exhibit higher respiration rates. Inhibition of glycolysis results in an *aak-2* dependent elevation of mitochondrial respiration and lifespan extension [19]. Moreover, we found that *flcn-1* mutants exhibit increased AAK-2 phosphorylation/activation which is required for their lifespan extension. We asked whether the increased rate of oxygen consumption in the *flcn-1* null mutant worms is regulated by AAK-2. We measured the rate to which *aak-2* mutant young adult worms and *aak-2;flcn-1* double mutants consume oxygen. We observe a decrease in respiration rates in the *aak-2* mutants compared to control animals and upon inhibiting the AAK-2 signalling pathway in the *flcn-1* null mutants, the respiration rate is decreased to the level of *aak-2* mutants (Figure 7F). Taken together, our findings indicate that the *flcn-1* mutant worms exhibit elevated rates of respiration via an AAK-2 dependent mechanism. Future experiments are required to shed some light onto whether increased respiration rates and triglyceride hydrolysis are required for the lifespan extension phenotype of the *flcn-1* null mutants.

It has been reported that induction of respiration causes elevated ROS production due to increased electron transfer in the respiratory chain [146, 147].According to the mitochondria theory of aging, the production of ROS by respiration causes oxidative damage in the mitochondria and inhibits the ETC leading to the generation of even more ROS which could eventually lead to aging and death [94]. Therefore, reducing ROS production might retard the aging process. Given that we observe elevated rates of respiration in the *flcn-1* null mutants, we wanted to determine whether this corresponds to

increased production of ROS. To this end, we quantified the levels of ROS generation in *flcn-1* adult mutants using DCF fluorescence. We show a two fold increase in ROS production in the *flcn-1* knockouts compared to the control animals (Figure 8A). We further investigated whether this increase in ROS production in the *flcn-1* null mutants is AAK-2 dependent by measure ROS levels in *aak-2* single mutants and *aak-2;flcn-1* double mutants (Figure 8A). Interestingly, we show that elevated ROS levels in the *flcn-1* knockouts are suppressed by inhibiting AAK-2 signalling since ROS generation levels in the *aak-2* single mutants and *aak-2;flcn-1* double mutants are very similar. If ROS production leads to a faster aging process and death, then how could the *flcn-1* null mutants have an extended lifespan while exhibiting elevated ROS levels? The answer to this question lies in the ROS detoxification machinery. This increase in ROS generation might up-regulate enzymes capable of oxygen radical detoxification causing increased defence capacity against ROS leading to lifespan extension [19, 148]. To determine whether the *flcn-1* mutant worms have elevated ROS resistance compared to control animals, we exposed *flcn-1* mutants and WT worms to paraquat which is known to act as a mitochondrial stressor capable of inducing ROS formation and we scored for survival. Upon treatment with 50mM paraquat, we observe a decreased maximal lifespan of WT worms from 22 days (untreated) to 4 days (treated) indicating that paraquat-induced ROS formation has a negative effect on lifespan (Figure 8B). However, *flcn-1* knockout worms show significantly increased survival rates when exposed to paraquat (Figure 8B) demonstrating increased stress resistance despite elevated respiratory activity and ROS production. Similarly, *daf-2* mutants show increased resistance to oxidative stress and decreased oxidative damage but still have higher levels of ROS production compared to wild type control animals [83, 84]. Thus at lower concentrations of ROS production, the stress level is sufficient to activate stress response mechanisms (ROS detoxification) leading to lower net stress levels and subsequently increased longevity. However, if the ROS levels are too high then the response might be the release of factors that activate cell death processes such as apoptosis leading to early death. Further experiments are required to determine the exact set of ROS detoxification enzymes that is up-regulated in the *flcn-1* mutants. We will perform western blot analysis on whole worm lysates from WT and *flcn-1* null mutant worms using SOD1 and SOD2 protein specific antibodies (kindly

provided to us by the laboratory of Dr. Siegfried Hekimi, McGill University) in addition we aim to look at the transcript levels of ROS detoxification enzymes [super oxide dismutases (SODs), glutathione peroxidise (GPX) and catalases (CAT)] using qRT-PCR to identify the up-regulated ROS resistance enzyme(s).

Previously, it was suggested in mammalian systems that mitochondrial ROS generation acts as a signal for autophagy activation [95]. Moreover, a selective elimination of damaged mitochondria by autophagy might be a key effector pathway downstream of mitochondrial dysfunction and ROS production required for increased resistance to oxidative stress (by eliminating ROS producing mitochondia) and the subsequent extension of lifespan. This will define a novel role for autophagy in regulating ROS generation and maintaining redox homeostasis to promote cell survival which to date has not been reported in *C.elegans*. We hypothesize that at lower concentrations of ROS, the stress level is sufficient to activate stress response mechanisms including autophagy and up-regulation of ROS detoxification enzymes leading to lifespan extension. Given that the *flcn-1* null mutants have increased stress resistance to ROS production and show elevated levels of autophagy both of which are required for lifespan extension, we asked whether autophagy is acting downstream of ROS generation as a ROS response mechanism leading to longevity. To this end, we measured the survival rates of *flcn-1* mutants and WT worms that are exposed to the ROS stressor paraquat upon inhibiting autophagy using *bec-1* RNAi. Both WT and *flcn-1* knockout worms show similar survival rates (2 days) however their survival is significantly decreased compared to the *bec-1* RNAi untreated animals (4 days and 5 days respectively) (Figure 8B). Interestingly, upon down-regulation of autophagy, the *flcn-1* mutants lose their survival advantage on paraquat. This suggests that in the *flcn-1* mutants and WT worms, autophagy is required for increased stress resistance to ROS leading to lifespan extension. Taken together, our findings potentially identify a novel role for autophagy as a downstream ROS regulatory mechanism required to maintain redox homeostasis and promote cell survival and longevity. Further work should be done in order to clarify the role of autophagy in regulation of ROS detoxification. One way is to pre-treat WT and *flcn-1* mutant worms with N-acetylcysteine (NAC), a membrane-permeable glutathione precursor known to recover the effects of ROS by mimicking the radical scavenging

potential of reduced glutathione, and measure autophagy levels and survival rates. This will determine whether ROS generation acts as a trigger to activate autophagy as a downstream mechanism regulating organismal survival.

Conclusions and Future directions

In this study, we identify a novel role of the *C.elegans* ortholog of the mammalian tumor suppressor FLCN in regulating aging. *flcn-1* is 27-28% identical to mammalian *BHD* and shares 64% homology at the C-terminus suggesting a functional importance and conservation of this region. We discovered a novel role of *flcn-1* in *C.elegans* aging using a *flcn-1(ok975)* null mutant and confirmed our findings by RNA mediated interference (feeding RNAi). We further identify *flcn-1* as a novel component of the insulin/IGF-1 signalling pathway that regulates organismal lifespan. Thus, *flcn-1* acts downstream of the insulin/IGF-1 receptor *daf-2* and regulates lifespan via a mechanism that is dependent on both DAF-16/FOXO transcription factor and AAK-2/AMP mediated kinase (AMPK).

We observe an increase in the abundance of the phosphorylated form of AAK-2 in the *flcn-1* null mutants and this phosphoryation of AAK-2 was not affected in the absence of PAR-4 kinase. Moreover, *par-4;flcn-1* double mutant worms live significantly longer than the *par-4* single mutants. Thus, FLCN-1 negatively regulates AAK-2 phosphorylation/activation through a novel mechanism that is independent of PAR-4/AMP sensing. An intriguing but not yet tested possibility is that FLCN-1 could be negatively regulating the expression levels or activity of another known or novel kinase which functions to phosphorylate/activate AAK-2. To determine whether FLCN-1 and AAK-2 directly interact, our laboratory is in the process of performing co-immunoprecipitation (co-IP) experiments in HEK293T cells transiently expressing *C.elegans* Myc-FLCN-1, Flag-AAK-2, HA-AAKB-1 and HA-AAKγ-1 in mammalian expression plasmids. To determine whether FLCN-1 is negatively regulating the activity or expression of CKK-1 kinase (ortholog of CaMKK) or the downstream CAM-1 kinase (ortholog of CaMK-1) which could be the kinases responsible for AAK-2 phosphorylation, we will generate *ckk-1(ok1033);flcn-1(ok975)* and *cmk-1(ok287);flcn-1(ok975)* double mutant worms (*ok287* is reported to be a null allele of *cmk-1* [149]).

Western blot analysis on whole worm lysates from WT(N2), *cmk-1(ok287)* single mutants, *ckk-1(ok287)* single mutants, *flcn-1(ok975)* single mutants, *cmk-1(ok287);flcn-1(ok975)* double mutants, and *ckk-1(ok1033);flcn-1(ok975)* double mutants using anti-phospho-AAK2 specific antibody will determine the phosphorylation status of AAK-2 in the *flcn-1* null mutants and whether it is altered in the absence of CKK-1 or CMK-1 expression.

We report that in *C.elegans, flcn-1* extends lifespan via a mechanism that independent of the inhibition of protein translation machinery as the lifespan of the *flcn-1* mutant worms was further increased upon the knockdown of *let-363* or *rsks-1*. We also show that *flcn-1* mutants have elevated levels of *let-363* independent autophagy which is required for lifespan extension. Thus, *flcn-1* regulates organismal lifespan via a mechanism that is autophagy, *aak-2* and *daf-16* dependent. An intriguing, but not yet tested, possibility is that *flcn-1* might be directly regulating the activity of *aak-2*, *daf-16,* or both upstream of autophagy to modulate longevity. We report that *flcn-1* mutants have elevated β-oxidation of fatty acids due to lower triglyceride levels. Indeed, the hydrolyzed triglycerides are converted through the respiratory pathway as *flcn-1* mutant worms show increased rates of oxygen consumption. Interestingly, this increase in β- oxidation of fatty acids and respiration is via a mechanism that is AAK-2 dependent. We aim to determine whether increased triglyceride hydrolysis and respiration in the *flcn-1* mutants influence lifespan. It is possible that the *flcn-1* negative regulation of AAK-2 might subsequently alter the activity of a downstream lipase and therefore influence adult lifespan. Further experiments are needed in order to identify the downstream lipase involved in this process.

Due to elevated rates of respiration, the *flcn-1* null mutants increase the production of reactive oxygen species (ROS). Our stress resistance experiments clearly indicate that the *flcn-1* mutants are more resistant to ROS. Therefore, this increase in ROS generation potentially acts as a stimulant for oxidative stress responses. Further experiments are required to determine the exact set of ROS detoxification enzymes that are up-regulated in the *flcn-1* mutants. To this end, we will perform western blot analysis on whole worm lysates from WT and *flcn-1* null mutant worms using SOD1 and SOD2 protein specific

antibodies. In addition, we will make use of qRT-PCR to shed some light on the up-regulated ROS detoxification enzyme(s) on a transcript level [super oxide dismutases (SODs), glutathione peroxidise (GPX) and catalases (CAT)]. Finally, we show a potential novel role for autophagy as a downstream ROS regulatory mechanism required to maintain redox homeostasis and to promote organismal survival. We propose a model by which *flcn-1* regulates lifespan in response to insulin/IGF-1 signalling (Figure 9). Further work should be done in order to clarify the role of autophagy in the regulation of ROS generation in the nematode.

Materials and Methods:

Strains and RNA interference

The Bristol isolate (N2) was used as wild type in all experiments. The following strains were used: *flcn-1(ok975)*, *daf-16(mu86)* [Both obtained Caenorhabditis Genetics Center (CGC, University of Minnesota)], *daf-2(e1370), aak-1(tm1944), par-4(it57), aak-2(ok524)* [all were a kind gift from the laboratory of Dr. Richard Roy, (McGill University)]. *flcn-1(ok975)* was out-crossed 8 times with WT (N2) animals to clear any mutational background. HT115 (DE3) bacteria transformed with vectors expressing dsRNA of *flcn-1* and *bec-1* were obtained from the Julie Ahringer's RNAi library [a kind gift from the laboratory of Dr. Richard Roy (McGill university)]. HT115 (DE3) bacteria transformed with vectors expressing dsRNA of *let-363* (TOR) and *rsks-1*(S6K) were a kind gift from the laboratory of Dr. Xiaomeng Long, Massachusetts General Hospital. All RNAi clones were grown at 37^{o}C and seeded onto NGM plates containing ampicillin (500ug/ml) and IPTG (1mM). L3 synchronized worms were placed on the *bec-1* RNAi plates as it has been reported to be most effective inhibitor of autophagy at this stage [51]. Young adult worms were placed on the *let-363* and *rsks-1* RNAi plates as it has been reported to cause developmental defects if applied prior to this stage [43]. L1 synchronized worms were placed on *flcn-1* RNAi plates for all *flcn-1* knockdown experiments.

Lifespan assays

Worm lifespan assays were performed at 20^{o}C. Worm populations were synchronized by treating a population of *C.elegans* with hypochlorite/NaOH solution and transferring the

resulting eggs to NGM agar plates seeded with the *E.coli* strain OP50. At the L4 molt, animals were transferred to plates containing 50 μM 5-fluoro-2′-deoxyuridine (FUDR, Sigma-Aldrich), which inhibits the development of the progeny and thus abrogate the need for transferring nematodes during lifespan assays. Control experiments indicated that this concentration of FUDR does not significantly affect the lifespan of nematodes during which no RNAi feeding was used. However, FUDR has been observed to affect different aspects relating to organismal aging, including RNAi-induced longevity phenotypes (please refer to "Methods" in ref [51]), therefore we excluded the use of FUDR in the lifespan analysis were feeding RNAi was used to knockdown genes of interest. Instead, we transferred the nematode populations every-other day into a fresh RNAi plate (with no FUDR) during the lifespan assays. Larval stage (L4) was counted as day one for all lifespan measurements. Worms were examined every other day until death and were scored as dead when they were no longer able to move even in response to prodding with a platinum pick. Every other day, any dead worms were removed from plates and the deaths were recorded. For each lifespan assay, 90 worms were used in 3 plates (30worms/plate). Animals that crawled off the plate or died from matricidal hatching (the bag-of-worms phenotype) or protrusion of the gonads through the vulva were censored. Censoring describes an event where partial information on the lifespan of the nematode is lost as a consequence of premature death. Censored animals were included in statistical analysis only until the day of the censoring event.

Plasmid constructions and transgenic line

2.8kb endogenous promoter of *flcn-1* was generated by PCR from WT(N2) genomic DNA (Forward primer:5'- AAAACTGCAGCGTCTTCTCGTTTCACAGTAGTCA-3and reverse primer: 5'-GCTCTAGATTGAATTCTGTAAAAACATGAATTTGA-3') and cloned into pPD 95.77 (GFP expression plasmid- A kind gift from the laboratory of Dr. Richard Roy, McGill University) at PstI and XbaI sites. *flcn-1* cDNA was obtained from an RT–PCR reaction performed on wild type worm RNA extracts using the following: forward primer 5'-GCTCTAGAATGCAAGCAGTAATAGCACTTTGT-3' and Reverse primer 5'-CGGGATCCACGAGCAGTAGAGGTTTGAGACTG-3'. *flcn-1* cDNA was subsequently cloned into pPD 95.77 (GFP expression plasmid-with *flcn-1* endogenous promoter region) at XbaI and BamHI sites. To generate the *flcn-1:: GFP* fusion in the

flcn-1(ok975) mutant, we micro-injected *flcn-1(ok975)* worms with the above generated GFP construct (pPD95.77: *flcn-1::*GFP) at 50–100 ng/ μl.

Protein extraction and western blotting analysis

Worm populations were synchronized by treating a population of *C.elegans* with hypochlorite/NaOH solution and allowed the eggs to hatch overnight in an M9 buffer solution. Next day, the L1 nematode populations were transferred to NGM agar plates seeded with the *E.coli* strain OP50 till they develop to the one day adult stage. Worm populations were separated from bacteria using sucrose flotation and washed three times with ice-cold M9 buffer. Optional, at this point animals could be frozen at -80^{o}C for future analysis or lysed for further gel analysis. Worm pellets were lysed with HB buffer (homogenization buffer: 15mM Hepes pH7.6, 10mM KCl, 1.5mM MgCl2, 0.1mM EDTA, 0.5M EGTA, 44mM Sucrose, 1mM DTT freshly added, protease inhibitor cocktail 1 tablet in 10ml of buffer freshly added [Roche Molecular Biochemicals]) using sonication 5 pulses (intensity 17%) for 5 seconds each with a 1 minute chill on ice between pulses. Samples were then centrifuged for 10 min at 12,000 × g to clear the lysate off of insoluble portions. Supernatants (referred to as whole worms lysate) were used for protein quantification using Bradford assay, and a portion was boiled in sample buffer and applied for SDS-PAGE. Proteins were then transferred for 1 hour and 10 minutes at 100V at 4^{o}C to nitrocellulose membrane (Bio-Rad). Blocking of membranes was done for one hour in 5% fat-free milk in PBST (0.1% Tween-20) at room temperature (RT). Primary antibodies: 1) rabbit monoclonal anti-phospho-Thr^{172} of human AMPK α (Cell Signaling Technology, Inc. Dilution 1:1000) to detect worm AAK-2 phosphorylated form was used. It is important to mention that the Thr^{172} is a phosphorylation site that is embedded in a sequence conserved between human and worm AAK-2 (recognizes same band as Thr^{243} of the AAK-2 protein) [19, 113, 114]. 2) Rat polyclonal anti-PAR-4 antibody (kindly provided to us by the laboratory Dr. Richard Roy, McGill University-Dilution 1:1000). 3) Rabbit polyclonal anti-STRAD-1 antibody (kindly provided to us by the laboratory of Dr. Richard Roy McGill university-Dilution 1:100). 4) mouse monoclonal α-tubulin (Sigma-Aldrich- Dilution 1:1000). 5) Rabbit polyclonal anti-GFP antibody (kindly provided to us by the laboratory of Dr. Richard Roy, McGill University). Bound antibodies were detected with horseradish peroxidase

(HRP)-conjugated anti-mouse (Jackson Laboratories) at 1:10,000 or HRP-conjugated anti-rabbit (Amersham) at 1:5000 using Western Lightening Plus-ECL chemiluminescent kit (Perkin Elmer) according to the manufacturer's instruction.

Slow growth assays

Slow growth assays were performed at 20^{o}C. Both WT (N2) and *flcn-1* worm populations were synchronized by treating with hypochlorite/NaOH solution and eggs were allowed to hatch overnight in an M9 buffer solution. Next day, the L1 nematode populations were transferred to NGM agar plates seeded with the *E.coli* strain OP50. Larval stage (L1) was counted as time point zero for growth assay experiments. Different larval stages were identified after 18h, 24h, 42h and 48h time point. Therefore, the developmental stage of the worms was assessed twice a day and recorded, until adulthood was reached during which the difference in development cannot be further detected. All experiments were performed in triplicates and for each growth assay experiment 30 worms were scored per NGM plate.

Egg-laying defect assays

Egg-laying defect were performed at 20^{o}C. Both WT (N2) and *flcn-1* worm populations were synchronized by treating with hypochlorite/NaOH solution and eggs were allowed to hatch overnight in an M9 buffer solution followed by plating on NGM agar plates seeded with the *E.coli* strain OP50. At the L4 molt, 6 nematodes of each strain were transferred onto their separate NGM plates seeded with the *E.coli* strain OP50. Larval stage (L4) was counted as day zero for all egg-laying measurement. The number of eggs laid per day by each nematode was recorded then the nematode was transferred to a fresh NGM plate thus preventing a mixture of generations. The number of eggs laid was quantified up until the adult nematodes arrested progeny formation. Egg-laying experiments were performed 6 times in two independent trials.

Quantification of total triglyceride content

Worm populations were synchronized by treating a population of *C.elegans* with hypochlorite/NaOH solution and allowed the eggs to hatch overnight in an M9 buffer solution. After 12-16 hours, the L1 nematode populations were transferred to NGM agar plates seeded with the *E.coli* strain OP50 until they develop to the L4 larval stage at

20°C. At the L4 molt, animals were transferred to plates containing 50 µM 5-fluoro-2′-deoxyuridine (FUDR, Sigma-Aldrich) to prevent progeny formation. After an incubation of 16 h, one day adult nematodes were harvested by three consecutive washes in ice-cold M9 buffer to separate nematodes from bacteria and worm pellets were weighed. Optional, at this point animals could be frozen at -80°C for future analysis or lysed for triglyceride content analysis. Worm pellets were lysed with HB buffer (homogenization buffer: 15mM Hepes pH7.6, 10mM KCl, 1.5mM MgCl2, 0.1mM EDTA, 0.5M EGTA, 44mM Sucrose, 1mM DTT freshly added, protease inhibitor cocktail 1 tablet in 10ml of buffer freshly added [Roche Molecular Biochemicals] and the ratio of lysis buffer to worm pellet weight was 3:1 (i.e. for every 100mg of nematode pellet 300ul of lysis buffer was used) followed by sonication 5 pulses (intensity 17%) for 5 seconds each with a 1 minute chill on ice between pulses. Samples were then centrifuged for 10 min at 12,000 × g to clear the lysate off of insoluble portions. Supernatants were used for total triglyceride quantification with a commercially available triglyceride determination kit (Sigma-Aldrich) as previously described [115]. Total triglyceride levels were normalized to protein content, which was determined according to the Bradford assay method. Total triglyceride quantification experiments were done in duplicates in three independent trials. The averages of the duplicates were compared in the three independent biological trials.

Oil-Red-O staining of fat content

Procedure was performed as described in O'Rourke *et al* [116]. Worm populations were synchronized by treating a population of *C.elegans* with hypochlorite/NaOH solution and allowed the eggs to hatch overnight in an M9 buffer solution. After 12-16 hours, the L1 nematode populations were transferred to NGM agar plates seeded with the *E.coli* strain OP50 until they develop to one day adult stage at 20°C. Oil-Red-O staining was conducted by washing 200-300 one day adult nematodes with 1x PBS. Worms were washed three times with 1x PBS pH 7.4 and allowed to settle by gravity to separate from bacteria. To permeabilize the cuticle, worms were resuspended in 120µl of PBS to which an equal volume of 2x MRWB buffer containing 2% paraformaldehyde(PFA) was freshly added (2x MRWB buffer: 160 mM KCl, 40 mM NaCl, 14 mM Na2EGTA, 1 mM spermidine-HCl, 0.4 mM spermine, 30 mM Na-PIPES pH 7.4, 0.2% ß-mercaptoethanol).

Samples were gently rocked for 1h at room temperature (allowing animals to rock inside the volume, without spreading the 240µl volume over the whole tube). Animals were allowed to settle by gravity, buffer was aspirated, and worms were washed with 1x PBS to remove PFA. Worms were then resuspended in 60% isopropanol and incubated for 15 minutes at room temperature (RT) to dehydrate. Oil-Red-O is prepared as follows: a 0.5g/100mL isopropanol stock solution equilibrated for 3 days was freshly diluted to 60% with water and rocked for at least 1h, then filtered with 0.45µm-filter. The Oil-Red-O solid poweder was kindly provided to us by the laboratory of Dr. Richard Roy, McGill University. After allowing worms to settle, isopropanol was removed, 1 mL of 60% Oil-Red-O stain was added, and animals were incubated overnight with rocking. Dye was removed after allowing worms to settle, and 200 µL of 1x PBS 0.01% TritonX-100 was added. Animals were mounted and imaged with a Leica colour camera outfitted with DIC optics. Images were taken at 63X magnification. All equipment was kindly provided to us by the laboratory of Dr. Richard Roy, McGill University.

Respiration assays

The procedure was performed as described in Feng *et al.* [77]. Worm populations were synchronized by treating a population of *C.elegans* with hypochlorite/NaOH solution and allowed the eggs to hatch overnight in an M9 buffer solution. After 12-16 hours, the L1 nematode populations were transferred to NGM agar plates seeded with the *E.coli* strain OP50 until they develop to young adult stage at 20^{o}C. Approximately 4000 worms were washed free of bacteria by sucrose flotation, resuspended in M9, and washed three times with M9 solution. Worm samples were incubated in a waterbath at 20°C for the duration of the entire experiment. Oxygen concentration was monitored with a Clark electrode in a closed chamber for 10-20 minutes. Worms were then collected from chamber, pelleted, and kept at−80°C for protein quantification. Worm sample pellets were lysed as described above and subjected to Bradford assay for protein quantification. Oxygen consumption was normalized to protein content of each individual sample. Respiration assays were performed in triplicates in 5 independent biological trails. All equipment and advice for respiration levels experiments were kindly provided to us by the laboratory of Dr. Seigfried Hekimi, McGill University.

Quantification of autophagy levels

The levels of autophagy in the WT (N2) and *flcn-1(ok975)* mutants was assessed using LGG-1:: GFP translational reporter previously characterized in Melendez *et al.* [92]. We generated a *flcn-1(ok975)* mutant that expressed a GFP-tagged LGG-1 by mating *flcn-1* mutants with the transgenic strain carrying the LGG-1:: GFP reporter. Animals were grown and maintained at 20^{o}C as described above. GFP positive puncta were counted in lateral hypodermal seam cells of WT (N2) and *flcn-1(ok975)* mutant L3 animals using a Zeiss Axiophot microscope equipped with fluorescent optics. Three to ten seam cells were examined in each of approximately 20 animals from two independent biological trials. Western blot analysis were performed as described above using an anti-GFP protein specific antibody to detect the levels of PE-LGG-1::GFP (bound to autophagosomal and pre-autophagosomal structures) and LGG-1::GFP found in the cytosol.

Quantification of ROS formation

The procedure was performed as described in Schulz *et al*. [19]. Worm populations were synchronized by treating a population of *C.elegans* with hypochlorite/NaOH solution and allowed the eggs to hatch overnight in an M9 buffer solution. After 12-16 hours, the L1 nematode populations were transferred to NGM agar plates seeded with the *E.coli* strain OP50 until they develop to one day adult stage at 20^{o}C. One day adult worms were collected and washed 3 times with cold M9 buffer to separate from bacteria. Animals were resuspended in M9 buffer, and a 50 µl volume of the suspension was pipetted in triplicates into the wells of a 96-well plate with opaque walls and transparent bottom and allowed to equilibrate to room temperature (RT). In the meantime, a fresh 100 µM 2,7-dichlorodihydrofluorescein-diacetate (H_2-DCF-DA) (Sigma-Aldrich) solution from a 100 mM stock solution in DMSO was prepared in M9 buffer, and a volume of 50 µl was pipetted to the suspensions, resulting in a final concentration of 50 µM. On each plate control wells containing nematodes from each treatment without H_2-DCF-DA and wells containing H_2-DCF-DA without animals were prepared in parallel. Immediately after addition of H_2-DCF-DA, basal fluorescence was measured in a microplate reader at excitation/emission wavelengths of 485 and 520 nm. Plate reader was kindly provided to us by the laboratory of Dr. Michael Tremblay, McGill University.

Plates were kept on a shaker at 20°C for 60 min and were measured under the previous conditions. The initial fluorescence and the fluorescence signals of the control wells were subtracted from the corresponding signals of each well after the second measurement. One milliliter of the initial animal suspension from each sample was centrifuged, and the pellets were kept at− 80°C for later protein quantification using Bradford assay to normalize the fluorescence signal. ROS quantification experiments were performed in three independent biological trials.

ROS resistance assays

The procedure was performed as described in Schulz *et al.* [19]. Worm populations were synchronized by treating a population of *C.elegans* with hypochlorite/NaOH solution and allowed the eggs to hatch overnight in an M9 buffer solution. After 12-16 hours, the L1 nematode populations were transferred to NGM agar plates seeded with the *E.coli* strain OP50 until they develop to the L3 larval stage at 20^{o}C. A population of 40-50 of each of WT (N2) and *flcn-1(ok975)* adult worms were maintained for 5- 6 days on regular NGM plates with OP50 *E.coli* bacteria at 20^{o}C, until progeny production ceased. Another 40-50 WT(N2) and *flcn-1(ok975)* L3 worms were maintained for 6 days on *bec-1* RNAi plates at 20^{o}C , until progeny production ceased. *bec-1* knockdown by RNAi feeding at the L3 stage has been previously shown to be the most effective stage to inhibit autophagy [51]. The 6 day treatment appeared necessary, as most animals died due to internal hatching if the stressor was applied earlier throughout the egg-laying period. After 6 days, nematodes were transferred to plates containing 50 mM paraquat (Sigma-Aldrich). Dead animals were scored as described above in lifespan assays.

References

1. Nystrom, T., *Aging in bacteria.* Curr Opin Microbiol, 2002. **5**(6): p. 596-601.
2. Mortimer, R.K. and J.R. Johnston, *Life span of individual yeast cells.* Nature, 1959. **183**(4677): p. 1751-2.
3. Friedman, D.B. and T.E. Johnson, *A mutation in the age-1 gene in Caenorhabditis elegans lengthens life and reduces hermaphrodite fertility.* Genetics, 1988. **118**(1): p. 75-86.
4. Partridge, L., *Some highlights of research on aging with invertebrates, 2008.* Aging Cell, 2008. **7**(5): p. 605-8.
5. Chalfie, M., et al., *Green fluorescent protein as a marker for gene expression.* Science, 1994. **263**(5148): p. 802-5.
6. Fire, A., et al., *Potent and specific genetic interference by double-stranded RNA in Caenorhabditis elegans.* Nature, 1998. **391**(6669): p. 806-11.
7. Chang, L., S.H. Chiang, and A.R. Saltiel, *Insulin signaling and the regulation of glucose transport.* Mol Med, 2004. **10**(7-12): p. 65-71.
8. Wolkow, C.A., et al., *Insulin receptor substrate and p55 orthologous adaptor proteins function in the Caenorhabditis elegans daf-2/insulin-like signaling pathway.* J Biol Chem, 2002. **277**(51): p. 49591-7.
9. Hertweck, M., C. Gobel, and R. Baumeister, *C. elegans SGK-1 is the critical component in the Akt/PKB kinase complex to control stress response and life span.* Dev Cell, 2004. **6**(4): p. 577-88.
10. Brazil, D.P., Z.Z. Yang, and B.A. Hemmings, *Advances in protein kinase B signalling: AKTion on multiple fronts.* Trends Biochem Sci, 2004. **29**(5): p. 233-42.
11. Lee, R.Y., J. Hench, and G. Ruvkun, *Regulation of C. elegans DAF-16 and its human ortholog FKHRL1 by the daf-2 insulin-like signaling pathway.* Curr Biol, 2001. **11**(24): p. 1950-7.
12. Narbonne, P. and R. Roy, *Inhibition of germline proliferation during C. elegans dauer development requires PTEN, LKB1 and AMPK signalling.* Development, 2006. **133**(4): p. 611-9.
13. Baugh, L.R. and P.W. Sternberg, *DAF-16/FOXO regulates transcription of cki-1/Cip/Kip and repression of lin-4 during C. elegans L1 arrest.* Curr Biol, 2006. **16**(8): p. 780-5.
14. Kenyon, C., et al., *A C. elegans mutant that lives twice as long as wild type.* Nature, 1993. **366**(6454): p. 461-4.
15. Tullet, J.M., et al., *Direct inhibition of the longevity-promoting factor SKN-1 by insulin-like signaling in C. elegans.* Cell, 2008. **132**(6): p. 1025-38.
16. Kenyon, C., *The plasticity of aging: insights from long-lived mutants.* Cell, 2005. **120**(4): p. 449-60.
17. Lee, S.J., C.T. Murphy, and C. Kenyon, *Glucose shortens the life span of C. elegans by downregulating DAF-16/FOXO activity and aquaporin gene expression.* Cell Metab, 2009. **10**(5): p. 379-91.
18. Wang, M.C., E.J. O'Rourke, and G. Ruvkun, *Fat metabolism links germline stem cells and longevity in C. elegans.* Science, 2008. **322**(5903): p. 957-60.
19. Schulz, T.J., et al., *Glucose restriction extends Caenorhabditis elegans life span by inducing mitochondrial respiration and increasing oxidative stress.* Cell Metab, 2007. **6**(4): p. 280-93.
20. David, D.C., et al., *Widespread protein aggregation as an inherent part of aging in C. elegans.* PLoS Biol. **8**(8): p. e1000450.

21. Apfeld, J. and C. Kenyon, *Cell nonautonomy of C. elegans daf-2 function in the regulation of diapause and life span.* Cell, 1998. **95**(2): p. 199-210.
22. Libina, N., J.R. Berman, and C. Kenyon, *Tissue-specific activities of C. elegans DAF-16 in the regulation of lifespan.* Cell, 2003. **115**(4): p. 489-502.
23. Wolkow, C.A., et al., *Regulation of C. elegans life-span by insulinlike signaling in the nervous system.* Science, 2000. **290**(5489): p. 147-50.
24. Murphy, C.T., S.J. Lee, and C. Kenyon, *Tissue entrainment by feedback regulation of insulin gene expression in the endoderm of Caenorhabditis elegans.* Proc Natl Acad Sci U S A, 2007. **104**(48): p. 19046-50.
25. Bishop, N.A. and L. Guarente, *Two neurons mediate diet-restriction-induced longevity in C. elegans.* Nature, 2007. **447**(7144): p. 545-9.
26. Bartke, A., *Insulin and aging.* Cell Cycle, 2008. **7**(21): p. 3338-43.
27. Yuan, R., et al., *Aging in inbred strains of mice: study design and interim report on median lifespans and circulating IGF1 levels.* Aging Cell, 2009. **8**(3): p. 277-87.
28. Selman, C., et al., *Evidence for lifespan extension and delayed age-related biomarkers in insulin receptor substrate 1 null mice.* FASEB J, 2008. **22**(3): p. 807-18.
29. Kappeler, L., et al., *Brain IGF-1 receptors control mammalian growth and lifespan through a neuroendocrine mechanism.* PLoS Biol, 2008. **6**(10): p. e254.
30. Kojima, T., et al., *Association analysis between longevity in the Japanese population and polymorphic variants of genes involved in insulin and insulin-like growth factor 1 signaling pathways.* Exp Gerontol, 2004. **39**(11-12): p. 1595-8.
31. Suh, Y., et al., *Functionally significant insulin-like growth factor I receptor mutations in centenarians.* Proc Natl Acad Sci U S A, 2008. **105**(9): p. 3438-42.
32. Li, Y., et al., *Genetic association of FOXO1A and FOXO3A with longevity trait in Han Chinese populations.* Hum Mol Genet, 2009. **18**(24): p. 4897-904.
33. Willcox, B.J., et al., *FOXO3A genotype is strongly associated with human longevity.* Proc Natl Acad Sci U S A, 2008. **105**(37): p. 13987-92.
34. Flachsbart, F., et al., *Association of FOXO3A variation with human longevity confirmed in German centenarians.* Proc Natl Acad Sci U S A, 2009. **106**(8): p. 2700-5.
35. Anselmi, C.V., et al., *Association of the FOXO3A locus with extreme longevity in a southern Italian centenarian study.* Rejuvenation Res, 2009. **12**(2): p. 95-104.
36. Pawlikowska, L., et al., *Association of common genetic variation in the insulin/IGF1 signaling pathway with human longevity.* Aging Cell, 2009. **8**(4): p. 460-72.
37. Kaeberlein, T.L., et al., *Lifespan extension in Caenorhabditis elegans by complete removal of food.* Aging Cell, 2006. **5**(6): p. 487-94.
38. Cypser, J.R., P. Tedesco, and T.E. Johnson, *Hormesis and aging in Caenorhabditis elegans.* Exp Gerontol, 2006. **41**(10): p. 935-9.
39. Lee, G.D., et al., *Dietary deprivation extends lifespan in Caenorhabditis elegans.* Aging Cell, 2006. **5**(6): p. 515-24.
40. Greer, E.L. and A. Brunet, *Different dietary restriction regimens extend lifespan by both independent and overlapping genetic pathways in C. elegans.* Aging Cell, 2009. **8**(2): p. 113-27.
41. Li, Y., et al., *SirT1 inhibition reduces IGF-I/IRS-2/Ras/ERK1/2 signaling and protects neurons.* Cell Metab, 2008. **8**(1): p. 38-48.
42. Kaeberlein, M., et al., *Regulation of yeast replicative life span by TOR and Sch9 in response to nutrients.* Science, 2005. **310**(5751): p. 1193-6.
43. Hansen, M., et al., *Lifespan extension by conditions that inhibit translation in Caenorhabditis elegans.* Aging Cell, 2007. **6**(1): p. 95-110.

44. Kapahi, P., et al., *Regulation of lifespan in Drosophila by modulation of genes in the TOR signaling pathway.* Curr Biol, 2004. **14**(10): p. 885-90.
45. Honjoh, S., et al., *Signalling through RHEB-1 mediates intermittent fasting-induced longevity in C. elegans.* Nature, 2009. **457**(7230): p. 726-30.
46. Rogina, B. and S.L. Helfand, *Sir2 mediates longevity in the fly through a pathway related to calorie restriction.* Proc Natl Acad Sci U S A, 2004. **101**(45): p. 15998-6003.
47. Greer, E.L., et al., *An AMPK-FOXO pathway mediates longevity induced by a novel method of dietary restriction in C. elegans.* Curr Biol, 2007. **17**(19): p. 1646-56.
48. Avery, L., *The genetics of feeding in Caenorhabditis elegans.* Genetics, 1993. **133**(4): p. 897-917.
49. Lakowski, B. and S. Hekimi, *The genetics of caloric restriction in Caenorhabditis elegans.* Proc Natl Acad Sci U S A, 1998. **95**(22): p. 13091-6.
50. Panowski, S.H., et al., *PHA-4/Foxa mediates diet-restriction-induced longevity of C. elegans.* Nature, 2007. **447**(7144): p. 550-5.
51. Hansen, M., et al., *A role for autophagy in the extension of lifespan by dietary restriction in C. elegans.* PLoS Genet, 2008. **4**(2): p. e24.
52. Wang, Y. and H.A. Tissenbaum, *Overlapping and distinct functions for a Caenorhabditis elegans SIR2 and DAF-16/FOXO.* Mech Ageing Dev, 2006. **127**(1): p. 48-56.
53. Kaeberlein, M., M. McVey, and L. Guarente, *The SIR2/3/4 complex and SIR2 alone promote longevity in Saccharomyces cerevisiae by two different mechanisms.* Genes Dev, 1999. **13**(19): p. 2570-80.
54. Berdichevsky, A., et al., *C. elegans SIR-2.1 interacts with 14-3-3 proteins to activate DAF-16 and extend life span.* Cell, 2006. **125**(6): p. 1165-77.
55. Heidler, T., et al., *Caenorhabditis elegans lifespan extension caused by treatment with an orally active ROS-generator is dependent on DAF-16 and SIR-2.1.* Biogerontology. **11**(2): p. 183-95.
56. Apfeld, J., et al., *The AMP-activated protein kinase AAK-2 links energy levels and insulin-like signals to lifespan in C. elegans.* Genes Dev, 2004. **18**(24): p. 3004-9.
57. Wullschleger, S., R. Loewith, and M.N. Hall, *TOR signaling in growth and metabolism.* Cell, 2006. **124**(3): p. 471-84.
58. Wang, X., et al., *Regulation of elongation factor 2 kinase by p90(RSK1) and p70 S6 kinase.* EMBO J, 2001. **20**(16): p. 4370-9.
59. Tee, A.R. and J. Blenis, *mTOR, translational control and human disease.* Semin Cell Dev Biol, 2005. **16**(1): p. 29-37.
60. Sonenberg, N. and A.C. Gingras, *The mRNA 5' cap-binding protein eIF4E and control of cell growth.* Curr Opin Cell Biol, 1998. **10**(2): p. 268-75.
61. Hay, N. and N. Sonenberg, *Upstream and downstream of mTOR.* Genes Dev, 2004. **18**(16): p. 1926-45.
62. Henderson, S.T., M. Bonafe, and T.E. Johnson, *daf-16 protects the nematode Caenorhabditis elegans during food deprivation.* J Gerontol A Biol Sci Med Sci, 2006. **61**(5): p. 444-60.
63. Vellai, T., et al., *Genetics: influence of TOR kinase on lifespan in C. elegans.* Nature, 2003. **426**(6967): p. 620.
64. Syntichaki, P., K. Troulinaki, and N. Tavernarakis, *eIF4E function in somatic cells modulates ageing in Caenorhabditis elegans.* Nature, 2007. **445**(7130): p. 922-6.
65. Jia, K., D. Chen, and D.L. Riddle, *The TOR pathway interacts with the insulin signaling pathway to regulate C. elegans larval development, metabolism and life span.* Development, 2004. **131**(16): p. 3897-906.

66. Pan, K.Z., et al., *Inhibition of mRNA translation extends lifespan in Caenorhabditis elegans.* Aging Cell, 2007. **6**(1): p. 111-9.
67. Harrison, D.E., et al., *Rapamycin fed late in life extends lifespan in genetically heterogeneous mice.* Nature, 2009. **460**(7253): p. 392-5.
68. Selman, C., et al., *Ribosomal protein S6 kinase 1 signaling regulates mammalian life span.* Science, 2009. **326**(5949): p. 140-4.
69. Wallace, D.C., *A mitochondrial paradigm of metabolic and degenerative diseases, aging, and cancer: a dawn for evolutionary medicine.* Annu Rev Genet, 2005. **39**: p. 359-407.
70. Lakowski, B. and S. Hekimi, *Determination of life-span in Caenorhabditis elegans by four clock genes.* Science, 1996. **272**(5264): p. 1010-3.
71. Jonassen, T., P.L. Larsen, and C.F. Clarke, *A dietary source of coenzyme Q is essential for growth of long-lived Caenorhabditis elegans clk-1 mutants.* Proc Natl Acad Sci U S A, 2001. **98**(2): p. 421-6.
72. Branicky, R., P.A. Nguyen, and S. Hekimi, *Uncoupling the pleiotropic phenotypes of clk-1 with tRNA missense suppressors in Caenorhabditis elegans.* Mol Cell Biol, 2006. **26**(10): p. 3976-85.
73. Braeckman, B.P., et al., *No reduction of energy metabolism in Clk mutants.* Mech Ageing Dev, 2002. **123**(11): p. 1447-56.
74. Miyadera, H., et al., *Altered quinone biosynthesis in the long-lived clk-1 mutants of Caenorhabditis elegans.* J Biol Chem, 2001. **276**(11): p. 7713-6.
75. Hihi, A.K., Y. Gao, and S. Hekimi, *Ubiquinone is necessary for Caenorhabditis elegans development at mitochondrial and non-mitochondrial sites.* J Biol Chem, 2002. **277**(3): p. 2202-6.
76. Lapointe, J. and S. Hekimi, *Early mitochondrial dysfunction in long-lived Mclk1+/- mice.* J Biol Chem, 2008. **283**(38): p. 26217-27.
77. Feng, J., F. Bussiere, and S. Hekimi, *Mitochondrial electron transport is a key determinant of life span in Caenorhabditis elegans.* Dev Cell, 2001. **1**(5): p. 633-44.
78. Dillin, A., et al., *Rates of behavior and aging specified by mitochondrial function during development.* Science, 2002. **298**(5602): p. 2398-401.
79. Lee, S.S., et al., *A systematic RNAi screen identifies a critical role for mitochondria in C. elegans longevity.* Nat Genet, 2003. **33**(1): p. 40-8.
80. Toth, M.L., et al., *Longevity pathways converge on autophagy genes to regulate life span in Caenorhabditis elegans.* Autophagy, 2008. **4**(3): p. 330-8.
81. Houthoofd, K., et al., *No reduction of metabolic rate in food restricted Caenorhabditis elegans.* Exp Gerontol, 2002. **37**(12): p. 1359-69.
82. Larsen, P.L., *Aging and resistance to oxidative damage in Caenorhabditis elegans.* Proc Natl Acad Sci U S A, 1993. **90**(19): p. 8905-9.
83. Honda, Y. and S. Honda, *The daf-2 gene network for longevity regulates oxidative stress resistance and Mn-superoxide dismutase gene expression in Caenorhabditis elegans.* FASEB J, 1999. **13**(11): p. 1385-93.
84. Brys, K., J.R. Vanfleteren, and B.P. Braeckman, *Testing the rate-of-living/oxidative damage theory of aging in the nematode model Caenorhabditis elegans.* Exp Gerontol, 2007. **42**(9): p. 845-51.
85. Dingley, S., et al., *Mitochondrial respiratory chain dysfunction variably increases oxidant stress in Caenorhabditis elegans.* Mitochondrion. **10**(2): p. 125-36.
86. Doonan, R., et al., *Against the oxidative damage theory of aging: superoxide dismutases protect against oxidative stress but have little or no effect on life span in Caenorhabditis elegans.* Genes Dev, 2008. **22**(23): p. 3236-41.

87. Petriv, O.I. and R.A. Rachubinski, *Lack of peroxisomal catalase causes a progeric phenotype in Caenorhabditis elegans.* J Biol Chem, 2004. **279**(19): p. 19996-20001.
88. Keaney, M., et al., *Superoxide dismutase mimetics elevate superoxide dismutase activity in vivo but do not retard aging in the nematode Caenorhabditis elegans.* Free Radic Biol Med, 2004. **37**(2): p. 239-50.
89. Kim, J., et al., *Effects of a potent antioxidant, platinum nanoparticle, on the lifespan of Caenorhabditis elegans.* Mech Ageing Dev, 2008. **129**(6): p. 322-31.
90. Klionsky, D.J. and S.D. Emr, *Autophagy as a regulated pathway of cellular degradation.* Science, 2000. **290**(5497): p. 1717-21.
91. Terman, A. and U.T. Brunk, *Myocyte aging and mitochondrial turnover.* Exp Gerontol, 2004. **39**(5): p. 701-5.
92. Melendez, A., et al., *Autophagy genes are essential for dauer development and life-span extension in C. elegans.* Science, 2003. **301**(5638): p. 1387-91.
93. Hars, E.S., et al., *Autophagy regulates ageing in C. elegans.* Autophagy, 2007. **3**(2): p. 93-5.
94. Harman, D., *The biologic clock: the mitochondria?* J Am Geriatr Soc, 1972. **20**(4): p. 145-7.
95. Scherz-Shouval, R., et al., *Reactive oxygen species are essential for autophagy and specifically regulate the activity of Atg4.* EMBO J, 2007. **26**(7): p. 1749-60.
96. Hardie, D.G., D. Carling, and M. Carlson, *The AMP-activated/SNF1 protein kinase subfamily: metabolic sensors of the eukaryotic cell?* Annu Rev Biochem, 1998. **67**: p. 821-55.
97. Hardie, D.G., *AMP-activated/SNF1 protein kinases: conserved guardians of cellular energy.* Nat Rev Mol Cell Biol, 2007. **8**(10): p. 774-85.
98. Kahn, B.B., et al., *AMP-activated protein kinase: ancient energy gauge provides clues to modern understanding of metabolism.* Cell Metab, 2005. **1**(1): p. 15-25.
99. Curtis, R., G. O'Connor, and P.S. DiStefano, *Aging networks in Caenorhabditis elegans: AMP-activated protein kinase (aak-2) links multiple aging and metabolism pathways.* Aging Cell, 2006. **5**(2): p. 119-26.
100. Greer, E.L., et al., *The energy sensor AMP-activated protein kinase directly regulates the mammalian FOXO3 transcription factor.* J Biol Chem, 2007. **282**(41): p. 30107-19.
101. Klass, M. and D. Hirsh, *Non-ageing developmental variant of Caenorhabditis elegans.* Nature, 1976. **260**(5551): p. 523-5.
102. Narbonne, P. and R. Roy, *Caenorhabditis elegans dauers need LKB1/AMPK to ration lipid reserves and ensure long-term survival.* Nature, 2009. **457**(7226): p. 210-4.
103. Greer, E.L. and A. Brunet, *Signaling networks in aging.* J Cell Sci, 2008. **121**(Pt 4): p. 407-12.
104. Tyner, S.D., et al., *p53 mutant mice that display early ageing-associated phenotypes.* Nature, 2002. **415**(6867): p. 45-53.
105. Maier, B., et al., *Modulation of mammalian life span by the short isoform of p53.* Genes Dev, 2004. **18**(3): p. 306-19.
106. Campisi, J., *Aging, tumor suppression and cancer: high wire-act!* Mech Ageing Dev, 2005. **126**(1): p. 51-8.
107. Garcia-Cao, I., et al., *"Super p53" mice exhibit enhanced DNA damage response, are tumor resistant and age normally.* EMBO J, 2002. **21**(22): p. 6225-35.
108. Matheu, A., et al., *Delayed ageing through damage protection by the Arf/p53 pathway.* Nature, 2007. **448**(7151): p. 375-9.

109. Bauer, J.H., et al., *Neuronal expression of p53 dominant-negative proteins in adult Drosophila melanogaster extends life span.* Curr Biol, 2005. **15**(22): p. 2063-8.
110. Tavernarakis, N., et al., *The effects of p53 on whole organism longevity are mediated by autophagy.* Autophagy, 2008. **4**(7): p. 870-3.
111. Gossage, L. and T. Eisen, *Alterations in VHL as potential biomarkers in renal-cell carcinoma.* Nat Rev Clin Oncol. **7**(5): p. 277-88.
112. Mehta, R., et al., *Proteasomal regulation of the hypoxic response modulates aging in C. elegans.* Science, 2009. **324**(5931): p. 1196-8.
113. Narbonne, P., et al., *Differential requirements for STRAD in LKB1-dependent functions in C. elegans.* Development. **137**(4): p. 661-70.
114. Lee, H., et al., *The Caenorhabditis elegans AMP-activated protein kinase AAK-2 is phosphorylated by LKB1 and is required for resistance to oxidative stress and for normal motility and foraging behavior.* J Biol Chem, 2008. **283**(22): p. 14988-93.
115. Ristow, M., et al., *Frataxin activates mitochondrial energy conversion and oxidative phosphorylation.* Proc Natl Acad Sci U S A, 2000. **97**(22): p. 12239-43.
116. O'Rourke, E.J., et al., *C. elegans major fats are stored in vesicles distinct from lysosome-related organelles.* Cell Metab, 2009. **10**(5): p. 430-5.
117. Baba, M., et al., *Folliculin encoded by the BHD gene interacts with a binding protein, FNIP1, and AMPK, and is involved in AMPK and mTOR signaling.* Proc Natl Acad Sci U S A, 2006. **103**(42): p. 15552-7.
118. Hasumi, H., et al., *Identification and characterization of a novel folliculin-interacting protein FNIP2.* Gene, 2008. **415**(1-2): p. 60-7.
119. Takagi, Y., et al., *Interaction of folliculin (Birt-Hogg-Dube gene product) with a novel Fnip1-like (FnipL/Fnip2) protein.* Oncogene, 2008. **27**(40): p. 5339-47.
120. Wang, L., et al., *Serine 62 is a phosphorylation site in folliculin, the Birt-Hogg-Dube gene product.* FEBS Lett. **584**(1): p. 39-43.
121. Rogina, B., et al., *Extended life-span conferred by cotransporter gene mutations in Drosophila.* Science, 2000. **290**(5499): p. 2137-40.
122. Kenyon, C.J., *The genetics of ageing.* Nature. **464**(7288): p. 504-12.
123. Dillin, A., D.K. Crawford, and C. Kenyon, *Timing requirements for insulin/IGF-1 signaling in C. elegans.* Science, 2002. **298**(5594): p. 830-4.
124. Hemminki, A., et al., *A serine/threonine kinase gene defective in Peutz-Jeghers syndrome.* Nature, 1998. **391**(6663): p. 184-7.
125. Jeghers, H., K.V. Mc, and K.H. Katz, *Generalized intestinal polyposis and melanin spots of the oral mucosa, lips and digits; a syndrome of diagnostic significance.* N Engl J Med, 1949. **241**(26): p. 1031-6.
126. Hawley, S.A., et al., *Complexes between the LKB1 tumor suppressor, STRAD alpha/beta and MO25 alpha/beta are upstream kinases in the AMP-activated protein kinase cascade.* J Biol, 2003. **2**(4): p. 28.
127. Woods, A., et al., *LKB1 is the upstream kinase in the AMP-activated protein kinase cascade.* Curr Biol, 2003. **13**(22): p. 2004-8.
128. Baas, A.F., et al., *Activation of the tumour suppressor kinase LKB1 by the STE20-like pseudokinase STRAD.* EMBO J, 2003. **22**(12): p. 3062-72.
129. Boudeau, J., et al., *MO25alpha/beta interact with STRADalpha/beta enhancing their ability to bind, activate and localize LKB1 in the cytoplasm.* EMBO J, 2003. **22**(19): p. 5102-14.
130. Hurley, R.L., et al., *The Ca2+/calmodulin-dependent protein kinase kinases are AMP-activated protein kinase kinases.* J Biol Chem, 2005. **280**(32): p. 29060-6.

131. Woods, A., et al., *Ca2+/calmodulin-dependent protein kinase kinase-beta acts upstream of AMP-activated protein kinase in mammalian cells.* Cell Metab, 2005. **2**(1): p. 21-33.
132. Anderson, K.A., et al., *Hypothalamic CaMKK2 contributes to the regulation of energy balance.* Cell Metab, 2008. **7**(5): p. 377-88.
133. Tokumitsu, H., et al., *Substrate recognition by Ca2+/Calmodulin-dependent protein kinase kinase. Role of the arg-pro-rich insert domain.* J Biol Chem, 1999. **274**(22): p. 15803-10.
134. Eto, K., et al., *Ca(2+)/Calmodulin-dependent protein kinase cascade in Caenorhabditis elegans. Implication in transcriptional activation.* J Biol Chem, 1999. **274**(32): p. 22556-62.
135. Kimura, Y., et al., *A CaMK cascade activates CRE-mediated transcription in neurons of Caenorhabditis elegans.* EMBO Rep, 2002. **3**(10): p. 962-6.
136. Baba, M., et al., *Kidney-targeted Birt-Hogg-Dube gene inactivation in a mouse model: Erk1/2 and Akt-mTOR activation, cell hyperproliferation, and polycystic kidneys.* J Natl Cancer Inst, 2008. **100**(2): p. 140-54.
137. Chen, J., et al., *Deficiency of FLCN in mouse kidney led to development of polycystic kidneys and renal neoplasia.* PLoS One, 2008. **3**(10): p. e3581.
138. Hartman, T.R., et al., *The role of the Birt-Hogg-Dube protein in mTOR activation and renal tumorigenesis.* Oncogene, 2009. **28**(13): p. 1594-604.
139. Hudon, V., et al., *Renal tumour suppressor function of the Birt-Hogg-Dube syndrome gene product folliculin.* J Med Genet. **47**(3): p. 182-9.
140. Kihara, A., et al., *Two distinct Vps34 phosphatidylinositol 3-kinase complexes function in autophagy and carboxypeptidase Y sorting in Saccharomyces cerevisiae.* J Cell Biol, 2001. **152**(3): p. 519-30.
141. Kihara, A., et al., *Beclin-phosphatidylinositol 3-kinase complex functions at the trans-Golgi network.* EMBO Rep, 2001. **2**(4): p. 330-5.
142. Kume, S., et al., *Calorie restriction enhances cell adaptation to hypoxia through Sirt1-dependent mitochondrial autophagy in mouse aged kidney.* J Clin Invest. **120**(4): p. 1043-55.
143. Mammucari, C., et al., *FoxO3 controls autophagy in skeletal muscle in vivo.* Cell Metab, 2007. **6**(6): p. 458-71.
144. Behrends, C., et al., *Network organization of the human autophagy system.* Nature. **466**(7302): p. 68-76.
145. Kroemer, G., G. Marino, and B. Levine, *Autophagy and the integrated stress response.* Mol Cell. **40**(2): p. 280-93.
146. Droge, W., *Free radicals in the physiological control of cell function.* Physiol Rev, 2002. **82**(1): p. 47-95.
147. Rea, S. and T.E. Johnson, *A metabolic model for life span determination in Caenorhabditis elegans.* Dev Cell, 2003. **5**(2): p. 197-203.
148. Kharade, S.V., et al., *Mrg19 depletion increases S. cerevisiae lifespan by augmenting ROS defence.* FEBS Lett, 2005. **579**(30): p. 6809-13.
149. Satterlee, J.S., W.S. Ryu, and P. Sengupta, *The CMK-1 CaMKI and the TAX-4 Cyclic nucleotide-gated channel regulate thermosensory neuron gene expression and function in C. elegans.* Curr Biol, 2004. **14**(1): p. 62-8.

Figure 1: C-terminus of FLCN-1 is Highly Conserved in the Nematode *C.elegans*.

(A) Alignment of the full length *C.elegans* FLCN-1 and mammalian FLCN c-terminal amino acid residues using ClustalW alignment software. The C-terminal region of FLCN-1 (a.a 425 to 635) is highly homologous to the mammalian FLCN. "*" means that the residues or nucleotides in that column are identical in all sequences in the alignment.":" means that conserved substitutions have been observed, according to the COLOUR table below."." means that semi-conserved substitutions are observed.

(B) Amino acid residues of wild type (WT) *C.elegans* FLCN-1 using ExPASy (Expert Protein Analysis System) software.

(C) Amino acid residues of mutant *C.elegans* FLCN-1 (mutFLCN-1) using ExPASy (Expert Protein Analysis System) software. The strain flcn-1(ok975) has 817 bp deletion causing a frameshift that introduces a stop codon after amino acid residue (a.a) 149**.**

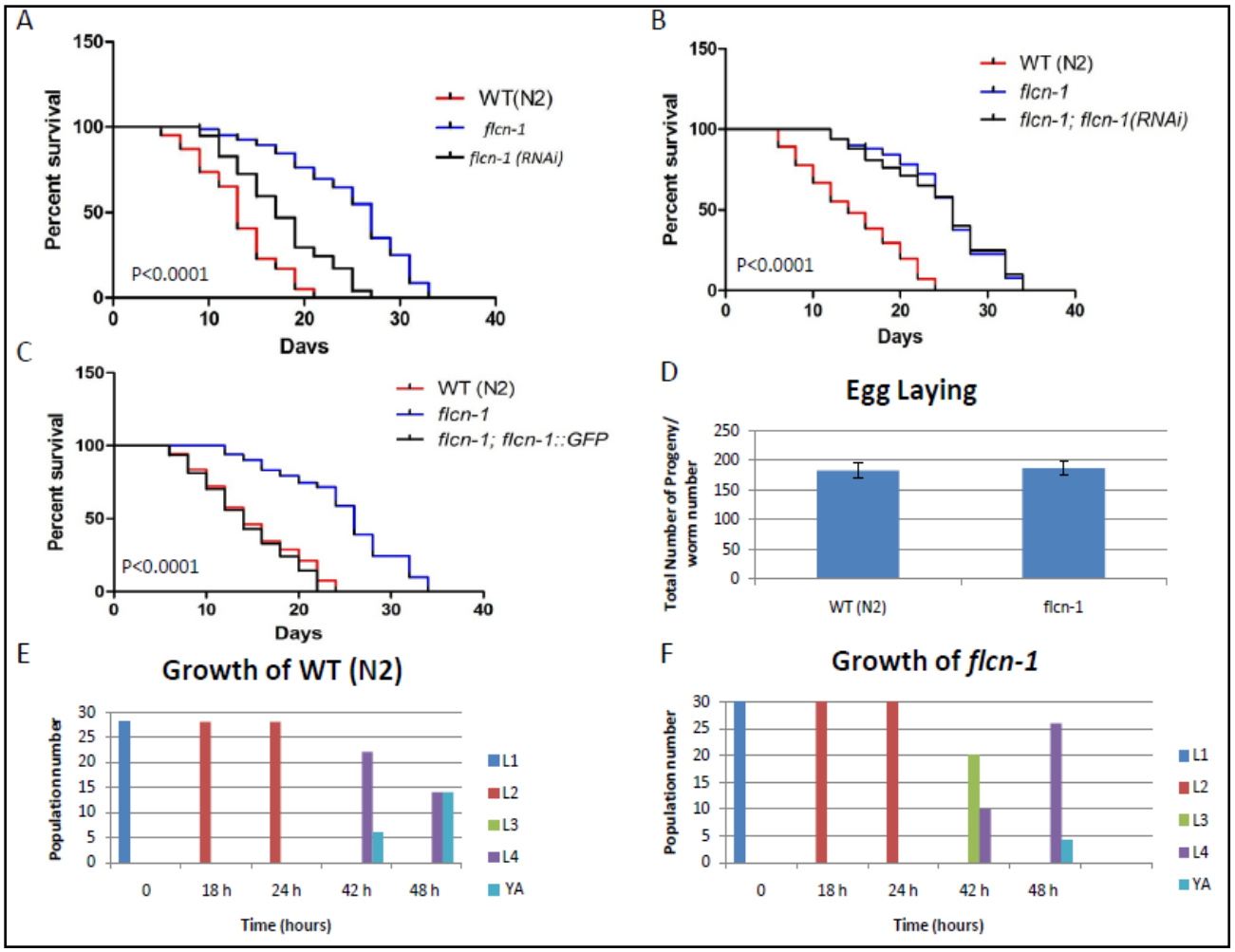

Figure 2: *flcn-1* knockout worms live 1.5 fold longer than WT (N2).

(A) Lifespan assay of *flcn-1(ok975)* mutant worms feed OP50 bacteria (Blue color), lifespan assay of WT (N2) (Red color) and lifespan assay of WT(N2) worms after knocking down *flcn-1* by RNAi feeding (Black color).

(B) Lifespan assay of *flcn-1(ok975)* mutant worms (Blue color) ,lifespan assay of WT (N2) (Red color) and lifespan assay of *flcn-1(ok975)* mutant worms after knocking down *flcn-1* by RNAi feeding (Black color).

(C) A transgene expressing flcn-1::GFP completely rescued the extended lifespan of *flcn-1(ok975)* null mutants.

(D) Egg laying assay of WT (N2) and flcn-1(ok975) null mutant worms.

(E) Growth assay of WT (N2) nematodes. L1 is first larval stage, L2 is second larval stage, L3 is third larval stage, L4 is fourth larval stage and young adult (YA) stage are shown.

(F) Growth assay of *flcn-1(ok975)* null mutants nematodes. L1 is first larval stage, L2 is second larval stage, L3 is third larval stage, L4 is fourth larval stage and young adult (YA) stage are shown.

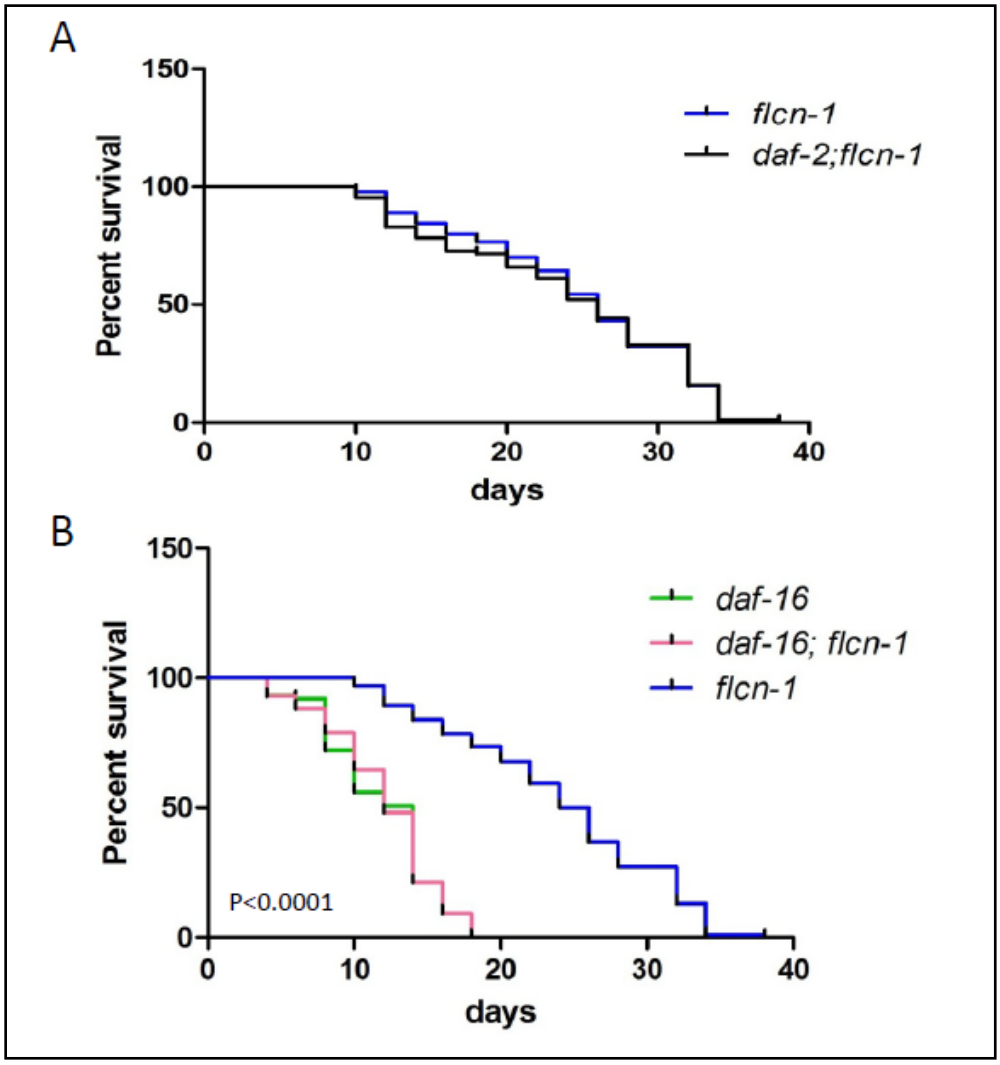

Figure 3: *flcn-1* a novel component of the Insulin/ IGF-1 like signalling pathway.

(A) Lifespan of *daf-2* mutants is *flcn-1* dependent: Lifespan assay of *flcn-1(ok975)* mutant worms (Blue color), lifespan assay of *daf-2;flcn-1* double mutant worms (Black color) and lifespan assay of *daf-2(e1370)* is still in progress (worms are still alive after 50days).

(B) Lifespan of *flcn-1* mutants is *daf-16* dependent: Lifespan assay of *flcn-1(ok975)* mutant worms (Blue color), lifespan assay of daf-16(mu86) (Green color) and lifespan assay of *daf-2;flcn-1* double mutant worms (Pink color).

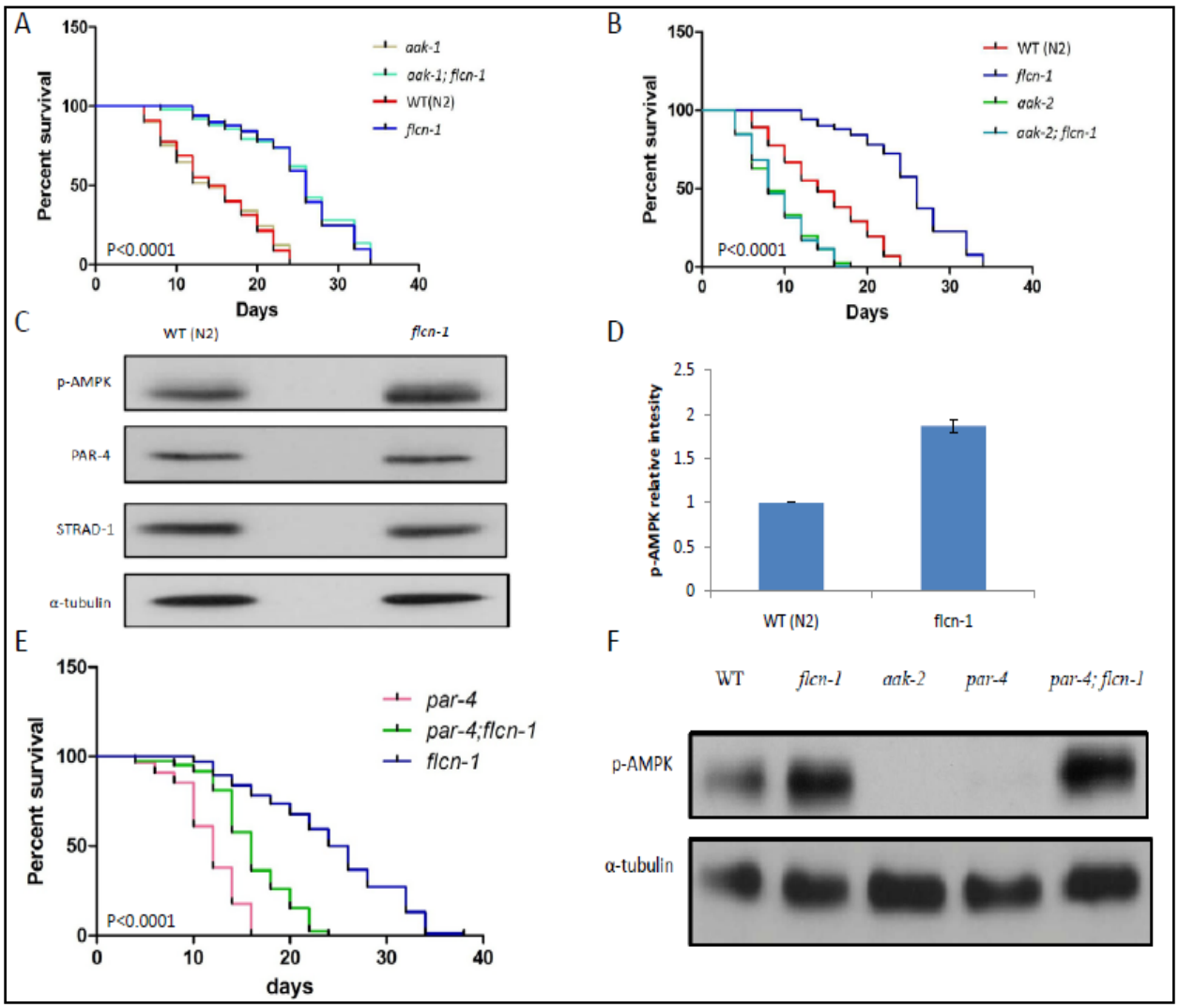

Figure 4 : *flcn-1* extends lifespan via an *aak-2* dependent and *par-4* independent mechanism.

(A) Lifespan of *flcn-1* mutants is *aak-1* dependent: Lifespan assay of *flcn-1(ok975)* mutant worms (Blue color), lifespan of WT(N2) nematodes (Red color), lifespan assay of *aak-1(tm1944)* null mutants (Gray color) and lifespan assay of *aak-1;flcn-1* double mutant worms (Sky blue color).

(B) Lifespan of *flcn-1* mutants is *aak-2* dependent: Lifespan assay of *flcn-1(ok975)* mutant worms (Blue color), lifespan of WT(N2) nematodes (Red color), lifespan assay of *aak-2(ok524)* null mutants (Green color) and lifespan assay of *aak-2;flcn-1* double mutant worms (Sky blue color).

(C) Abundance of the phosphorylated form of AAK-2/AMPK (refer to materials and methods) is increased in the *flcn-1(ok975)* null mutants compared to WT(N2) worms . No differences in the PAR-4 and STRAD-1 expression levels were observed.

(D) *flcn-1(ok975)* null mutants have a 2 fold increase in phosphorylated form of AAK-2/AMPK relative to WT(N2) nematodes. Relative levels of p-AMPK/AAK2 were quantified using Scion image softer and normalized against α-tubulin levels.

(E) Lifespan of *flcn-1* mutants is *par-4* independent: Lifespan assay of *flcn-1(ok975)* mutant worms (Blue color), lifespan assay of *par-4(it57)* mutants (Pink color) and lifespan assay of *par-4;flcn-1* double mutant worms (Green color).

(F) Abundance of the phosphorylated form of AAK-2/AMPK (refer to materials and methods) is increased in the *flcn-1(ok975)* null mutants compared to WT(N2) worms. No phosphorylated form was detected in the *aak-2(ok524)* deficient strain and *par-4 (it57)* mutant strain. Abundacne of the phosphorylated form of AAK-2/AMPK is increased in the *par-4;flcn-1* double mutants compared *par-4* mutant strain.

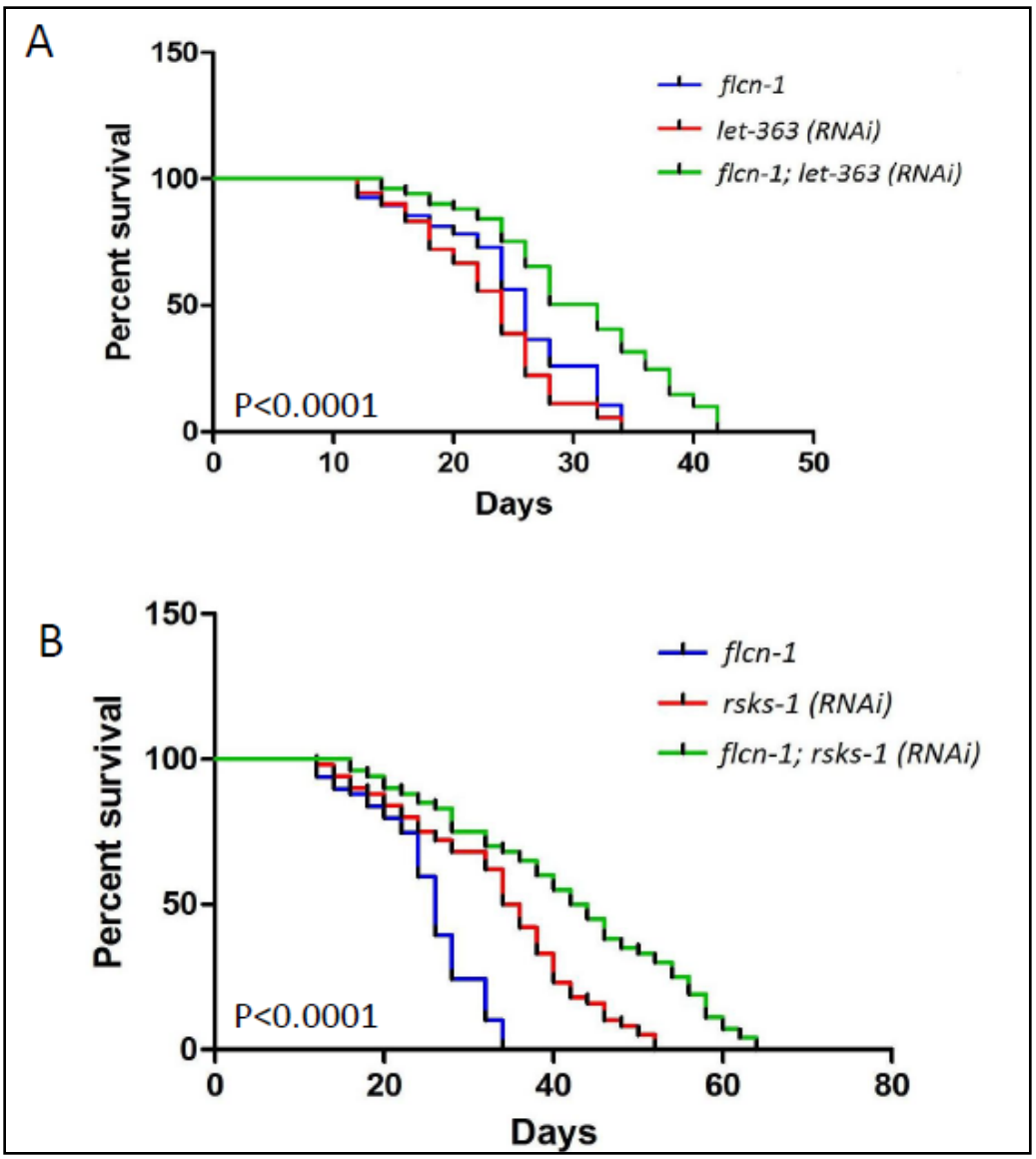

Figure 5: *flcn-1* Longevity is independent of the Protein Translation Machinery.

(A) Lifespan of *flcn-1* mutants is independent of *let-363*: Lifespan assay of *flcn-1(ok975)* mutant worms (Blue color) ,lifespan assay of WT (N2) after knocking down *let-363* by RNAi feeding (Red color) and lifespan assay of *flcn-1(ok975)* mutant worms after knocking down *let-363* by RNAi feeding (Green color).

(B) Lifespan of *flcn-1* mutants is independent of *rsks-1*: Lifespan assay of *flcn-1(ok975)* mutant worms (Blue color) ,lifespan assay of WT (N2) after knocking down *rsks-1* by RNAi feeding (Red color) and lifespan assay of *flcn-1(ok975)* mutant worms after knocking down *rsks-1* by RNAi feeding (Green color).

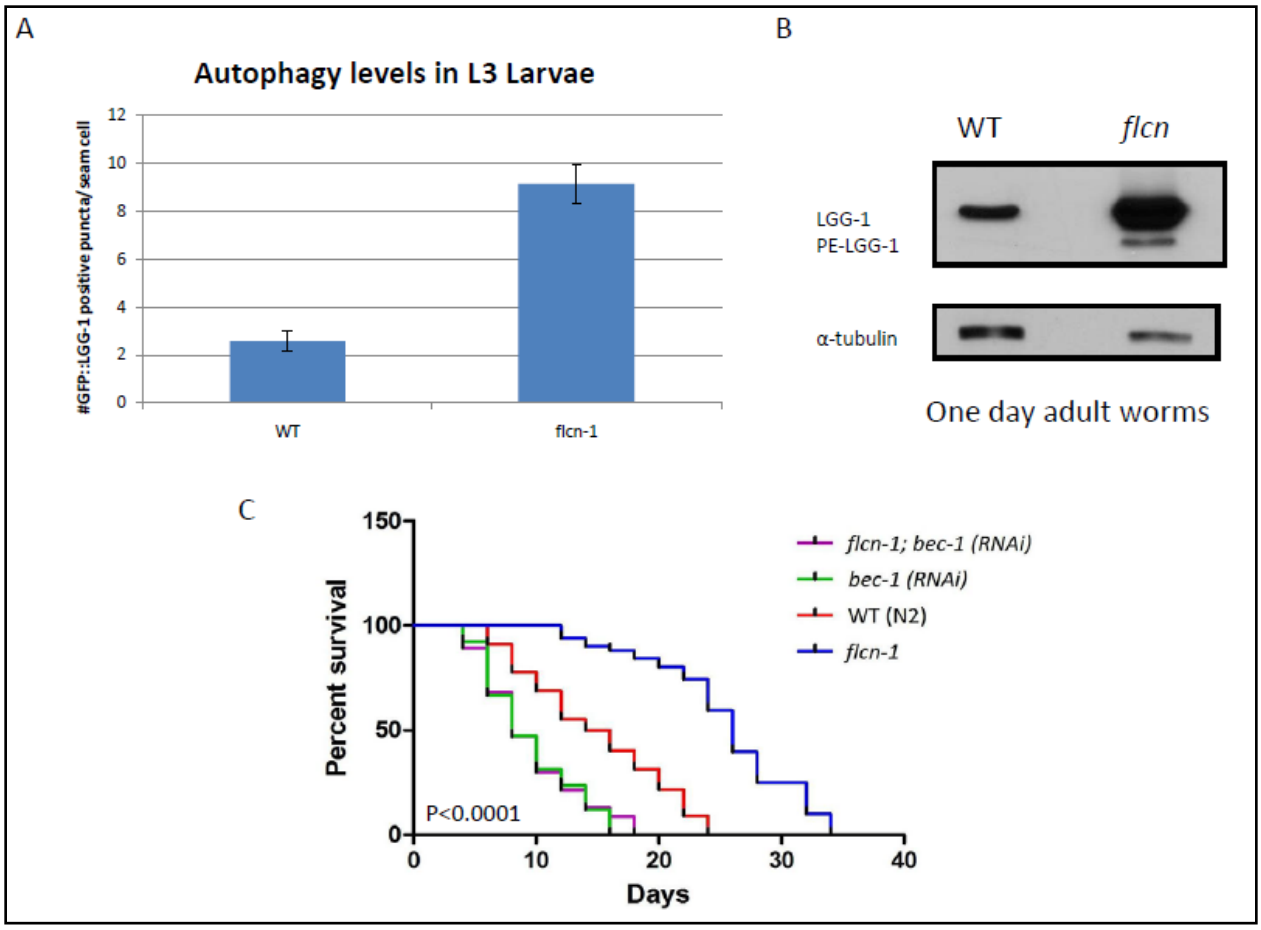

Figure 6 : Autophagy is required for *flcn-1* mediated Lifespan Extension.

(A) Elevated levels of Autophagy in the *flcn-1(ok975)* mutants. The *gfp::lgg-1* reporter gene for autophagy was expressed in the *flcn-1(ok975)* mutants and the numer of GFP::LGG-1 positive puncta in seam cells were counted in the L3 Larvae. *flcn-1* mutants increased the number of positive *gfp::lgg-1* puncta compared to WT(N2) nematodes.

(B) Western blot analysis of *flcn-1(ok975)* and WT(N2) strains expressing *gfp::lgg-1* reporter gene. Abundance of both PE-LGG-1 and LGG-1 is significantly increased in the flcn-1 null mutants compared to WT(N2) indicating elevated levels of autophagy.

(C) Lifespan of *flcn-1* mutant nematodes is autophagy dependent. Lifespan assay of *flcn-1(ok975)* mutant worms (Blue color) , lifespan assay of WT (N2) (Red color), lifespan assay of WT (N2) after knocking down *bec-1* by RNAi feeding (Green color) and lifespan assay of *flcn-1(ok975)* mutant worms after knocking down *bec-1* by RNAi feeding (Purple color).

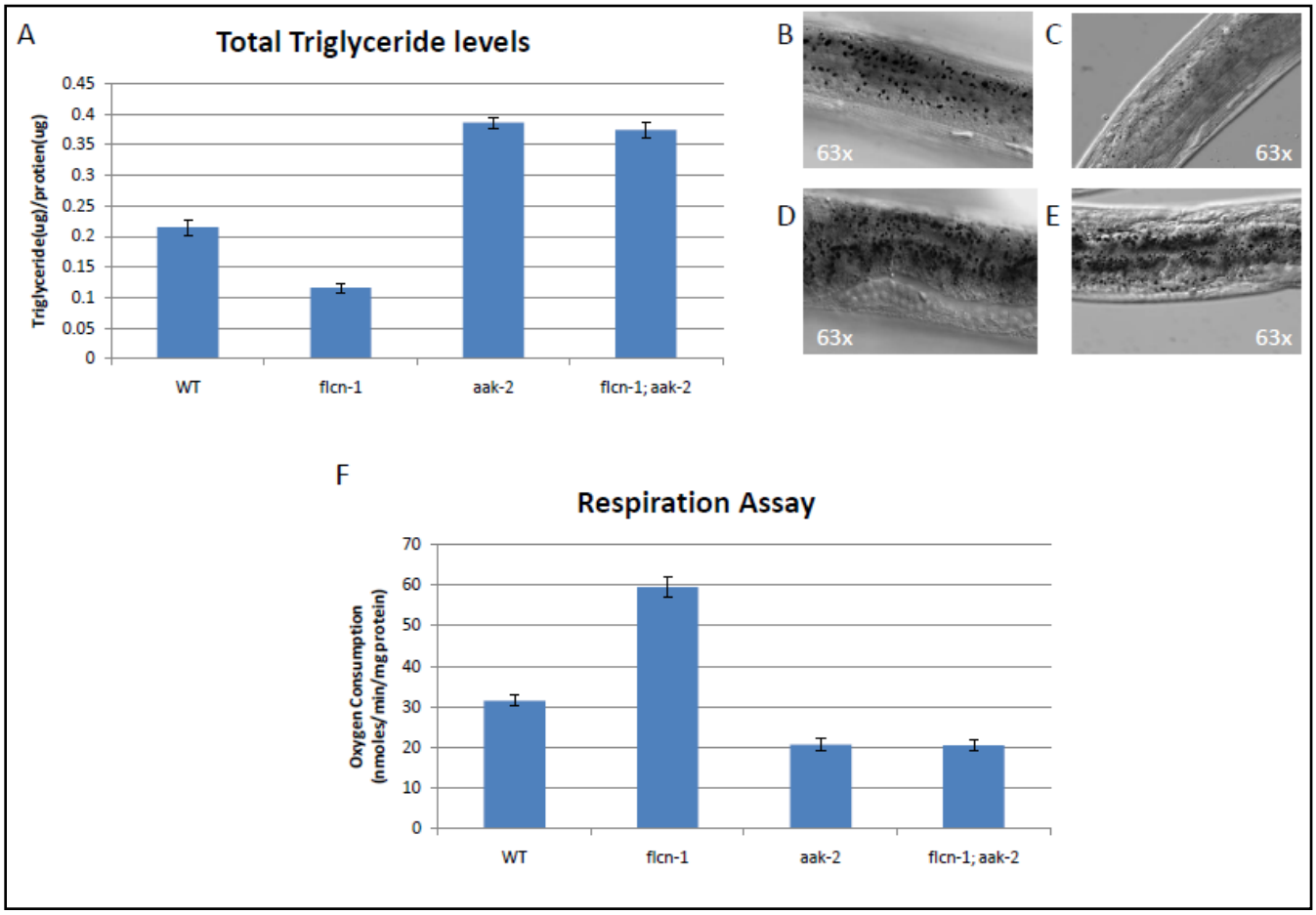

Figure 7 : *flcn-1* mutants show Elevated Respiration and Lower Triglyceride Levels through AAK-2 Activation.

(A) Triglyceride content in WT(N2), *flcn-1(ok975)* mutants, *aak-2(ok524)* mutants and *flcn-1;aak-2* double mutant worms.

(B) Oil-Red-O fat staining of WT(N2) worms

(C) Oil-Red-O fat staining of *flcn-1(ok975)* mutant worms

(D) Oil-Red-O fat staining of *aak-2(ok524)* mutant worms

(E) Oil-Red-O fat staining of *flcn-1;aak-2* double mutant worms

(F) Oxygen Consumption of young adult WT(N2), *flcn-1(ok975)* mutants, *aak-2(ok524)* mutants and *flcn-1;aak-2* double mutant worms normalized to total protein content.

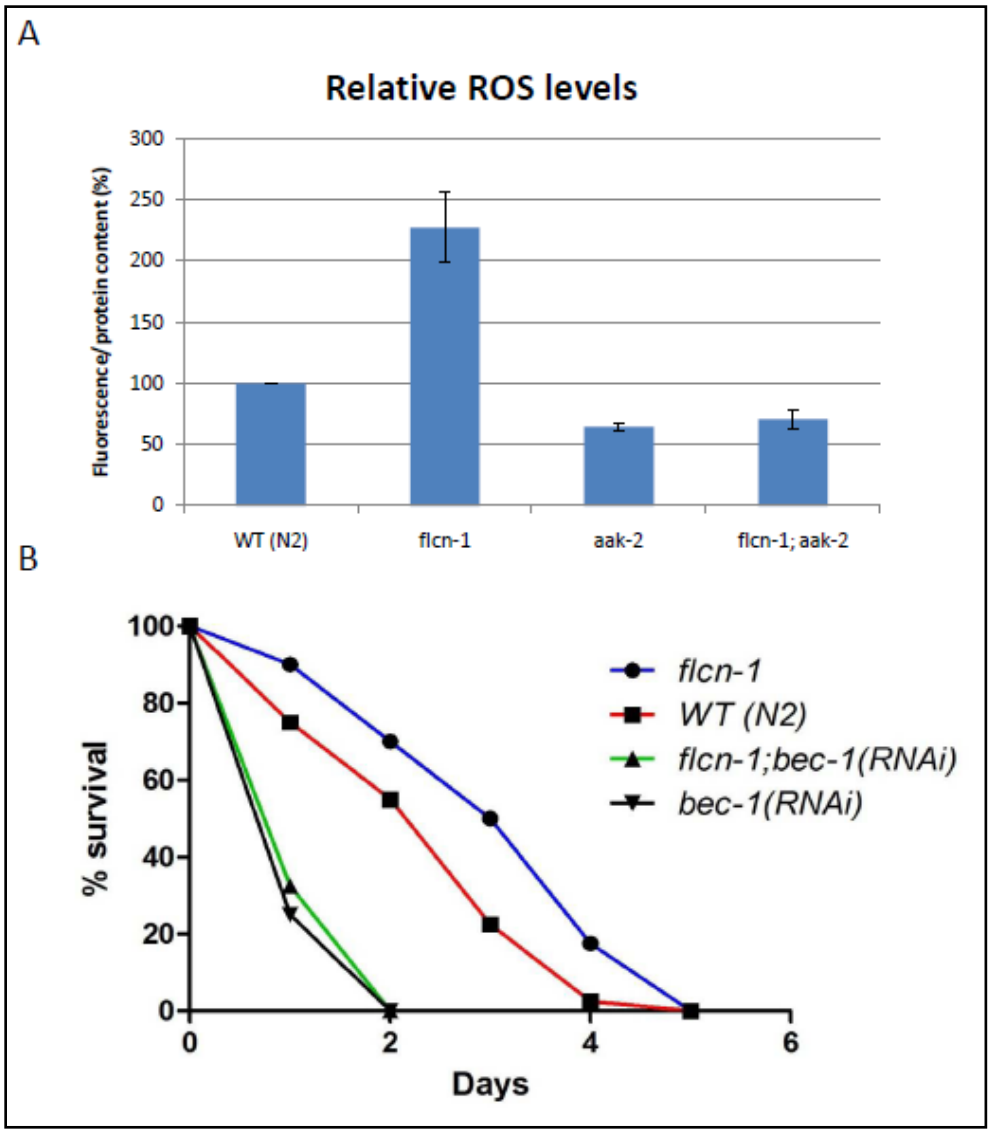

Figure 8 : *flcn-1* mutants show Elevated ROS Levels and Increased Oxidative Stress Resistance which is Autphagy dependent.

(A) Relative formation of reactive oxygen species (ROS) in WT(N2), *flcn-1(ok975)* mutants, *aak-2(ok524)* mutants and *flcn-1;aak-2* double mutant worms.

(B) Survival of nematodes on NGM plates containing 50mM paraquat. Survival of *flcn-1(ok975)* null mutants (Blue color), survival of WT(N2) worms (Blue color), survival of *flcn-1(ok975)* null mutants after knocking down *bec-1* by RNAi feeding (Green color) and survival of WT(N2) worms after knocking down *bec-1* by RNAi feeding (Black color)

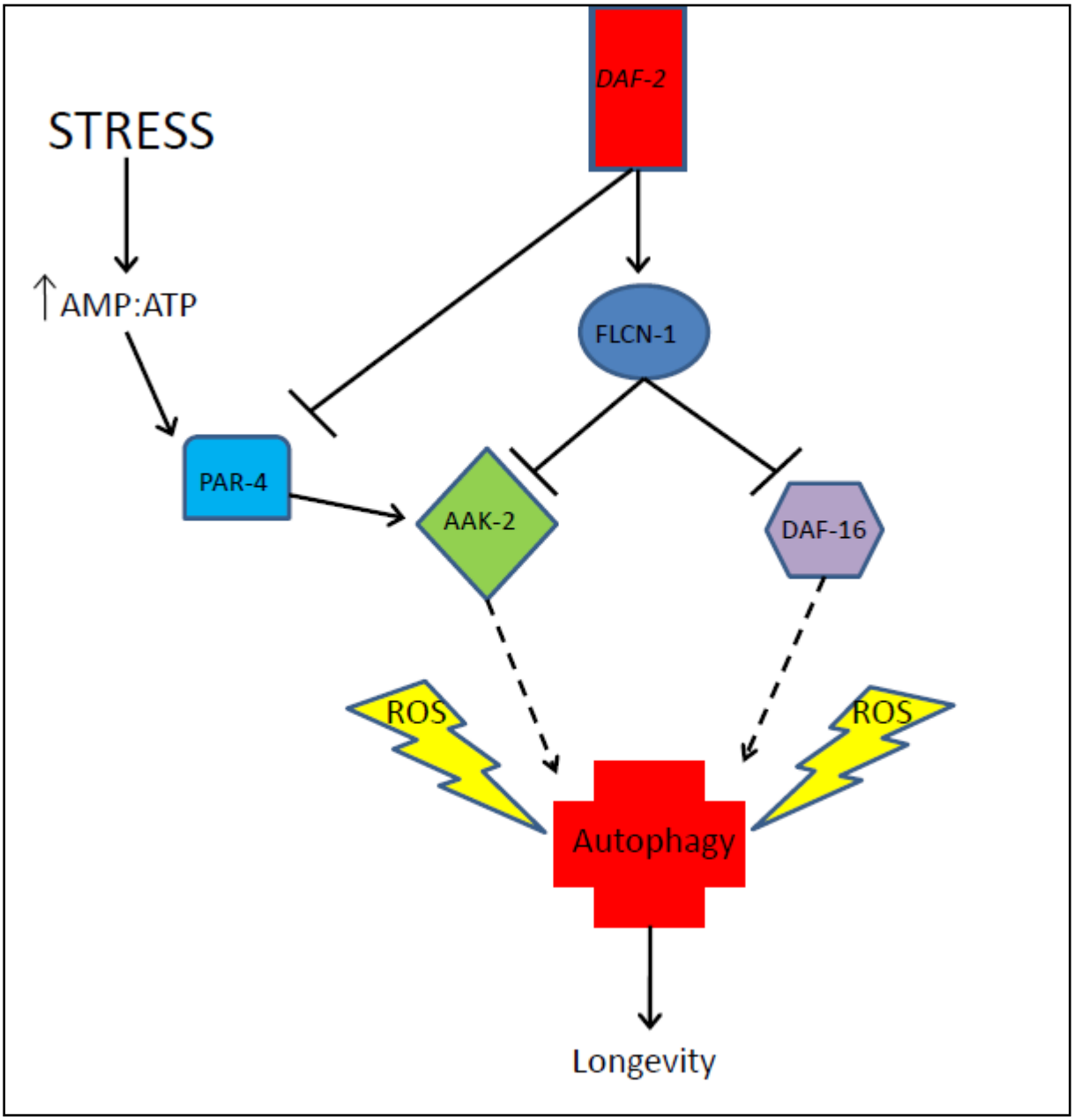

Figure 9: Model.

Flcn-1 regulates lifespan in response to insulin/IGF-1 signalling via a mechanism dependent on aak-2, daf-16 and autophagy.

Table 1: Mean adult lifespan of various mutants in relation to *flcn-1*. All lifespan assays were performed at 20^{o}C (P<0.0001).

Genotype	Mean adult lifespan (days) (n = 90-200)
Wild type (N2) [WT]	14
flcn-1(ok975)	26
flcn-1(RNAi)	17
daf-2(e1370); flcn-1(ok975)	26
daf-16(mu86)	10
daf-16(mu86); flcn-1(ok975)	10
aak-1(tm1944)	14
aak-1(tm1944); flcn-1(ok975)	26
aak-2(ok524)	8
aak-2(ok524); flcn-1(ok975)	8
par-4(it57)	12
par-4(it57) ; flcn-1(ok975)	16
let-363(RNAi)	24
flcn-1(ok975); let-363(RNAi)	32
rsks-1(RNAi)	35
flcn-1(ok975); rsks-1(RNAi)	43
bec-1(RNAi)	8
flcn-1(ok975); bec-1(RNAi)	8